Development of Self-Aspirated Two-Layer Porous Radiant Burners for LPG Cooking Applications

A thesis submitted in partial fulfillment of the requirements for the degree of

Doctor of Philosophy

by

Niraj Kumar Mishra

(Roll No: 10610321)

Department of Mechanical Engineering

Indian Institute of Technology Guwahati

Guwahati – 781039, India

September 2015

Department of Mechanical Engineering
Indian Institute of Technology Guwahati
Guwahati – 781039, India

THESIS CERTIFICATE

It is certified that the work contained in the thesis entitled **Development of Self-Aspirated Two-Layer Porous Radiant Burners for LPG Cooking Applications** by **Niraj Kumar Mishra**, a student in the Department of Mechanical Engineering, Indian Institute of Technology Guwahati, India, for the award of the degree of the **Doctor of Philosophy** has been carried out under our supervision and that this work has not been submitted elsewhere for the degree.

Dr. Subhash C. Mishra
Professor
Department of Mechanical Engineering
Indian Institute of Technology Guwahati
Guwahati – 781039, Assam, India.

Dr. P. Muthukumar
Professor
Department of Mechanical Engineering
Indian Institute of Technology Guwahati
Guwahati – 781039, Assam, India.

Dedicated to

My Family

Acknowledgement

I am deeply indebted to my thesis supervisors, **Prof. Subhash C. Mishra** and **Prof. P. Muthukumar**, for their invaluable guidance and steady encouragement throughout my Ph.D. program. The vigour and attention bestowed by them in taking my research ahead in difficult times will never be forgotten. Starting from framing the problems to the final experimental results and their physical interpretations, they remained deeply involved in my thesis work. They provided me with most innovative ideas, helpful books and journals that were very helpful in successfully completing the present thesis. I have immensely benefited from each and every moment of my association with them. I am highly inspired by their intellectual prowess and exemplary professionalism. I enjoyed each and every moment working under their supervision and learnt a lot of things from them, which will be an asset for my future research.

I wish to express my deep gratitude to all those who have helped me in various ways during the tenure of my PhD work at IIT Guwahati. I have been supported and accompanied by many people and each one has played an indispensable role during my work. I am grateful to all of them.

I am thankful to my Doctoral Committee members, Prof. Niranjan Sahoo, Dr. C. Somayaji and Dr. Tapas K Mandal for their valuable suggestions and encouragement during the period of my research work.

I specially thank Mr. D. Chetri, Mr. J. Basumatary, Mr. Nip Borah and Mr. R. Saikia for their help during the course of fabrication of the setup and also their assistance when needed during my experimental studies.

I am thankful to Dr. Vijaya Pantangi, Dr. B. Satya Sekhar, Dr. S. Anbarasu, Dr. Rupesh Singh, Dr. Koushik Das, Mr. Shyamkumar, Mr. Swapnil kharche, Mr. Shaurabh Sharma, Mr. Snehasish Panigrahy, Mr. Gyan Sagar Sinha, Mr. Chilaka Ravi Chandra Rao, Mr. Hakeem Niyas, Mr. B. Kiran, Mr. Satisha, Mr. Vivek Selvan, and Mr. Vijay Mishra, with whom I had

healthy discussions and they made my stay a pleasant one at IIT Guwahati. I may have missed out a few names in the following list; my sincere apologies are due for any such inadvertent oversight.

I would like to express my sincere gratitude to my parents Mr. Subhash Chandra Mishra and Mrs. Anjani Devi, my brother Mr. Pankaj Mishra, whose blessings, prayers and never ending support is the real impetus that continuously motivates me to produce my best. Last but not the least, my deepest gratitude goes to my wife Mrs. Shwetesh Mishra for her constant encouragement, patience and motivation for the completion of this thesis work.

I bow my head and record my sincere gratitude to the God Almighty for giving me the strength, health and the spirit to complete my research work.

Niraj Kumar Mishra

Abstract

Globally, the major share of energy requirement is met by conventional combustion devices working on fossil fuels. Depletion of fossil fuel reserves, and ever increasing environmental imbalance caused by pollutants from combustion devices, has become a great concern. This has, thus necessitated the need to search for alternative sources of energy, and also some design modifications in the existing devices. The main focus of the design modifications is to conserve energy to the maximum possible extent, and to minimize the emissions. Hence, a continuous effort on improving the performance of combustion devices has remained a paramount task for the policy makers and researchers dealing with energy conservation and environmental pollution.

A conventional combustion device is characterized by free-flame in which the combustion takes place in the open air environment, and convection is the main mode of heat transfer. As compared to heat conducting solids, gases have very low thermal conductivities and emissivities, in conventional combustion devices, contributions of conduction and radiation from the post flame to pre flame zone is insignificant. Thus, due to poor heat transport, these devices are less efficient, and they have undesirable features such as low flammability limits, low power density, high level of pollutant emissions, etc. Conventional liquefied petroleum gas cooking stoves fall under this category.

In India and many other countries, for cooking stoves, LPG is the most commonly used fuel. In these stoves, a premixed air-fuel mixture combust in the gaseous environment and the flame stabilizes over the perforated metallic burner head. The free-flame combustion in these burners is similar to that of the Bunsen burner. In free-flame combustion, the reaction zone is very thin, and because of which, the temperature gradient across the flame is very high. The measured thermal efficiencies of the conventional domestic LPG cooking stoves (1 – 3 kW) available in the Indian market are in the range of 60-68%, and that of the medium-scale (5 – 15 kW) are in the range of 30-45%. These efficiencies are low. Due to the aforesaid reasons, the free-flame combustion is not desirable for the LPG cooking stoves.India is the fourth largest consumer of

LPG, and it ranks third in the domestic sector. The total domestic consumption of LPG in India is almost comparable to other petroleum products used in industrial applications. According to the 2014 Annual Report, "Basic Statistics on Indian Petroleum & Natural Gas" the number of the domestic LPG consumers in India is increasing year by year, and the total number of LPG consumers in 2014 was about 150 million. Analysis of the consumers' data of previous years shows a steady growth of about 10%. Due to increasing number of consumers, the demand of LPG is also increasing. The total LPG requirement during 2016-17 is projected to be 21.83 MMT which is 1.66 times more than India's indigenous production. To meet the demand, therefore, India has to import LPG, and for this, a huge amount of foreign exchange is paid. As consumers cannot afford the actual price of LPG, the Government provides a substantial amount of subsidy. In the year 2014, the total subsidy on LPG for cooking stoves given by Government was (INR) 483.62 billion.

Apart from inefficient utilization of energy in the existing LPG cooking stoves, and expenditure of the foreign exchange, huge amount of pollutant emissions is a serious concern. CO and NOx emissions from conventional domestic LPG cooking stoves (1 – 3 kW) are in the range of 220 ppm to 550 ppm and 5 ppm to 25 ppm, respectively. The same for the medium scale (5 – 15 kW) LPG cooking stoves are 355 ppm to 1165 ppm and 28 ppm to 110 ppm, respectively. These emissions levels are above the current standards of World Health Organization. Thus, curtailment of CO and NOx emissions further necessitates development of the efficient burners for cooking applications.

Instead of combustion in the gaseous environment, like in the conventional burners, if a fuel is made to combust in a conducting and radiating porous matrix, thermal efficiency goes up, and emissions of CO and NOx come down. This is owing to enhanced heat transfer. This combustion in the porous matrix utilizes the principle of excess enthalpy combustion. By preheating the premixed fuel-air mixture, even the lean mixture and low calorific value fuel can be combust in the porous matrix. This preheating in combustion in the porous matrix is realized due to the manifestation of the volumetric thermal radiation. Apart from preheating of the incoming premixed fuel-air mixture, volumetric radiation, conduction and increased convection owing to higher surface area per unit volume of the porous matrix, homogenization

of temperature, and hence the volume of the reaction zone gets elongated. These all lead to a higher thermal efficiency and reduced emissions.

Impressed with the performance of the devices based on porous medium combustion in diverse applications, recently, some researchers have extended its usage to LPG cooking stoves. They have reported enhanced thermal efficiency and reduced emissions. A critical review of previous studies reveals that their developments lacked utility for domestic cooking as well as cooking for a mass, as these required the supply of compressed air. The supply of compressed air is not feasible, and it is also unnecessary for the cooking applications. The present work, addresses this issue through the development of self-aspirated two-layer porous radiant burners for LPG domestic as well as medium-scale cooking stoves.

The present work, therefore, is aimed at the development of the LPG cooking stoves that utilizes the principles of porous medium combustion. For the domestic cooking, the burner power of the range 1-3 kW is developed. With cooking for a large number of people (say 50 or 100) in hostels, hotels, community centres in mind, a medium scale burner with power range 5 – 15 kW is also developed. The developed cooking stoves with porous radiant burners are stand-alone systems. Unlike the burners of other researchers, for their operation, these burners do not require supply of any external air. Making the developed stoves independent of external air, the design has been substantially changed. The changes are discussed in detail in the thesis.

The work contained in the thesis has been carried out in three parts. In the first part, the performance analyses have been carried out for the medium-scale LPG cooking stove with a porous radiant burner. Though working on external air supply, the objective of the first study has been to understand the stability range of the burner, and to fix the geometric and operating parameters. The second part of the study is dedicated to the development of self-aspirated domestic LPG cooking stove with a porous radiant burner (PRB). The development of self-aspirated medium-scale PRB for LPG cooking stoves is the third study. To compare the improvements in terms of thermal efficiency and emissions in the developed LPG cooking stoves, experiments were also performed with that of the conventional LPG cooking stoves of the same power input available in the market.

In the first part of the study, the burner input power range considered was 5–10 kW. For the two-layer LPG cooking stove with a PRB working on external air, performances have been investigated at power inputs in the range 5–10 kW. And, for the stable combustion, the equivalence ratio was found from 0.54 to 0.72. The combustion behaviour within the burner has been also studied by measuring radial and axial temperature distributions. The temperature measurement has been done using both thermocouple and IR camera. For different power inputs, the thermal efficiency of the PRBs were found in the range 42 – 58% and the respective values for the conventional burner was in the range of 35 – 45%. This increase in thermal efficiency is attributed to improved combustion in PRB. Also emissions were lower than the conventional burner. As mentioned before, the LPG cooking stove with PRB operating on external air lacks utility, the two studies address the development of self-aspirated LPG cooking stoves with PRB with the input power ranges 1 – 3 kW and 5 – 15 kW.

Placement of porous matrix in the flow path adds to the resistance, and to overcome that in previous studies, researchers had to use compressed air. And, this has been one of the major limitations in using the LPG cooking stoves with PRB for cooking applications. To overcome this limitation, the design modifications in terms of LPG supply pressure, orifice, burner port, mixing tube and burner casing were done. For power input 1-3 kW LPG cooking stove with a PRB, for air entrainment, two slots in the burner port was introduced. The orifice diameter too was changed. The LPG supply pressure was increased to 1.2 bar (gauge). With the improved design of the burner assembly, thermal efficiency, emission characteristics and temperature distribution were studied for power input in the range of 1 - 3 kW. A significant improvement in thermal efficiency (63-75%), and large reduction in emissions (CO: 30- 140 ppm and NOx: 0.2-3.5 ppm) were observed.

For the medium scale (5 – 15 kW) LPG cooking stove with PRB, the design of the burner is completely different from the one with 1-3 kW considered in the second study, and also of the conventional ones of the same input power range (5 – 15 kW). Instead of one burner port in the previous one (1 -3 kW), to meet the requirement of large volume of air, four burner ports with four orifices were incorporated. Each of the four burner port was fitted with an orifice.

All the four orifices were connected to the same LPG supply line. For the better radiant output, the diameter as well as the thickness of the porous matrix for the combustion zone was optimized. The thermal efficiency was found to improve significantly (44 – 55%), and the emissions (CO: 60 – 190) ppm and NOx: 2 – 10 ppm) also reduced considerably.

For both self-aspirated domestic as well as medium-scale cooking stoves with PRB, the measured emissions were found lower than the conventional burner. Significant amount of LPG can be saved by using developed LPG cooking stove with a two-layer PRB. Newly developed burners with PRB showed a steady-state operation without any flashback and blow-off. It was observed that the radial temperature distribution of the burner with PRB was almost uniform. As both developed stoves are self-aspirated, it works on the natural draft. It is ideally suited for LPG cooking applications everywhere.

Nomenclature

Symbols	**Units**	**Comments**
A/F	-	Air-fuel ratio
C_L	-	Loss coefficient
CV	kJ/kg	Calorific value
$C_{W,p}$	kJ/kg-K	Specific heats of water and aluminium pan
d_m	m	Mean pore diameter
D_I	mm	Inlet diameter of orifice
D_P	mm	Burner port diameter
k	W/m-K	Thermal conductivity
m_f	kg	Fuel consumed to raise the water temperature from T_1 to T_2
m_p	kg	Mass of pan along with the lid and stirrer
m_w	kg	Mass of water
Pe	-	Peclet number
r	cm	Radius of PRB
R	-	Entrainment ratio
S_L	m/s	Flame velocity
T_1 and T_2	°C	Initial and final temperatures of water
η_{th}	%	Thermal efficiency
ρ	kg/m^3	Density
σ	-	Relative density of gas

Abbreviations

CB	Conventional burner
CZ	Combustion zone
DOM	Discrete ordinates method
FF	Free-flame
INR	Indian rupees
LPG	Liquefied petroleum gas
MMT	Mega metric ton
MW	Mega watt
ppi	pores per inch
ppm	part per million
PB	Porous burner
PM	Porous matrix
PMB	Porous medium burner
PMC	Porous medium combustion
PRB	Porous radiant burner
PRRB	Porous radiant re-circulated burner
PSB	Porous surface burner
PSC	Porous surface combustion
PZ	Preheating zone
SAC	Super adiabatic combustion
SB	Swirl burners
SCH	Surface combustor heater
WHO	World Health Organization

Contents

List of Figures

List of Tables

Chapter 1

Introduction

1.1 Motivation

In India and other developing countries, majority of the energy requirements are fulfilled by the conventional combustion devices working on fossil fuels. The diminishing fossil fuel reserves and the rise in environmental imbalance due to pollutants originating from combustion processes have demanded the necessity to look for an alternative sources of energy. At the same time, some design modifications are also required to make the existing combustion systems more efficient. The main focus of these design modifications is to conserve the energy to the maximum possible extent and to minimize the emissions. Hence, a continuous effort on improving the performance of such devices has remained an utmost interest for the policy makers and researchers dealing with energy conservation and environmental pollution.

A conventional combustion device is categorized by a free flame. This type of combustion takes place in the open air environment where the convection is the main mode of heat transfer. As the gases have a very low thermal conductivity and low emissivity, the contributions of conduction and radiation modes of heat transfer from the post flame to pre flame zone is insignificant. Thus, due to poor heat transport, the conventional combustion devices are less efficient, and they have undesirable features such as low flammability limits, low power density, high level of pollutant emissions, etc. Conventional cooking gas burner is such device that falls with this category of high emission levels, low thermal efficiency and power modulation. In India and many other developing countries, for

cooking gas burners, LPG is the most commonly used as a fuel. LPG is synthesized by refining petroleum, and is usually derived from fossil fuel sources. LPG has a high calorific value than kerosene and wood, and burns without any soot. The properties of LPG have been presented in Appendix – I.

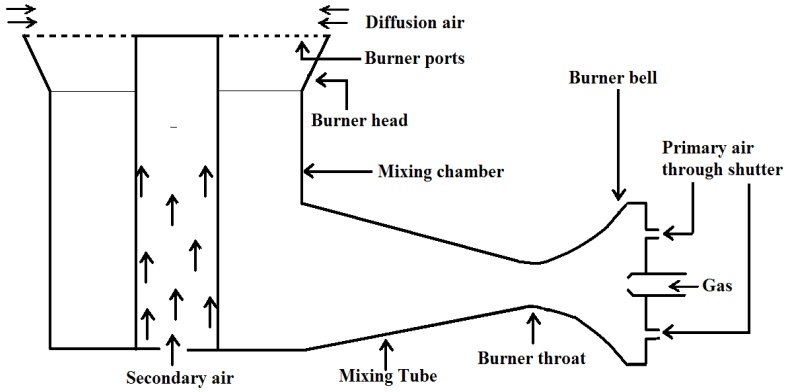

Fig. 1.1. Schematic of the conventional domestic LPG cooking stove [Pantangi, 2010]

Fig. 1.2. Pictorial view of the free flame in conventional domestic cooking stove

1.1.1 Conventional domestic LPG cooking stove

All kinds of conventional burners used in domestic LPG cooking stove and commercial LPG cooking stove work on the principle of a Bunsen burner. The details of burner assemblies and different types of burners are presented in Chapters 3 and 4. The schematic

of a typical burner of a conventional domestic LPG cooking stove is shown in Fig. 1.1. It consists of an orifice for LPG supply, two slots for primary air source, a venturi-shaped mixing tube, and a burner head with holes in it mounted on top of the mixing chamber. The tapered zone of the mixing tube is called as throat, which diverges into the rear part called its bell. The positions of the two primary air opening or shutters relative to the LPG supply orifice vary according to manufacturers. In some burners, they are positioned somewhat downstream of the gas inlet orifice. The high velocity LPG jet generates a low static pressure in the burner bell and as a result suction of primary air through the two primary air shutters. Air and LPG are getting mixed in the mixing tube and through the mixing chamber it delivers out in the form of jets through the holes of the burner head. Combustion takes place on top of the burner head. The equivalence ratio of the mixture (air and LPG) hardly reaches to 1. Consequently, the combustion of conventional burner (CB) is always fuel rich. The holes are closely situated circumferentially and thus the jet flames from the individual holes combine to form a single flame. The secondary air is entrained to the combustion zone from the bottom of the mixing chamber and air also spreads to the combustion zone from the circumferential area surrounding the flame. Therefore, the combustion in the burner of a domestic LPG cooking stove is a partially premixed one. The combustion products are at a high temperature, thus rise vertically away from the flame, transferring heat to the air close to the top of the flame. The heated air moving upward direction due to density difference that pulls in the cooler secondary air to the base of the flame.

The combustion in the burner of a domestic LPG cooking stove takes place in a gaseous environment and the flame becomes stable over the metallic surface of the burner as shown in Fig.1.2. This combustion is called as free flame combustion. In free flame combustion,

the reaction zone is very thin and because of which the temperature gradient across the flame is very high. Due to the above reasons the free flame combustion is not desirable for cooking stoves.

1.1.2 Energy crisis

India is the fourth largest consumer of the LPG, and it ranks third in the domestic sector [Chandra A, 2012]. As the living standards of the people in India are improving, the number of LPG consumers is also increasing. The measured (laboratory conditions) thermal efficiencies of the current domestic LPG cooking burners available in the Indian market are in the range of 60-68 %, also the thermal efficiencies of medium-scale conventional LPG burners are in the range of 30-45% . These efficiencies are very low.

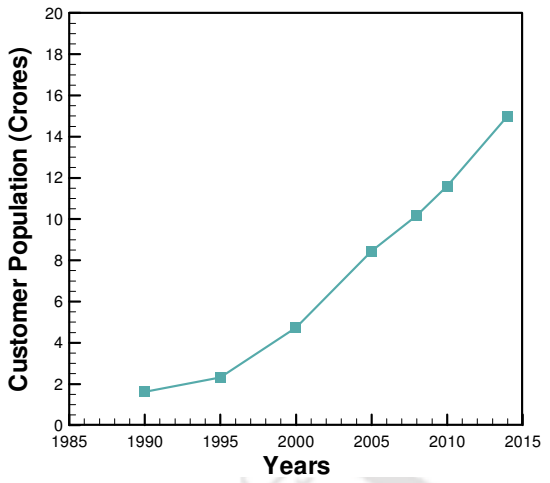

Fig.1.3. Year-wise total number of LPG domestic consumers in India

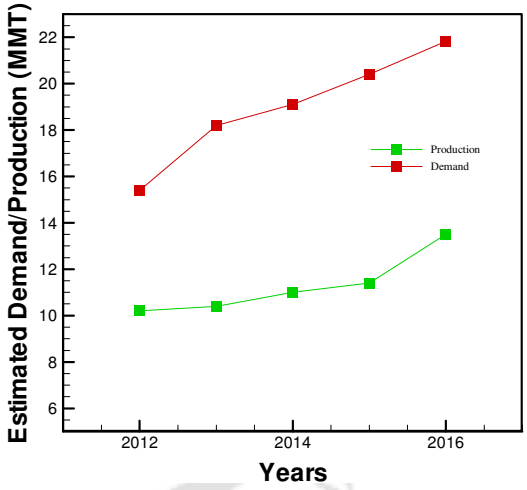

Fig.1.4. Estimated demand and planned production of LPG in India

The total domestic consumption of LPG in India is almost comparable with other petroleum products used in industrial applications. Basic Statistics on Indian Petroleum & Natural Gas, Annual Report (2013-2014) suggest that the number of LPG domestic consumers in India is increasing year by year and the total number of LPG consumer in 2014 is about 15 Crores. Analysis of the consumers' data of previous years shows a steady growth of about

10% as shown in Fig.1.3. Due to increasing number of customer the demand is also increasing. As illustrated in Fig. 1.4, the total LPG requirement during 2016-17 is 21.83 MMT (mega metric ton) which is 1.66 times higher than India's indigenous production. This will also lead to huge amount of foreign exchange.

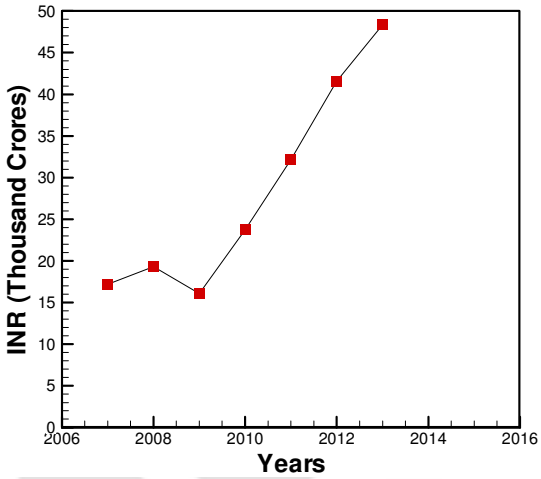

Fig. 1.5. Year-wise total subsidy by Government of India on domestic LPG

In India LPG is highly subsidized from the Government of India. In year 2014, total subsidy given by Indian Government is 48,362 Crores INR (shown in Fig. 1.5). Hence, Government of India has to spend Crores of rupees as subsidies in every year. In order to cut down the increasing subsides, the amount of LPG consumed should to be reduced by improving the combustion characteristics of the existing burners.

Another serious issues related to the combustion is the formation of pollutants, which are having undesirable health effects on human and living species. Pantangi et al., [2011] reported the CO emissions of the conventional domestic LPG cooking stoves are in the range of 220 ppm to 600 ppm and NO_X emissions are in the range of 5 ppm - 25 ppm. The similar data for the medium-scale LPG cooking stoves are in the range of 355 ppm to 1165 ppm and 28 ppm to 109 ppm, respectively. All measurements have been done following the procedure described in Bureau of Indian Standards (BIS) 4246:2002. The details of

measurements are discussed in Chapter 3. These emissions levels are above the current standards prescribed by World Health Organization, Kandpal *et al.*, [1995].

1.1.3 Pollutant formation and their Effects

The pollutant formed from the combustion process effects the environment and health in several ways. The pollutant formation occurs in two ways: one is primary air pollutants which are emitted directly from the source and the other is secondary pollutants which are formed through the reactions involving primary pollutants in the atmosphere. The primary pollutants discussed in this Section are carbon monoxide (CO), nitric oxide (NO) and nitrogen dioxide (NO_2) because they dominate during the gas combustion process. The general effects and physical properties are presented in Table 1.1 [Avdic, 2004].

Carbon monoxide is the most abundant pollutant in the lower atmosphere. The physical properties and effects are presented in Table 1.1. The effects vary normal cough to death depending upon the exposure levels. Fig. 1.6 illustrates the different effects of CO exposure levels.CO generally is the major species formed during the rich combustion. For stoichiometric and slightly lean mixtures, CO is found in substantial quantities at typical combustion temperatures as a result of the dissociation of CO_2. Carbon monoxide concentrations rapidly fall with temperature [Turns, 2000]. According to Basu *et al.* [2000], 0.1 s of residence time is necessary for complete combustion. In furnaces, for example, where the residence time is measured in seconds, to reach conditions for complete combustion is not difficult. In IC engines the temperature rapidly falls and the residence time is not sufficiently long to approach conditions for complete combustion.

In order to decrease the formation of CO concentrations in flue gases, the residence time must be as long as possible. Higher combustion temperatures are one more advantageous

for CO reduction and lean air mixture (excess air) ratio is also preferred for CO reduction. At lower air fuel (AF) ratio, the CO emission is higher and the CO equilibrium concentration is high. For high AF, the oxidation velocity decreases owing to the lower temperatures in the combustion zone. One should emphasize that the above considerations are valid only for pre-mixed combustion processes.

Table 1.1: Some important physical properties and effects of the primary pollutants

Pollutant	Physical properties	Source		Effects on humans
		Humans	Natural	
CO	Colourless, odourless, flammable, toxic gas, slightly soluble in water	Combustion of fossil fuels	Atmospheric oxidation of methane and other biogenic hydrocarbons	Decreases the oxygen carrying capacity of blood. The other effects vary from headache, vomit, collapse and death depends on the levels of exposure.
NO	Colourless, Odourless gas; non-flammable and slightly soluble in water; toxic	Combustion	Bacterial action, Natural combustion processes.	Damage respiratory air ways; can cause burns on the skin/eyes.
NO_2	Reddish-orange brown gas with sharp, pungent odour; toxic and highly corrosive.	Combustion	---	Risk of respiratory symptoms such as acute bronchitis and cough and phlegm, particularly in children.

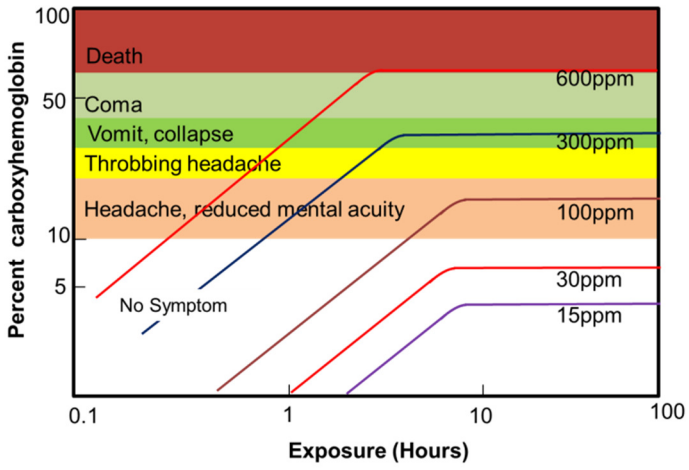

Fig. 1.6. Effects of different levels of CO exposure on humans [Turn, 2000]

Nitrogen oxides are also one of the important pollutants formed from the combustion of fossil fuels. The major sources are automobiles and coal, oil and gas fired power plants. Both nitric oxide NO, and nitrogen dioxide NO_2, are produced in combustion, but NO is a major proportion. Both the emission species are frequently clubbed together with the title NO_x. Nitric oxide is formed both from atmospheric nitrogen N_2, and from nitrogen contained in some fuels. The latter source depends on the fuel composition and is not important for fuels with low nitrogen contents but former is a major source of NO_x, e.g., coal combustion. Nitric oxide can be formed, though, when any fuel is burned in air because of the high-temperature oxidation of N_2. Everyone is exposed to small extents of nitrogen oxides in ambient air. Higher exposure may occur by burning kerosene, wood, near gas stoves or if one smokes. The effects are presented in Table 1.1. The important thing regarding NO prescription is that there is no antidote for NO poisoning.

1.2 Porous medium combustion

1.2.1 Working principle of porous medium combustion

The heat transfer mechanism in a Porous Burner (PB) is totally different from the CB, which is characterized by a free flame as discussed in Section 1.1. The PMC operates a novel concept of using a 3-D porous matrix in the combustion zone for enhanced heat transport from the burned to unburned portion of the air-fuel mixture. Fig.1.7 shows the photographic view of the PRB taken at Thermal Science Lab, IIT Guwahati. Since the porous matrix has high thermal conductivity and good radiative properties, the contributions of conduction and radiation in the PMC are very important. Also, due to a large surface area of the porous matrix and high heat transfer coefficient, the convective heat transfer is also better than the free flame combustion. The better heat transport (through the combined modes of conduction, convection and radiation) results a homogeneous

temperature distribution in the combustion zone. Depending on the flow velocity and thermo-physical properties of the porous material, the flame may stabilize either inside or on the surface of the porous matrix.

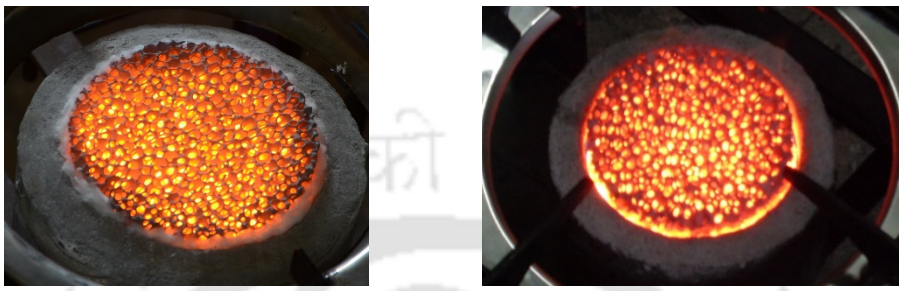

Fig. 1.7. The photographic views of PRB taken at IIT Guwahati.

The PMC is characterized by a high burning velocity, reduced temperature drop across the reaction zone, high radiant output, high peak flame temperature and reduced enthalpy of flue gas. Unlike the conventional burners, in the porous burners, a low calorific fuel can also be combusted. In general, based on the type of media used, the PMC is categorized into catalytic and inert. The former one utilizes a catalytic medium, which is coated on the solid matrix and participates in the combustion process; whereas the latter one remains inert but augments the heat transfer process. Further, depending upon whether the flame is stabilized above the surface or within the porous matrix, the PMC can be classified as surface stabilized or matrix stabilized. In matrix stabilized combustion (Fig.1.8.a), the flame stabilizes close to the inlet and combustion takes place completely inside the porous matrix. The gas temperature reaches its maximum value in the reaction zone and decreases in the downstream due to cooling. Unlike this, in surface stabilized combustion (Fig.1.8.b), the flame stabilizes on the downstream surface of the porous matrix and the maximum volumetric heat release there.

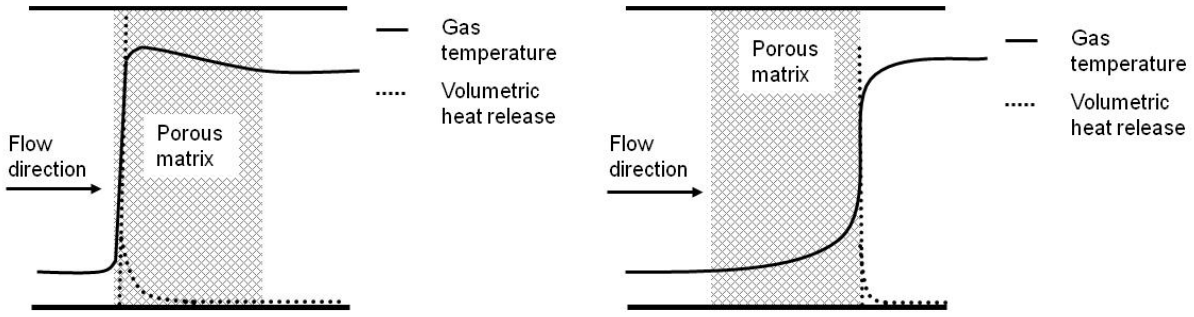

(a) (b)

Fig.1.8. Schematic of (a) matrix stabilized and (b) surface stabilized PM [Pantangi, 2010]

The dependency of the flame position on porosity has led to the concept of a double layered PB having different porosities [Kulkarni and Peck, 1996]. A double layered PB consists of a preheating zone (PZ) and a combustion zone (CZ) (Fig.1.9). The PZ, which has a low porosity, prevents possibility of ignition and flame propagation thereby occurrence of flashback. The air-fuel mixture is preheated in this zone and it helps in improving the combustion efficiency and enhance the flammability limit. Further, preheating improves the stability of the combustion regime too. In the CZ, due to high porosity, combustion takes place and flame propagates. In this, the reaction zone is enlarged and because of homogenization of temperature, the NOx formation is reduced. The interface of the two zones serves as a flame holder.

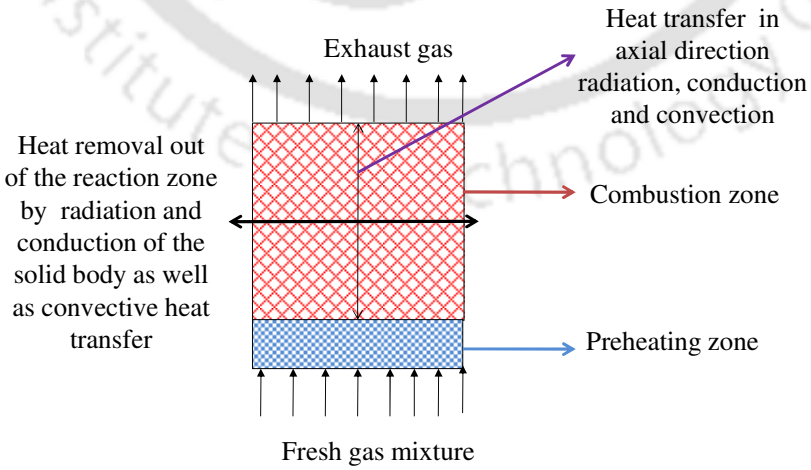

Fig. 1.9. Schematic of a double layered PB [Durst and Trimis, 2002]

Babkin *et al.* [1991] provided the criterion for flame stabilization inside a PB as a function of Peclet number, *Pe* (ratio of heat flow by convection transport to heat flow by conduction), based on mean pore diameter. They proposed the following limiting condition for the flame propagation

$$Pe \geq 65$$

$$\text{where, } Pe = \frac{S_L d_m c_p \rho}{k} \tag{1.1}$$

where, S_L is the laminar flame velocity, d_m is the mean pore diameter, c_p is the specific heat, ρ is the density and k is the thermal conductivity of the gas. For a stable operation, a double layered PB should be designed in such a way that the *Pe* for the pre-heating zone should be less than 65, and the same for combustion zone should be greater than or equal to 65. The optimization of porosities as well as the thermal conductivities of the two zones gives rise to a better heat utilization and temperature homogenization. Under certain conditions, the heat recirculation gives rise to a kind of flame called excess enthalpy flame.

1.2.2 Excess enthalpy combustion

Weinberg [1971] first introduced the concept of excess enthalpy. He reported that minimization of heat loss from a combustion device to the surrounding through heat recirculation from exhaust gases, generates a kind of flame called “excess enthalpy flame”. The combustion, in which the excess enthalpy flame generates, is called “excess enthalpy combustion” or “super adiabatic combustion” (SAC). The typical characteristic of an excess enthalpy flame is that its peak temperature is higher than the corresponding adiabatic flame temperature.

Weinberg [1971] proposed several recuperative schemes, in which heat from exhaust could be extracted and used for pre-heating of incoming reactants. Among all the schemes, the one with internal heat recirculation appeared to be very promising as it led to the generation of excess enthalpy flame. He showed some of the benefits of excess enthalpy flame such as high combustion efficiency, thermodynamic efficiency, lower emission of pollutants, etc. Hardesty and Weinberg [1974] found that owing to a high heat feedback, for a given equivalence ratio, at high gas velocities, the peak temperature of the combustible mixture increased. At high gas velocities, the reaction zone also found to widen. Fig.1.10 illustrates the enthalpy comparison with and without heat recirculation.

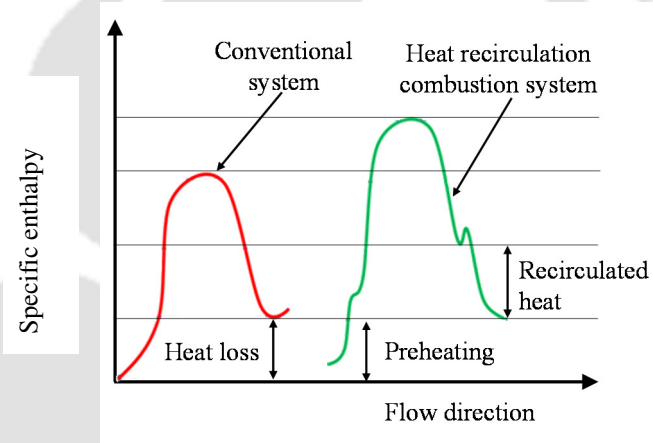

Fig. 1.10. Enthalpy comparison with and without heat recirculation [Pantangi, 2010]

1.2.3 Advantages of porous medium combustion

The major advantages of PMC are as follows;

- Good heat transfer properties and keep the burner's surface temperature lower which in turn lowers NO_x emissions.
- Due to increase of residence time, the formation of CO emission is low.

- A portion of heat released is transported in the upstream direction which preheats the fresh mixture causing the greater flame speeds as compared to free flame combustion.
- Operates at lower equivalence ratios.
- The burner can be operated on wide range of power modulation.
- Complex combustion chambers geometries are possible in case of a porous burner.
- This method improves the heat transfer process due to good radiation and conduction properties of porous medium.

1.2.4 Applications of porous medium combustion

Some of the important applications of porous medium combustion based porous burner are given below and same have been presented in details in Chapter 2.3

- Household, for example porous burners for cooking and heating systems
- Burner for automobiles.
- Burner for gas turbine and propulsion.
- Burners for heat exchangers.
- Miscellaneous applications like thermoelectric conversion, steam generation etc.

1.2.5 Materials used in porous medium combustion

Ceramics (Fig.1.11) are most suitable for porous medium applications because of their high operating temperatures, resistance to erosion and thermal shock, chemical stability and wear. The most commonly used high temperature ceramics are alumina (Al_2O_3), silicon carbide (SiC) and zirconia (ZrO_2) and their respective thermo-physical properties are summarized in Table 1.2.

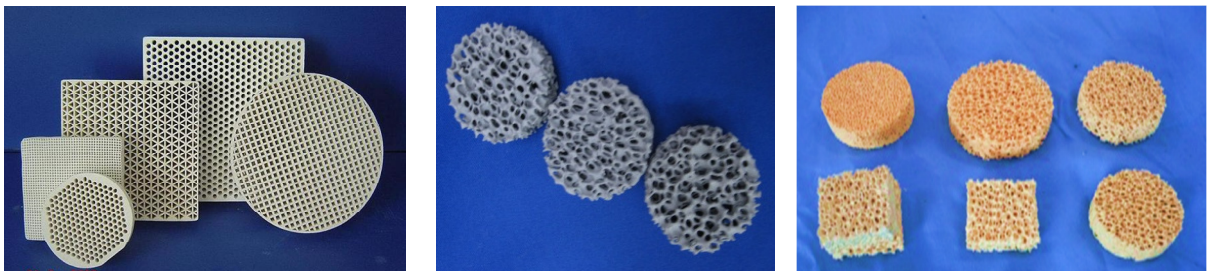

(a)Aluminum oxide ceramic (b) SiC ceramic (c) Zirconium ceramics

Fig. 1.11 Different types of ceramics

Alumina is the most popular, working both in a packed bed and as a lamella structure. It has a high temperature resistance and has good resistance to wear and corrosion, as well as economical too. It has a moderate thermal conductivity and emissivity, but has a large coefficient of thermal expansion and poor thermal shock resistance. The properties of any alumina-based ceramic depend on the actual alumina content. Ceramics with higher silica contents will typically have lower maximum usage temperatures and higher thermal conductivities. SiC and SiSiC (silicon infiltrated silicon carbide) ceramics oxidize at around 600 °C but as long as the resulting surface layer of silica remains stable, can be used up to reasonably high temperatures. Compared to alumina, they have high thermal conductivity, emissivity, and lower coefficient of thermal expansion. Zirconia-based ceramics on the other hand generally have a very high temperature but a low thermal conductivity, high coefficient of thermal expansion, and moderate thermal shock resistance and emissivity. Trimis and Durst [2002] investigated different porous structures viz. ceramic pebbles, ceramic foams, metal foils and wires for use in the PMC. They reported that the heat transport properties of the porous medium depend on the form of the structure and the foam material.

Table 1.2: Thermo-physical properties of most commonly used ceramics for PMC applications [Avdic, 2004]

Parameter	**Units**	**Al_2O_3**	**SiC**	**ZrO_2**
Thermal expansion coefficient α (20-1000 °C)	10^{-6} 1/K	8	4-5	10-13
Thermal conductivity λ at 20 °C	W/m·K	20-30	80-150	2-5
Thermal conductivity λ at 1000 °C	W/m·K	5-6	20-50	2-4
Specific thermal capacity	J /g·K	0.9-1	0.7-0.8	0.5-0.6
Thermal stress resistance parameter, hard shock, R = sigma/ (E.alpha)	K	100	230	230
Thermal stress resistance parameter, mild shock, R'= R.lambda	10^{-3} W/m	3	23	1
Total emissivity at 2000 K	-	0.28	0.9	0.31

1.3 Aim and objectives

In order to cut down the increasing subsides and energy crisis, and to reduce the formation of pollutants, there is a need for research and development activities for improving the combustion performances of the burners used for cooking applications. It was observed that most of the researchers explored the use of porous medium combustion in cooking application for low thermal load in the range of 0.5-2 kW with the help of external air supply. No researchers have reported the use of two layered porous radiant burners (PRBs) in domestic cooking application without external air supply. It was also found that no researcher tested the two layered PRB with the capacity range of 5-15 kW for medium-scale cooking application.

Hence, this thesis is devoted to investigate the applications of the PRBs particularly concentrating on self-aspirated domestic as well as medium-scale cooking applications. This thesis contains of six Chapters and the contents presented in each Chapter are discussed in the following sections.

1.4 Organization of thesis

In the second chapter, an overall view on porous medium combustion covering the significant developments till date is presented. Chapter 2 also presents the state of the art on porous medium and surface combustion technologies. The state of the art mainly on PMC is sub-divided into experimental and numerical investigations, and applications of porous burners ranging from industry to domestic sectors. The chapter ends with concluding remarks on the literature review and then aims of the present thesis.

Chapter 3 deals with the experimental investigation on double layer PRB for medium-scale LPG cooking stoves. Thermal efficiency and emissions have been measured for different conventional medium-scale burners (5-10kW) available in Indian market. For same power input, the two-layer PRB have also been investigated. The combustion behaviour within the burner was also studied using the temperature distribution at different positions of the burner. It was observed that there was a possibility of replacing the CB with PRB. But only thing is that existing burner assembly need to be re-designed, so that it can work without any compressed air.

Chapter 4 deals with the different stages of self-aspirated domestic LPG cooking stove developments with PRB. The comprehensive efforts have been made for the use of PRB in domestic cooking application, without external air supply. Initially, the prototype PRBs assembly mounted on existing CB. But due to lack of air-entrainment design, it was not showing the stable combustion. Later, orifice, burner port, mixing chamber and burner casing design were modified for getting better air-entrainment and improved combustion. With the improved design, the thermal efficiency and the emission characteristics were studied at different power inputs.

Chapter 5 deals with the development of self-aspirated medium-scale LPG cooking stove with PRB for medium scale cooking applications (5-15kW). Initially, the existing cooking stove was used with PRB. But due to poor air-entrainment, it was found not suitable. Further, a self-aspirated medium scale cooking stove has been developed. For getting high air-entrainment and improved combustion, multi ports have been incorporated with new burner assembly. Burner's components such as orifices, slots and connector have been redesigned for accommodating the stable combustion. Conclusions and future work are presented in Chapter 6.

Chapter 2

State-of-the-Art

In this chapter, an extensive literature survey on the initial developments of porous medium combustion that lead to the establishment of the technology for different applications have been presented. The experimental and numerical investigations on flame stability, emission characteristics, and radiation output of porous medium combustion carried out by different researchers are discussed. Research works done on the porous surface burners are also discussed. The various applications of Porous Burner are discussed in detail. The objectives of the thesis are presented at the end of this chapter followed by the closure of the literature survey.

2.1 History of porous medium combustion

The PMC is a two-century old technology. Its first research activity started in the beginning of the 19th century [Avdic, 2004]. Though, due to non-commercialization, the interest in this technology faded away with time. The non-commercialization was due to the problems in flame stabilization and flash back, and so the burner's categorization could not be done and was left unexplored. There were a large time gap between the early findings and the continued exploration for applications of the PMC. In recent years, due to strict legislation on ecological protection and conservation of fuel, the attention in this technology has revived and many of its practical applications have been recognized. The following paragraphs give a brief review of the PMC technology from its early development in the 19th century to till date with emphasis in the important developments of the technology and possible commercial applications.

2.1.1 Initial developments

Sir Humphry Davy was the first to report a work relevant to PMC and more specifically the so called porous surface combustion [Avdic, 2004]. He made two important discoveries. His first discovery concluded that the combustion cannot occur in tubes below a certain radius. This minimum radius was called as "quenching radius". His second discovery established the fact that even without a flame, a gas can be burnt below its ignition temperature. This was termed as "flameless combustion". These days, both the concepts are widely used in design and development of devices based on the PMC. The further developments and patents are clearly discussed by Avdic [2004] until before the end of 19th century.

Echigo [1984] reported two major developments. The first one was related to the reduction of thermal NOx production and unburnt matters, such as CO and hydrocarbons. This was achieved through a homogenization of temperature in the combustion zone. The second one was related to enhancement of the combustion efficiency by a method wherein combustible mixture burnt in the porous matrix. In 1987, Fleming [1987] designed and patented a porous combustor and analysed the radiation energy generation process. He invented a combustor that comprised of a porous plate with at least two distinct adjacent layers. The bottom layer was of lower thermal conductivity as a preheating zone and the top layer had high thermal conductivity and emissivity which acted as a source for radiation. This design was found very effective in generation of radiant energy with improved energy efficiency, enhanced combustion intensity, and reduced emissions of noxious pollutants along with reduced flashback.

In 1991, Babkin *et al.* [1991] reported some important results related to flame propagation velocity in porous matrix. They measured the flame propagation velocity for methane-air and propane-air mixtures in four kinds of porous media. Their results established five steady-state regimes for gas combustion in an inert porous medium. They clarified the phenomenon of flame quenching within the porous medium, which was important for defining combustion stability. They provided the criterion of Peclet number '*Pe*' that became the basis for flame stabilization. After this invention, later, many others [Sathe *et al.*, 1989a; Hsu *et al.*, 1993a and b., Mital *et al.*, 1997] simplified the stability regime for other fuels and investigated few other issues viz. effect of pre-heating, radiation output, flame propagation, etc. In recent times, a few newer designs of the PB have emerged [Tong *et al.*, 1990; Durst and Trimis, 2002; Jugjai and Rungsimuntuchart, 2002; Wei *et al.*, 2002; Shinoda *et al.*, 2002] and some more possible applications have been identified. The same are reported in the later part of the thesis.

2.1.2 Some recent patents based on PMC

With the knowledge of the above early developments, Durst [1996a] and co-researchers patented a porous radiant burner with heat exchanger that can work at low wattage (1-8 kW) with stable combustions and no flash back. This development was mainly meant for European home heating systems. Their burner has increase in the pore size from the inlet to the outlet of the burner. This also allowed the burner to run at high inlet pressures.

Some of the recent patents in this area are as follows:

- A porous burner for gas turbine application which was built by Ellzey and William [2004].

- Volkert and peter [2006] patented a porous radiant burner for gas and air mixture. Burning of a gas/air mixture in porous radiant burner leads to improved heat transfer also, they reported low values of emissions.
- Bellucci *et al.* [2006] built a premixed burner with a swirl generator along with two perforated plates which are kept at a defined distance from one another in the inflow region of the combustion air in such a manner that the burner simultaneously allows damping of acoustic combustion chamber pulsations during operation.
- A pore-type burner with silicon–carbide porous body was built by Hoetger *et al.* [2006] which was designed for burning a fuel–air mixture and to generate a hot flue gas. The invention relates to a pore-type burner for burning a fuel/air mixture for the purpose of generating a hot flue gas. The burner includes a housing in which a pore material consisting of porous, high-temperature-resistant silicon carbide (SiC) is provided for combustion, in order to apply a hot stream of flue gas to a steam super heater.
- Redwood and John [2007] invented high efficiency radiant burner, incorporated with heat exchanger.
- Kaeding and Lawrence [2008] invented a burner with a Porous structure. The burner having a burner chamber filled partially by a porous body, an evaporation zone, an igniter for igniting the combustion mixture of evaporated liquid fuel and air supplied. They reported that the developed burner can burnt the liquid fuel with improved combustion.
- Fabrice and Beatrice [2008] designed compact exchanger reactor using a plurality of porous burners. The discovery relates to a novel exchanger for implementing highly endothermic chemical reactions such as steam reforming reactions of naphtha or natural gas reactor.

- Ellzey and Schoegl [2009] developed a Super adiabatic Counter flow Reactor. They reported that in one particular embodiment, fuel/oxidizer mixtures may be reacted in channels in a counter flow arrangement so, that heat from one channel preheats the gas in the neighbouring channel which leads to improved combustion.
- Assmann *et al*. [2010] developed a porous burner for especially for heating, drying and keeping hot especially a tundish of a continuous casting installation.
- Franz and Götz [2010] developed a device for burning a fuel/oxidant mixture. The invention consists of a reactor with a combustion chamber containing two different porous material zones. They developed the burner for higher operating temperature up to 2400 °C.
- Yoshida [2011] invented burner for manufacturing porous glass preform. The invention relates to a burner for manufacturing a porous glass preform, which can improve deposition efficiency and gas mixing efficiency without increasing turbulence of the flame.
- Claerbout *et al.* [2012] developed an improved radiant burner which comprises a premixing chamber and a combustion chamber. The premixing chamber was separated from the combustion chamber through radiant burner plate which had multiple levels of burner surface for getting improved combustion.
- Alexander [2012] invented a radiant Burner. The objective of the invention was to provide a radiant burner with high energy efficiency, high radiant power and high flame stability.
- Hwang [2014] designed a special type porous plate burner. The development made for a combustion device, which has a simple structure and burns wood chips, wood pellets or other fuel to achieve high heat efficiency and strong thermal power and generate less soot or air pollution.

2.2 Combustion of gaseous fuels in porous medium burners

The experimental and numerical investigations have been explored by many researchers in the area of PMC. Experimental measurements in the PMC are difficult because the complex porous structure prohibits movement of mechanical or optical probes for any direct measurement of quantities of interest inside the porous matrix. Numerical modelling of the PMC too is complex and challenging, since it needs solution of coupled fluid flow, heat and mass transfer and chemical reactions in the porous matrix. Due to dependency of solid and fluid properties on temperature and/or concentration, governing equations are non-linear and they pose difficulty in solution. Further, unavailability of precise thermo-physical and optical properties add to the limitations in numerical modelling. Though, in spite of the above limitations, even with some simplifying assumptions, a good amount of numerical as well experimental works have been carried out to understand the physics of the PMC and to study the thermal performances of different PRBs.

In the recent past, many experimental and numerical studies have been conducted to analyse the combustion behaviour of gaseous air-fuel mixture in PRB. A few have thrown light on the structure of radiation controlled flame, flame stabilization and effects of various parameters influencing flame propagation and emissions. The following paragraphs discuss some of the important experimental and numerical investigations.

2.2.1 Experimental investigations

Flame stabilization

Soete [1966] measured flame speeds and the rate of propagation of the reaction zone through packed beds of sand for methane/oxygen/nitrogen mixtures. They found that combustion in porous media was mainly controlled by the rate at which the reaction was

accelerated by heat recirculation and retarded in the presence of solid wall. He observed a decrease in the flame speed with the decrease in the grain size.

The flame in a PB is called radiation-controlled flame, as radiation dominates over the other two mode of heat transfer [Sathe *et al.*, 1989a]. The position of such a flame is dependent on various operating parameters such as physical and optical properties of the porous material, equivalence ratio, flow rate of the flowing fluid (air-fuel mixture), convective heat transfer coefficient between solid and fluid and thermal conductivity of solid. A balance between chemical reaction rate and two phase energy transfer rate through adjustments of porosity of the material, leads to stabilization of the flame within a porous medium. Babkin *et al.* [1991] and Dillon [1999] gave stabilization criteria of flame as a function of *Pe.* The findings of Babkin *et al.* [1991] have already been discussed in Section 1.2.1. They evaluated *Pe* for hydrocarbon fuel. Dillon [1999] calculated *Pe* for hydrogen. He found critical *Pe* as 37 against 65 of hydrocarbon fuel [Babkin *et al.*, 1991]. He thought that the difference was probably due to different chemistry of the fuel used (hydrogen versus hydrocarbon) and the absence of buoyancy effect, since the experimental combustion tube for his study was horizontal (this was vertical in Babkin *et al.*, 1991 experiments).

The stabilization of flame during the combustion is of great interest because an un-stabilized flame may lead to the condition of lift-off/flash back or quench. Min and Shin [1991] in their investigations extended the flammability limits of propane-air mixture inside a honeycomb cordierite PB which was mainly due to the recirculation of heat to the incoming air-fuel mixture. At flow rates less than the normal burning velocity, flame moved to downstream of the burner which was considered due to the heat loss to the combustor. It was noticed that at higher flow rate and equivalence ratio, flame stabilized fully inside the combustor. Mital *et al.* [1997] studied the flame stabilization phenomena in a reticulated

PB made of cordierite with a silicon-carbide based coating using methane as fuel. They observed the lift off limit between the equivalence ratio of 0.6 - 0.7 and the lean limit (complete extinguishment of the flame) between 0.5 and 0.6, depending on the firing rate. Below a firing rate of 300 kW/m^2, no flashback was observed. It was observed that at flash back condition, the measured laminar flame speed was 5 times greater than the corresponding adiabatic flame speed indicating the rise in flame speed with increase in equivalence ratio.

Flame speed is dependent on structure of the media used. Different media (with different porosity) induces different flow field and hence the flame speed varies. Babkin *et al.* [1991] measured the flame propagation speeds of premixed methane–air mixture. They used different types and shapes of porous media. They found the flame speeds were proportional to the cube of the laminar flame speed and to the square of the mean cell size of the porous media. Koester *et al.* [1994] studied methane-air combustion in a tube open at both ends. They found that the equivalence ratio determined the direction and rate of propagation of the reaction zone within the tube. Korzhavin *et al.* [1997] made experimental and numerical investigations of flame propagation and the dynamics of combustion in the subsonic regime.

The gas phase combustion in porous media, especially at elevated pressures (88.5 - 433 kPa, higher than the atmospheric pressure) and in low velocity regime was studied by Sanmiguel *et al.* [2003]. At an elevated pressure, the width of the combustion front appeared to be small. The maximum temperatures at elevated pressures were lower than those observed for the same mixtures and fluxes at atmospheric pressure. As the operating pressure increased, the combustion front velocity was found to decrease. However, the

observed burning velocity was 40 times higher than the velocity of the same mixture in an open space.

Cho *et al.* [2001] investigated the combustion characteristics of LPG and coke oven gas in a metallic fiber mat. They reported that depending on the combustion rate and excess air, the combustion of premixed fuel could occur in two modes viz. radiant mode and convective mode. In the radiant mode combustion takes place inside the mat, which heats to incandescence. This releases a considerable amount of energy by thermal radiation. In the convective mode a blue flame hovers above the surface of the permeable mat. The region between the fully radiant and blue flame modes was referred to as transient mode.

Thermal performance

The recirculation of heat in the PMC helps in better utilization of fuel and it also allows to burn gas/liquid fuels at very low equivalence ratios. In the following paragraphs, the literature, related to the power output, thermal efficiency, flammability limits and excess air ratios in the PBs are presented.

Xiong *et al.* [1995] examined the combustion stability and heat transfer rate in a PRB made of SiC and Al_2O_3. They found high combustion intensity up to 2.5 MW/m^2 and high heat transfer rate up to 310 kW/m^2. They examined the thermal efficiency of the combustor with SiC and Al_2O_3 and found higher with SiC at higher excess air. This was because the higher emissivity of SiC enhanced the radiation from the porous material to the tube surface. It was also found that in SiC PB, the flame could stabilize over a large range of excess air. On the other hand, at high excess air, Al_2O_3 was found to show lift off behaviour. They also concluded that there was a strong interaction between combustion, combined convective-radiative heat transfer and fluid dynamics within the burner.

Mohamad *et al.* [1994] modelled a combustor made of packed bed with embedded cooling tubes to study the influence of excess air on thermal efficiency. They found that with increase in excess air, the flame gradually shifted to the downstream side of the burner causing a decrease in thermal efficiency. An opposite effect i.e. increase in thermal efficiency and decrease in pressure drop with increase in the particle diameter. Tomimura *et al.* [2004] proposed a new multi-layered gas to gas heat exchanger using porous media and investigated the heat transfer characteristics. For 2 - 5 layers and two types of walls (bare or finned), they conducted a series of experiments for inlet gas temperatures in the range 300 - 700°C and optical thickness in the range 0 - 15.4. The heat recovery section was found to play an effective role in lowering the outer wall temperature and increasing the total heat recovery rate. It was concluded that the optical thickness of about 8 was enough to obtain sufficient total heat recovery rate with finned walls

Hoffman *et al.* [1997] observed a stable combustion against an extremely low equivalence ratio (Φ = 0.026). Premixed fuel-air mixture was allowed to pass from both side of the porous medium and the flow direction was reversed at regular intervals, which represents the half cycle of the system. The effects of flow velocity, half cycle and equivalence ratio on the temperature profiles and CO and NO_x emissions were studied with a re-circulated PRB. They found an increase in the exhaust gas temperature along with the equivalence ratio. The velocity profile was found similar to temperature profiles. The half cycle was found to affect both temperature profile and combustion efficiency. The latter decreased with decrease in the half cycle. The combustible limit was found to improve for a medium having high porosity. Shinoda *et al.* [1998] optimized the design of the burner using the criteria of fractional heat recirculation rate. They found that the fractional heat recirculation rate was almost constant as the equivalence ratio varied, but it was dependent on *Re* and

aspect ratio of the burner. It was also seen that with increase in the number of passes of the burner, there was a minimal increase in fractional heat recirculation rate.

Mare *et al.* [2000] experimentally and numerically analysed the flame structure and extinction mechanisms in the combustion of propane-air and methane-air mixtures. They studied the effects of physical and geometrical properties of the solid porous matrix on the flammability limits for methane-air and propane-air mixtures. Separate solid and gas phase energy equations were used and they were coupled using convective heat transfer between the solid and gas phases. Despite the single step chemistry, a good quantitative agreement between the numerical and experimental results was obtained. They concluded that flammability limit was more sensitive to geometric properties of the porous medium than to physical properties. Their results also confirmed that the flammability limits were independent of properties of the solid porous material.

The flammability limits, longitudinal temperature profiles of the burner in a two-stage gas turbine were found out experimentally and compared with the numerical results by Tanaka *et al.* [2001]. Taking different equivalence ratios, *Re*, diameter of the cylindrical body and keeping the height constant, the burner was optimized for heat recirculation rate and the thermal efficiency.

Shinoda *et al.* [2002] used the experimental burner of Tanaka *et al.* [2001] and evaluated the performance with methane-air mixture. Later, they compared the same with the low calorific value fuel. The experimental results showed that the peak heat recirculation rate of the burner with low calorific–fuel combustion was about one fourth of the value obtained for methane-air mixture. Similarly, the maximum thermal efficiency of low calorific fuel-air combustion was three fourth of methane-air combustion. The thermal efficiency for low

calorific fuel was 45% and that for methane-air mixture it was 60%. Huang *et al.* [2002] experimentally studied the effect of preheating and other operating conditions on SAC and found that a stable combustion required a minimum equivalence ratio and for the initiation of SAC, the preheating of inert porous media must be high enough for stable combustion. With decreasing firing rate, the preheating rate was found to increase. With an increase in operational equivalence ratio, a stable combustion mode was found to exist.

Kamal and Mohamad [2005] investigated the effect of swirl on the combustion efficiency and radiation flux from a non-premixed flame PB by motorizing the burner with variable speed motor (vane rotary burner) and fuelled by natural gas. The radiation spectrum at the burner exit was measured and compared for different swirl numbers. The results presented an enhancement of radiation by 5.7 times with optimization of the gap between the flame base and the base of the porous medium. This improvement was attributed to superior air-fuel swirl mixing. The swirl improved the flame quality greatly as it became highly turbulent and spread more in the radial direction. CO and unburned hydrocarbon emissions were reduced noticeably due to higher mixing rate. NO_x emission decreased to a level below 10 ppm due to the improved heat transfer. Cookson and Floyd [2005] studied the performance characteristics of reticulated open metal foam (FeCrAlY) burner and compared it with ceramic tile burner. The pore size and the porosity of the porous emitter were 420 μm and 95%, respectively. The results revealed that for the same input, the metal foam burner operated at higher temperature than the conventional ceramic tile burner and was more efficient.

Scribano *et al.* [2006] designed a prototype PRB and examined the flame behaviour as a function of burner operating conditions such as *Re*, input thermal power, equivalence ratio and fuel to air momentum ratio. They found that all these parameters had significant effect

on flame length, axial distribution of gas temperature and a homogeneity of radiant tube temperature and pollutant emissions.

Gao *et al.* [2012] investigated combustion on double layer packed pellets of different diameters. They found the stable operating region can be enhanced with the increased diameter of packed pellets. The flame and surface temperatures increased more evidently with increased flame speed for the single-layer burner than for the double-layer one. The flame temperature for the double-layer burner decreased with the increased pellet diameter of the downstream at a fixed equivalence ratio and flame speed. Keramiotis *et al.* [2013] investigated on a porous burner fuelled with a simulated biogas mixture, in terms of thermal efficiency and pollutant emissions. The combustor is a rectangular two-layer porous burner with an Al_2O_3 flame trap and SiSiC foam of 10 ppi. The burner was operated with a mixture of 60% methane and 40% carbon dioxide. Gas and solid phase temperature profiles were measured using thermocouples and infrared thermography respectively. The results revealed wide stability with respect to thermal loads, low NO_x and CO levels.

Byeonghun *et al.* [2013] conducted experiment to compare the emission characteristics and thermal efficiency of different types of porous-media burners. They developed three types of porous-media burners; metal fiber (MF), ceramic (CM) and stainless steel fin (SF) with a commercial heat exchanger and tested for various equivalence ratios and burner capacities. They concluded the smaller the burner porosity was (porosity: SF < CM < MF), the higher the CO emission and the lower the thermal efficiency. Based on the thermal efficiency, turn-down ratio and NOx and CO emissions with respect to the Korean industrial standard and European norms, the most appropriate burner type for the condensing boiler is the MF burner.

Radiation output/ efficiency

Radiation efficiency is the measure of radiation output at the exit of the burner to the input power. Radiation output depends on various parameters like optical thickness, extinction coefficient, scattering albedo, and thermal conductivity of the solid medium, heat transfer coefficient between the gas and solid phase and dimensions of the fibrous porous media. It is recognized as one of the most important parameters to estimate the thermal performance parameters of PB. It is dependent on firing rate, equivalence ratio, flame support layer thickness, flame position, temperature distribution and porosity of the material.

Mital *et al.* [1997] measured the thermal efficiency with two different thicknesses of flame holder. It was found that, at a specific power and equivalence ratio, the thermal efficiency is higher in case of 3.2 mm than 6.5 mm. They pointed out the effects of other factors viz. flame position and resultant temperature distribution on radiation output. Barra and Ellzaey [2004] studied the effect of equivalence ratio and flame speed on radiation output. It was also found that the radiation output efficiency increases with decrease in equivalence ratio but the actual quantity of radiation was lower than at higher equivalence ratio. The flame speed decreases with the increase in equivalence ratio. The actual flame speed was at a low of 2 times the adiabatic flame speed due to the recirculation of heat to the downstream section of the burner because the total heat release rate at is very low at lower equivalence ratio. The results were in consistent with Khanna *et al.* [1994]

It has been found that for similar operating conditions, there is a wide variation (15 - 50%) in radiation efficiency reported by different researchers. This variation is attributed to the lack of a standard methodology. To partially overcome this problem, Mital *et al.* [1998] proposed a standard procedure. Later, this method was adopted by Leonardi *et al.* [2002]

for measurement of combined (radiation plus convection) efficiencies for metal fiber (Fecralloy-Acotech, EN29001) burners. Experimental data were reported for a range of firing rates at three different equivalence ratios. It was found that the burner surface temperature and exit temperature increased with the firing rate and was higher for the double layered fiber pad than for a single layered pad. The radiation efficiencies measured for a double layered pad were about 5% higher than single layered pad. The radiation efficiency was found to increase with equivalence ratio and power. Abdelaal *et al.* [2013] investigated the combustion in porous inert media with mullite as a burner and LPG as a premixed fuel with air to show the effect of equivalence ratio and firing rate on the radiation efficiency, surface and exhaust gas temperatures. They achieved radiation efficiency up to 45%. The improvement of the burner performance, using oxygen enriched air was explored. The oxygen in the combustion air was increased up to 25%. The experimental results showed that the radiation efficiency of the burner was increased noticeably with increasing oxygen concentrations in the combustion air. The surface temperature also increased, though the exhaust gas temperature decreased.

Emissions

There is a comprehensive literature available on the emissions of PMB. Some of the most important are discussed below. Goeckner *et al.* [1992] used the radiant tube burners with porous ceramic inserts with natural gas as fuel. NO_x was found to reduce by 30%. Temperature distribution along the burner axis was found uniform. Hoffman *et al.* [1997] made a exhaustive study of CO emissions and found it to be strongly dependent on the operating conditions along with the type of the porous media. They found an extremely low level of NO_x (1 ppm) in the operating range. Xiong *et al.* [1995] conducted an experimental study on 60 kW bench-scale porous matrix combustor heaters with two rows of water

cooled tube coils. They reported ultra-low emissions. NO_x and CO were less than 15 ppm and total hydrocarbon (THC) was less than 3 ppm.

Mital *et al.* [1997] measured the emission indices of CO, HC and NO_x. They found the CO and HC pollution indices were relatively low, CO: 0.1 - 3.6 g/kg and HC: 0.1 - 1.2 g/kg. CO and HC emissions were found to decrease with decrease in equivalence ratio and increase in the firing rate. NO_x emission was found relatively low, 0.1 - 0.35 g/kg. It was found that the NO_x emissions had decreased with decrease in equivalence ratio, but increased with increase in the firing rate. The decrease in emission was attributed to higher energy release per unit area and to an increase in preheating at the higher firing rates. Suzukawa *et al.* [1997] developed an experimental burner for the industrial purpose and was able to reduce NO_x level by 50% compared to the conventional low NO_x burners.

Scribano *et al.* [2006] investigated the emission characteristics of self-recuperative radiant tube burner fuelled with natural gas in non-premixed mode. NO_x was found to reduce with intense exhaust gas recirculation. They suggested a new design to recirculate exhaust gas to CZ and found 50% reduction in emissions for a wide range of power 12 - 18 kW and equivalence ratio of 0.5 - 0.8. CO emission was also found very low. Keramiotis et *al.* [2012] developed two-layer rectangular porous burner with an Al_2O_3 flame trap and SiSiC foam of 10 ppi. They operated the burner with methane and LPG both as a fuel. They measured NO_X and CO along the axis of burner.

2.2.2 Numerical investigations

Flame stabilization

Like experimental studies, the stabilization phenomenon of flame within the porous medium has also been studied analytically and numerically by many researchers. For a

given equivalence ratio and a range of flow rates, the flame can stabilize at different locations within a porous medium [Sathe *et al.*, 1989a; Hsu *et al.*, 1993a; Sathe *et al.*, 1989b]. Buckmaster and Takeno [1981] defined the conditions for blow-off and flashback. They found that the flame stabilization depended on some parameters like flow velocity, heat transfer coefficient and the thermal conductivity of the porous matrix. Their results also confirmed the dependency of combustion location and upstream internal heat transfer and vice versa. Chen *et al.* [1987] studied the effect of thermal conductivity, volumetric heat transfer coefficient and exit boundary conditions on temperature and flame speeds in the 1-D porous medium without considering the effect of radiation. The flame speed was found to reduce when the volumetric heat transfer coefficient reduced below 10^7 W/m^3-K and a significant difference between the solid and gas temperatures were observed. The temperature profile was not affected when the thermal conductivity was varied from its value for air to that of pure zirconia. A little effect was found on temperature profiles. However, due to increased preheating of gas through the upstream conduction from the flame front, a significant effect on the flame speed was observed.

Yoshizawa *et al.* [1988] applied a 1-D two-phase model with single-step kinetics and analysed the effect of radiation on the structure and behaviour of the premixed flame in the porous medium. They found that the temperature profiles and burning velocities were highly dependent on radiative properties, especially absorption coefficient of the porous medium. The burning velocity, flame thickness and gas phase temperature were highest when the reaction zone was close to the centre of the porous medium. An increase in absorption coefficient caused not only an increase in the optical thickness of the reaction zone, but also an increase in the surface area of particles leading to an increasing role of the inter-phase heat transfer and an accompanying decrease of the maximum temperature and

burning velocity, and increased thickness of the reaction zone. The temperature and flame speed increased with the increase in the thickness of the medium along with decreasing reaction zone thickness keeping absorption coefficient constant. Yoshizawa *et al.* [1988] and Sathe *et al.* [1989b, 1990a] found that with increase in porosity, the flame velocity increased owing to increased conduction and radiation.

Sathe *et al.* [1989a] studied the flame behaviour of methane, in the equivalence ratio range of 0.55 - 0.6. From their study, they concluded that depending upon the firing rate; flame could be stabilized at two different regions. One at the interface of the two porous zones (PZ and CZ, refer to *Fig.*), and second one at the region before the exit plane of the combustion zone. However, the best radiant output could be obtained if the flame was located near the burner centre. They also reported that near the edge of the porous matrix, the flame speed variation was controlled by conduction, whereas radiation became a contributing factor for flame propagation in the interior. Later, the stabilization of flame at two different locations was confirmed by Hsu *et al.* [1993a].

Hanamura and Echigo [1991] studied the detailed temperature profiles, reaction rates and energy balance of methane air combustion in the equivalence ratio range Φ = 0.55 - 0.66. With increase in equivalence ratio, the flame position was to found to locate near the porous plate. The flame blew off at an equivalence ratio Φ = 0.66. It was found that with decrease in mass flow rates, the flame moved upstream of the PB and the temperature of the porous zone was increased. Kendall *et al.* [1992] also investigated the flash back phenomena in two different types of porous media viz. reticulated ceramic foam and packed ceramic fiber. The packed ceramic fiber was found to be least prone to the flashback as its inner surface temperature was low and the reticulated ceramic foam was found the most prone to flashback, as it conducted heat more effectively to upstream.

Sahraoui and Kaviany [1994] found that the flame speed was strongly affected by the geometry of the porous medium. With decrease in pore size, the flame speed was found to increase. Their conclusion was based on the result of their 2-D direct simulation of the PB consisting of either discrete or connected square cross-section element and using single step chemistry. The same group formulated one more model using volume averaged properties. With that model, they were able to predict the flame speed, but not the local super-adiabatic temperatures in the gas phase. Escobedo and Viljoen [1994] used a 1-D model with single-step chemistry and found that for a given equivalence ratio, with increase in the heat transfer coefficient, the range of stable flow rates of fuel-air mixture increased. Kulkarni and Peck [1996] studied the effect of extinction coefficient in a double-layered burner and they found that increase in upstream extinction coefficient resulted in decrease in effective flame speed.

Zhdanok *et al.* [1998] numerically studied the flame localization inside an axis-symmetric cylindrical and spherical PB. The main advantage with these configurations was natural stabilization of combustion front in the medium due to decrease in the filtration speed and the heat loss from the flame across the radius. They also found dependency of heat losses at the outer boundary of the burner on the fuel flow rate, heat content of the mixture and the external radius. Combustion front localization showed a dependency on the ignition radius. The burner was found to have a narrow combustion region in case of low calorific value fuels and at limited flow ranges.

To stimulate the flow in a 3-D porous structure, Yamamoto *et al.* [2005] used the Lattice Boltzmann method. They solved distribution functions for flow, temperature and concentration fields and compared them with the empirical correlations. Both were in good agreement. The porous structure considered was Ni-Cr metal obtained by the 3-D computer

tomography technique. Their objective was to improve the design of diesel particulate filter for diesel powered vehicles. An inhomogeneous flow was observed in regions where local temperatures were high. The information was considered to be vital for better design of diesel particulate filter. The simulation was also helpful in better understanding the soot combustion.

In all the above numerical simulations, the reaction zone thickness was assumed negligible. With two-temperature approximation, Bubnovich and Toledo [2007] analytically studied the thickness of the reaction zone. They provided analytical solutions for three different zones: PZ, reaction zone and the zone occupied by combustion products (CZ). The thickness of the reaction zone was found to be 9.16 mm. They compared their analytic results with those of the numerical simulation and a good agreement was found.

Thermal performance

Yoshida *et al.* [1990] analysed transient characteristics of combined conduction, convection and radiation heat transfer in a homogenous porous medium. They validated their results with experiments. With decrease in gas velocity, the time constant of the system was found to increase and it varied widely in the porous medium. The transient response was much faster at the entrance of the porous medium than at its exit. As a result, the net radiative heat-flux at the entrance of the porous medium reached steady state fast. Hsu *et al.* [1993b] numerically studied premixed methane-air combustion in a double layered PB. The burner consisted of two cylinders of the same length and diameter but with different pore sizes stacked together and insulated around the circumference. The simulations were performed for equivalence ratio in the range, $\Phi = 0.1 - 0.43$. The predicted lean limits were lower than

the limit for a free laminar flame. The maximum flame speed occurred close to the exit plane.

To predict the thermal efficiency, flame location, temperature distribution and pressure drop, Mohammad *et al.* [1994] used a 2-D model for matrix stabilized PMC with single-step kinetics. They predicted the possible amount of excess air, firing rate, pore size, geometry, for a range of design and operating parameters and system configurations. They compared their numerical results with available experimental data and found $\pm$ 15% variation. Hayashi *et al.* [2004] proposed a 3-D modelling of a double layered porous media. Their model was valid to operate in the range of 5 - 20 kW and considered a mixture of air and fuel (a blend of fuel-oil and vegetable oil) for domestic heating. The range of equivalence ratio was 1 - 1.8. They applied a single-step mechanism for describing combustion in the porous media and n-heptane was considered to model the actual fuel. Their work mainly aimed at a better understanding of the PMC to develop efficient household combustion systems. For most of the operating conditions, the flame was found to stabilize at the interface of the two layers. But the exceptions were found at the low power and excess air conditions for which it was suggested to reduce the pore size of the bottom perforated plate.

A comparison of gas phase reactions using single-step and multi-step kinetics was made by Hsu *et al.* [1993b, 1991b, 1991a]. It was observed that the consideration of single-step kinetics in the PMC modelling provided similar results as that with the multi-step kinetics for lean mixture. In case of models with single-step chemistry, the reduced accuracy in predicting the reacting flow was counterbalanced by lower levels of uncertainties in the heat transfer coefficient, turbulence, etc. than the model with multi-step kinetics. Hsu *et al.* [1993c] developed a 1-D model wherein they considered both the single step and multi-

step chemical kinetics. They concluded that it is necessary to use multi-step kinetics only if accurate predictions of temperature distribution, energy release rates are desired. Their model was able to predict CO emissions accurately and over predicted NO.

The previous investigations [Weinberg, 1971; Sathe *et al.*, 1989a; Xiong, 1991] provided the qualitative information about the heat recirculation and the conduction and radiation modes of heat transfer in the PMC. However, there was no quantitative information. Using 1-D transient formulation with complete chemistry of methane combustion, Barra and Ellzey [2004] numerically quantified heat recirculation, radiation efficiency, solid conduction, and solid-solid radiation and flame speeds at different stable conditions. For better understanding, for equivalence ratio in the range 0.55 - 0.9, the above parameters were non-dimensionalised. High heat recirculation efficiency (ratio of solid-gas convection in preheating zone to firing rate) was observed for a high flame speed ratios (ratio of effective flame speed to laminar flame speed) at lower equivalence ratio. Solid conduction as well as solid-solid radiation was found to be important for heat recirculation efficiency. The radiation efficiency for preheating at high equivalence ratio was more than conduction efficiency at low equivalence ratios. The non-dimensional exit temperature was almost constant at equivalence ratio Φ = 0.9. The radiation efficiency was higher at lower equivalence ratio but the magnitude of radiation was less when compared at higher equivalence ratios. The variation in the length of the burner had no effect on the amount of heat recirculation as well as on conduction and radiation.

Leonardi *et al.* [2003] and Chen [1987] made an extensive investigation to study the effects of the volumetric heat transfer coefficient, solid matrix emittance, effective thermal conductivity, extinction and scattering coefficients as well as firing conditions on the thermal performance of the PB.

Radiation output/ Radiation efficiency

Many researchers have recognized the importance of radiation in the PMC. An initial contribution towards the development of mathematical model accounting radiation was attributed to Echigo *et al.* [1986]. Due to unavailability of the exact thermo-physical and transport properties, they made simplified assumptions and used arbitrary property values along with single-step kinetics. They did not consider any reaction at the exit of the porous medium. Later Echigo and his co-researchers [Echigo, 1991; Yoshizawa *et al.*, 1988; Echigo *et al.*, 1986] studied the exchange of energy within a highly porous medium due to conduction, convection and radiation. In early experimental and numerical works, Echigo *et al.* [1982, 1986] found that the heat re-circulated in the upstream direction through the metal mesh screen was approximately 60°C higher than the downstream. Upstream temperature was found to increase with increasing the optical thickness. The effect of radiation was noticed due to high temperature drop across the screen. They also reported that the lean flammability limits was extendable in the experimental burner made of porous ceramic plate enclosed in a permeable cylinder of stainless steel mesh. However, they did measure the radiation efficiency. Tong and Sathe [1988] performed a parametric study for a fibrous porous medium and considered the effect of absorption, emission and isotropic scattering. Solid conduction and scattering of radiation were observed to have a significant influence on radiation output, while the gas conduction had a negligible effect on burner's performance.

Tong *et al.* [1987] also discussed the dependency of the size of the porous fiber on radiation output. They performed 1-D analysis of porous PRBs having sub-micron size fiber of silica and alumina. They found that with reduction in fiber diameter, the single scattering albedo was reduced and this led to increase in radiation output. They also found a rapid increase

in radiation output when the diameter of the fiber decreased below 1 mm. At a temperature of 1000 °C, for a fiber of approximately 0.2 mm, the radiation output was found to increase to 65 % and 109 % for silica and alumina, respectively as against the reference case of 0.5 mm fiber diameter. The same group of authors [Tong and Li, 1995] numerically showed that the radiation output increased with optical thickness, for low conductive and low scattering albedo materials. A similar study was undertaken by Andersen [1992] and Baek [1989]. They studied the effect of fiber size of porous ceramic on radiative output. It was found that fiber diameter of less than 1.0 mm produced significantly higher radiant output. For a temperature of 1500 °C, the output increased by 72 % for the silica and 150 % for alumina materials. Yoshizawa *et al.* [1988] pointed out the relevance of the absorption coefficient and total optical thickness in calculating temperature profiles, radiant energy density and the position of the flame within the PB. They found that with decrease in absorption coefficient, the maximum temperature increased, the size of the reaction zone decreased and its position shifted upstream. An optically thick porous layer maximized radiant output and a highly scattering porous media ensured more homogenous solid temperature distribution [Chen *et al.*, 1988; Shinoda, 2002; Kulkarni and Peck 1996].

Sathe *et al.* [1990b] investigated the radiation efficiency of the porous PB and found the same in the range of 26 – 40 % when the flame stabilized in the upstream half of the porous medium. Sathe *et al.* [1989, 1990a] concluded that the best radiation efficiency was achieved if the flame stabilized at the centre of the burner having an optical thickness of about 10 and low scattering albedo, low solid thermal conductivity and high heat transfer coefficient. The results were in good agreement with the experimental results of Sathe *et al.* [1990a], which used lithium-aluminium-silicate foams with methane as fuel. At the lean mixture conditions, with shifting of flame to the surface, Leonardi *et al.* [2003] found a drastic drop in the radiation efficiency of the burner.

Singh *et al.* [1991] observed that low scattering albedo improved radiation efficiency due to high absorption. They concluded that for better performance, one should choose a porous material which possesses neither a very high nor a very low scattering albedo. Lim [1997] concluded that increasing the scattering albedo in the post-flame region of a two layer PB resulted in an increase of the gas and solid temperature in the post flame zone. However, increasing scattering albedo at the pre-heating zone resulted in lowering the peak- and post-flame temperature. Malico and Pereira [2001] did a study on the influence of radiative properties on flame speed, temperature distribution etc. They found that increase in extinction coefficient caused in a higher post-flame temperature gradient, improved heat transfer to pre-flame zone and a reduced peak temperature.

Kulkarni and Peck [1996] made a numerical study on a 5 cm long double layered PB. They investigated the effect of porosity, length, extinction coefficient and albedo on radiant output from the burner. They concluded that for maximization of radiation output, the upstream layer of PB should have lower porosity, higher scattering albedo, shorter length and higher optical thickness than the downstream section. Further, the downstream section should be non-scattering. For the downstream section, they found the optimum extinction coefficient ranged 1 - 2 cm^{-1}. They concluded that the optimization of extinction coefficient was important because large extinction coefficient (large pore diameter) resulted in insufficient radiation to pre-heat the mixture. Similarly, smaller extinction coefficient (large pore diameter) resulted in spreading of radiation over a large distance. Barra *et al.* [2003] also studied the effect of material properties on stable operating range of the double layered burner. In their model, they kept the scattering albedo constant and varied the extinction coefficient. The optimized extinction coefficient for the downstream section was found to be 2.6 cm^{-1}.

To overcome the limitations of the 1-D models, Sahraoui and Kaviany [1994] considered the 2-D direct numerical simulation using single-step kinetics without radiation. They considered combustion in a porous medium consisting of discrete or connected square cylinders arranged in-line or staggered. The same was compared with the model based on volume averaged properties. The results showed that the direct numerical simulations predicted the flame speeds more accurately.

Tong and Li [1995] made a theoretical study to examine the effect of the fiber coatings on the radiation output. The burners made of coated silica fibers were considered along with the coatings of silicon carbide, graphite and platinum. It was found that silicon carbide coatings resulted in minimal enhancement. Both graphite and platinum coatings provided significant enhancement in the emittance by a factor of three and six at the mean temperature of 1000 K and 1500 K, respectively.

Hackert *et al.* [1999] examined a honeycomb geometry consisting of many small parallel plates. Their model gave quantitative temperature distribution, flame velocity and interfacial heat transfer. Nevertheless, it could not predict detailed effects of process in the flame. In their study, they found that with an increase in wall emissivity, the burning rate and radiation output increased. Talukdar *et al.* [2004] analysed heat transfer in a 2-D rectangular PB taking into account the effect of radiation effect. The non-local thermal equilibrium between gas and solid phases was considered. It was found that the radiant output decreased if the emissivity of the top and the bottom boundaries of the burner increased. They further observed that in the transient state, with the passage of time until the steady state, when the solid temperature became very high, both radiative and convective fluxes increased.

For the purpose of uniform heating, consideration of directional radiative behaviour of heating devices is important. To study the parameters affecting the directional radiative behaviour, Li *et al.* [2005] developed a model for a gas fired porous PB having a bundle of reflecting tubes. The energy equations were solved by the finite volume method and the radiative source terms were computed using the Monte Carlo method. They found a need for a trade-off between the radiation efficiency and uniform radiative heating of the object.

In order to analyse the thermal characteristics of porous burners, Keshtkar et al. [2009a] numerically solved the coupled energy equations for the gas and porous medium in steady condition. They used the discrete ordinates method to compute the radiative information. In another work heat transfer analysis of a cylindrical porous radiant air heater under the influence of a 2-D axisymmetric radiative field was carried out by the same authors [2009b]. In order to determine the thermal characteristics of the proposed porous radiant air heater, a two-dimensional model was used to solve the governing equations for porous medium and gas flow and DOM (discrete ordinates method) was used to obtain the distribution of radiative heat flux in the porous media.

Emissions

Bouma and Goey [1995] studied combustion of a lean premixed methane air mixture stabilized in a ceramic foam burner. The combustion model was formulated using 15 species, including the chemistry of NO_x formation. It was shown that in radiant mode operation, the flue gas temperature was considerably low and hence the emissions of CO and NO_x were found lower compared to blue flame mode. Hsu and Matthews [1993c] did a numerical study to predict concentrations of different constituents of the exhaust gas and

compared the same with the experimental data. At lower equivalence ratio, due to low flame temperature, NO_x concentration was found low.

To study the emissions from a 2-D PB with integrated heat exchanger, Malico *et al.* [2000] incorporated the detailed kinetic mechanism in their previous model [Malico and Pereira, 1999]. The results were compared with the experimental data reported by Durst and Trimis [1996b]. It was found that CO emissions were under predicted and NO emissions were over predicted, especially for richer mixture. This observation was similar to Hsu and Matthews [1993c] results. Their results also revealed that with increase in solid conductivity and heat transfer coefficient between solids and fluids, the peak temperature was lowered and hence the NO emission was also low. However, an increase in the extinction coefficient did not show an obvious effect on NO emissions.Brenner *et al.* [2000] used pseudo-homogeneous heat transfer and flow model for the porous material to study the combustion behaviour and also the predictability of the code. Al_2O_3 and SiC lamella were considered as porous mediums. The model was found difficult in simulating the conditions of flame stabilization between the combustion and preheating zones where most of the NO_x formed. Hence the NOx prediction was not accurate. Their results showed a better radiant output and low CO emissions in the case of SiC.

2.3 Applications of porous medium burner

Owning several advantages, the applications of the PBs are extensive. They are used both in industrial and in domestic sectors. Gas fired PBs are used in a number of manufacturing processes such as paper drying, paper finishing, powder and paint curing, baking, textile drying, polymer processing, etc. They are also used in household air and water heating system, IC engines (pre-heaters of vehicles), gas turbine combustion chamber, steam

generator and electricity generation. Some of the important applications of the PB are discussed in the following sections.

2.3.1 Domestic applications

Jugjai and Rungsimuntuchart [2002] implemented the idea of the PMC in a LPG cooking stove for improved efficiency. In doing so, they proposed a new concept named as semi confined porous radiant re-circulated burner (PRRB) where the primary air was preheated to higher temperatures than CB. With the former, they could achieve 12 % higher thermal efficiency than the 30 % for the CB, and with the latter, it was just double the CB. This led to an energy saving of around 50 %. The NOx and CO emissions were found significantly low in the PRRB (SB) than PRRB (CB). But, they have not used the porous burner for combustion zone.

Qui and Hayden [2006] designed and fabricated a PB made of fiber felt along with a recuperator using natural gas. The main objective was to study the performance of the existing gas-fired lanterns equipped with porous medium. The different modes of combustion in the fiber felt, performance at various operating conditions and the effect of heat recuperation were studied. Flame stabilized in the porous ceramic fiber felt was found to be strongly dependent on the firing rate and excess air ratio. The stable flame was obtained in the range 16 - 54.5 W/cm^2. The effect of recuperation was also considerable. The light output was measured and it was found to increase with combustion air temperature

Patangi *et al.* [2007] investigated the efficiency, emission and energy cost for the conventional domestic LPG cooking stoves with and without the usage of various porous media likes metal balls, pebbles and metal chips. With the usage of porous media, they

investigated energy cost analysis and showed a saving of about 10 % and the ppm of CO was found to decreases from 225 to 118. Pantangi *et al.* [2011] studied the applicability of PRBs in domestic LPG cooking applications. They investigated the thermal efficiency and emission characteristics of two layered Porous Radiant Burners at various equivalence ratios and thermal loads. Result showed that maximum efficiency of the PRB was about 68 % and measured CO and NO emissions were significantly low in PRB than the conventional LPG cooking stoves. They also investigated the effect of burner diameter on the thermal efficiency of the PRB and found that increase in the diameter of the burner from 6 cm to 9 cm increase the efficiency from 55% to 68%.

Muthukumar *et al.* [2011] tested the performances of a SiC based PRB (80 mm diameter and 90 % porosity) used in LPG cooking stove. They studied the performance of the burner at different equivalence ratios and power intensities. The results showed that the maximum thermal efficiency of the PRB was about 71% at 1.24 kW, equivalence ratio of 0.68 at an ambient temperature of 31 °C. They also observed that CO and NOx emission of PRB was very low compared to the CB. They investigated influence of ambient temperature on the thermal efficiency of the PRB.

Mujeebu *et al.* [2011] developed two compact premixed LPG burners based on submerged and surface combustion modes in porous medium. They compared combustion and emission characteristics of these burners with the CB. For a thermal load of 0.62 kW, they found the thermal efficiency of submerged and surface combustion burners as 59 % and 71 % respectively.

Yoksenakul and Jugjai [2011] developed a self-aspirating, porous medium burner (SPMB) with the packed bed of alumina spheres. They used the same mixing tube and the same fuel

nozzle as used in CB. They found stable combustion in the firing rate range from 23 to 61 kW. Burner performance and combustion characteristics of SPMB were done in terms of temperature profiles along the axial direction of the packed bed, emissions of CO and NOx at the burner exit and they also calculated radiative heat loss and radiation efficiency.

Muthukumar and Shyamkumar [2013] optimized the PRB. They found the thermal efficiency of PRB was 75 %. For a given wattage of 1.7 kW and equivalence ratio of 0.54, the efficiency of PRB was found to decrease from 75% to 71% when the porosity of PRB decreased from 90 % to 80 %. Thermal efficiencies of all the tested PRBs gradually decrease with increase in the equivalence ratios and power intensities. Stable combustion of the burner is possible in the equivalence ratio range 0.52–0.7. Emission indices of all PRB were lower than conventional domestic cooking stoves.

Boggavarapu *et al.* [2014] have worked on the thermal efficiency and emission improvements in the LPG conventional cooking stoves. They introduced a radiation shield in the conventional LPG cooking stoves and reported 3% improvement in thermal efficiency. By modifying the nozzle dimensions, Basu *et al.* [2008] reported about 3 % improvement in the thermal efficiency of the conventional LPG cooking stoves. However, both the work has been carried out for conventional porous metal burner based on free-flame combustion.

2.3.2 Gas turbines and boilers

Tanaka *et al.* [2001] explored the possible application of the PB in the combustor of the second stage of the chemical gas turbines developed by Arai *et al.* [1999]. The aim of their investigation was to utilize the unused chemical energy of the exhaust in the second stage combustor equipped with porous medium, so that the flammability limits would widen and

thermal efficiency be improved. For this, they optimized the burner in terms of chemical, fluid mechanical and geometrical parameters using thermal efficiency and heat recirculation rate as the criteria. From their results, they concluded that use of the porous medium in the chemical gas turbine would be a good choice.

Delalic *et al.* [2004] successfully used porous media heat exchangers as an integral component in the low temperature (condensate) boilers. The results showed a better heat exchange efficiency and combustion stability. The thermal efficiency was found to be higher than 95% for both 5 kW and 9 kW burners at different excess air-ratios. It was possible due to the fact that a part of the latent heat of the water condensation from exhaust gas was transferred to water in the heat exchanger. NO_X and CO_2 emissions were low due to improved energy efficiency. The system was found to be applicable for central heating system also.

2.3.3 Fuel cell and hydrogen production

Mjaaness *et al.* [2005] experimentally investigated the possible use of the PMC as a reformer in the fuel cell. They used PBs of two types: double layered alumina foam and double layered alumina beads to convert methanol, methane, octane and automotive grade petrol for the generation of hydrogen which is used in the fuel cell. The experiments showed that the alumina beads had long lifetime than foams and the conversion efficiency of the burner was also high.

In the recent past, Raviraj and Janrt [2006] did an experimental study with an aim of achieving higher conversion efficiency along with the parameters affecting the conversion efficiency. They could achieve 65 % net conversion efficiency for a particular equivalence

ratio and inlet velocity of the methane. For better conversion efficiency, they suggested low specific heat and low thermal conductivity porous media.

2.3.4 Furnaces, process and IC engines

With an objective of heat transfer enhancement, Zhang *et al.* [1997] proposed a novel application of PB in a partially bypass flow system. They assumed hydro-dynamically fully developed and thermally developing laminar flow inside a circular duct incorporated with porous core in which heat was transferred from high temperature gaseous medium to a heat absorbing wall. The numerical results showed that the use of porous medium was very effective to enhance both convective to radiative heat transfers. The system was found suitable for a gas medium having a weak emittance, lower wall temperature and low velocity.

Liu and Hsieh [2004] conducted experiments in the PBs using the LPG under steady-state and transient conditions. In their experiments, they introduced cooling tubes in the post flame zone to recover the maximum heat used to preheat the incoming air–fuel mixture unlike conventional PMC. The heating of working fluid passing through the cooling tubes has found many applications such as in water and air heaters, boilers and chemical processes. A particular phenomenon called metastable combustion (having single flame speed at a particular equivalence ratio) was observed due to the changes of heat balance in the burner. It was also observed that the metastable combustion ceased during transient state and drove the flame out of the packed bed. The CO and NO_x emissions were also reported for the particular burner.

Kesting *et al.* [1999] developed a high temperature staged Oxy-fuel PB. The main aim was to succeed in keeping the temperatures of the radiation burner below the known material

limits (< 1800 °C), although pure oxy-fuel combustion was realized, which normally yields to very high temperatures (> 2800 °C). They found that the burner could be operated at nearly stoichiometric condition without reaching very high combustion temperature. This was made possible by adjusting the radiant surface of the burner in such a way that the necessary heat could be transferred by radiation. With continuous staged combustion, the radiation output was controlled and a better heat recirculation was achieved. The radiation efficiency of the burner was found higher and the temperature within the CZ was homogenous. The emission was low and hence it was identified as ultra-low emission burner. The burner is mainly aimed at glass melting furnaces, surface treatment, and metal treatment.

Mo¨ßbauer *et al.* (2001) designed and tested a compact ultra-low emission steam engine based on PMC technology for automotive application. The prototype showed a possible application of PMB to the current car engines along with the steam generator which can offer advantages over the state-of-the art existing technologies. Durst and Weclas [2001] first applied PB technology to the diesel engines. Weclas [2005] explored the application of the PMC in IC engines and he found improvements in many respect. The main benefit was the reduction of NOx and elimination of soot. The combustion was found homogeneous and flameless. The media was found effective to control gas flow, fuel injection and its spatial distribution, vaporization, homogenization, ignition and combustion. The investigations showed encouraging results.

2.3.5 Combined heat and power generation and miscellaneous applications

The idea of combined heat and power with the PMB was put forward by Echigo *et al.* [1993, 1994, and 1995] and a system was developed by Hunt *et al.* [1994, 1995] for hybrid electrical vehicles. PMB is also taking its place in thermo-photovoltaic power generation [Qui and Hayden, 2007]. The usage of PMB in combination with solar water heaters for home and commercial heating was studied by Avdic [2004]. In the near future the PMB will be the most prospective ingredient for combined heat and power generation. Very recently, few researchers have focused on micro and meso-scale applications of PMC technology [Marbach and Agrawal, 2006; Marbach *et al.*, 2007; Li *et al.*, 2008; Sadasivuni and Agrawal, 2009; Kamijo *et al.,* 2009]. Dobrego *et al.* [2005, 2006, and 2007] made a remarkable contribution by eliminating highly polluting volatile organic compounds (VOCs) such as formaldehyde, benzole, asphenol, acetone etc; through oxidation in PMB. Ismail *et al* [2013] investigated the application of porous medium burner (PMB) with micro cogeneration system. They fixed Thermoelectric (TE) cells with the PMB constituted the cogeneration system. The TE cells attached to the hexagonal walls absorbed the heat of combustion. A mobile phone was coupled to the TE charger system to demonstrate the ability of the cogeneration system to generate electric power. They showed that the PMB can be used for heating and cell phone charging.

2.4 Porous surface combustion

As discussed earlier the flame is stabilised on the surface of the porous matrix not more than 1 mm. The hot gases from the combustion heats up the porous matrix and then the surface starts radiating. The initial work in this direction were carried out by Bone [1912], Lucke [1913], and Hays [1937]. The first notable numerical contribution in this direction

was by Hanmura and Echigo [1991]. They explained the detailed behaviour of the flames in the surface burners with respect to time for understanding the stabilization mechanism along with the three critical limits for blow-off, flash back and extinction associated to the flame velocity, flame structure and thermal radiation propagation.

Williams *et al.* [1992] conducted the experimental investigations on surface combustion with methane and air premixed mixtures inside and close the downstream of the porous matrix. The maximum rate of heat release was found at or above the surface of the porous matrix. The major contributor in the formation of NO_x was prompt NO. Itaya *et al.* [1992] and Nakamura *et al.* [1993] observed a steady flame in methane air combustion over a porous ceramic plate in an open atmosphere. The ceramic plate was found to act as a flame holder. Nakamura *et al.*[1993] studied the methane–air premixed combustion on the surface of the combustions and found that the maximum height the flame should be stabilized is 1 mm for better balance between the velocity of the combustion and gas flow to avoid flash back. The temperature on the surface was found proportional to the thickness of the porous matrix because the air-fuel mixture will have enough time to preheat to high temperatures. The peak surface temperature reaches at a particular thermal load and after that the flame gradually detaches from the surface and the surface temperature starts decreased. Itaya *et al.* [1994] also made study on surface combustion of methane and air on a porous ceramic plate in a cylindrical furnace. They found extension of lean flammability limit and higher temperature of ceramic plate owing to the higher thermal radiation from the furnace wall.

Bouma *et al.* [1995] and Bouma and Goey [1999] studied the porous surface combustion experimentally and numerically. The formation of major CO and NO were studied in detail. The levels of both the emissions above the porous matrix surface at different heights were illustrated. Both the experimental and numerical results were in good agreement. To predict

the CO emission more accurately, the authors suggested having gas radiation in the modelling. It was found that, prompt NO as well as thermal NO was important for the prediction of the total NO. Lammers and Goey [2004] studied the effect of gas radiation experimentally and numerically on the surface temperature decrease on the porous surface burner and inturn the emissions.

Jugjai and Sawananon [2004] studied a surface combustor heater coupled with a heat exchanger, with a new concept of cyclic flow reversal combustion for residential and commercial complexes, steam super heaters and thermal fluid heaters of industrial applications. The authors claimed that, the proposed concept could provide the basis for development of state-of-the-art technology for new versions and more advanced thermal systems, such as highly efficient ultra-low-pollutant-emission boilers, for efficient utilization of energy. Both interior and surface combustion processes using silicon carbide-coated, carbon - carbon composite porous media were investigated by Marbach and Agrawal [2005], and Nemoda *et al.* [2004]. Outcomes confirmed PMC as an effective method to extend the blow-off limit in lean premixed combustion. Recently, Marbach *et al.* [2007] presented a numerical study of heat recirculation in an annulus around a surface combustor made of silicon carbide-coated carbon foam. The proposed model was validated for methane combustion in chamber volume of 0.364 cm^3 and overall system volume of 1.5 cm^3. Experiments were conducted for reactant flow velocities varying from 0.25 - 1.0 m/s in the equivalence ratio range of 0.50 - 0.80. Results showed an excellent agreement between measured and computed temperature profiles at different reactant flow rates. The proposed combustion system design achieved a significant reduction in the heat loss as compared to the baseline design tested experimentally.

2.5 Literature closure

Due to some undesirable features such as sharp temperature gradient, thin reaction zone, large sized combustor, low power density, low power modulation range, low efficiency and high level of pollutant emissions associated with combustion devices based on free flame technology, the need for combustion inside an inert porous medium which addresses the above problems are discussed. A brief history of research and developments in the PMC is provided. It is found that till date, the actual conditions governing the excess enthalpy flame generation have not been clearly specified. This leaves a scope to further study the actual parameters affecting it and hence, research is still underway to have a better understanding of the complete phenomena.

The results of various studies on flame stabilization phenomena within single as well as double layered PBs are reported. It is observed that the flame is found to stabilize even at low equivalence ratio due to heat recirculation. Heat recirculation is the heat transfer in the PRB from downstream section to upstream by the radiation and conduction. Flame stabilized at the upstream section of the centre of the single layered and at the interface of a double layered PB provided better performance. The flame speed was found higher than the laminar flame speed that helped in enhancing the degree of preheating of the incoming air-fuel mixture. However, the flame stabilization phenomenon for low calorific fuel is still under investigation.

A good amount of research works have been done to investigate the thermal performance of the PB made of different materials having different power outputs, different firing rates, equivalence ratios, and optical properties. Because of better heat recirculation, the lean flammability limit was found to be extended for all types of fuels. For a double layered PB, it has been found that the porosity of the PZ should be lower than that of the CZ.

Radiation greatly influences the thermal performance of the PB. The radiation output has been found to depend on various parameters like equivalence ratio, firing rate, flame support layer thickness, porosity and aspect ratio which in turn influence combustion and thermal efficiencies. In the absence of a standard procedure, a wide variation (15 - 50%) in radiation efficiency has been found. A doubled layered PB showed higher radiation efficiency than the single layered PB. In the PMB, because of heat recirculation, the CZ temperature is lowered and the combustion is nearly complete with sufficient residence time. Reduced temperature has been found to be one of the most effective means to control thermal NO_x and because of nearly complete combustion, CO level is considerably low. Further research considering complete chemistry of NO_x formation is still under investigation.

Researchers explored many areas of application for PMB. Depending upon the applications, researcher reported the thermal efficiency ranging from 60 to 75%. It was observed from the literature survey that most of the researchers explored the use of porous medium combustion for cooking application for low thermal load in the range of 1-2 kW, with the help of external air supply. No researchers have explored the application of two layered PRB in domestic cooking application without external air supply. It was also found that no researcher tested the two layered porous PRB with the capacity range of 5-15 kW for medium-scale cooking applications.

2.6 Objectives of the present work

In view of the above conclusions made on the available literatures, the following objectives are considered for present work.

- To test a two layered porous radiant burner for medium-scale (5-10 kW) LPG cooking application and also investigate the effects of the power input and equivalence ratio on the thermal efficiency and emissions of the two layer porous radiant burner.
- To develop a self-aspirated two layered porous radiant burner for LPG domestic cooking application in the power range 1-3 kW and to study the effects of the power input on the thermal efficiency and emissions of the self-aspirated two layer porous radiant burner.
- To develop a medium-scale self-aspirated improved air entrainment LPG cooking stove with a two-layer porous radiant in the power range 5 - 15 kW and to investigate the effects of the power input on the thermal efficiency and emissions for the same.
- To ascertain the applicability of the porous radiant burner for LPG domestic cooking as well as medium-scale cooking applications.

Chapter 3

Development of Medium-Scale LPG Cooking Stove with Porous Radiant Burner

In this chapter, the design of PRB and fabrication of experimental set-up for the medium-scale conventional cooking stove and medium-scale PRB stove are presented. A brief discussion about the experimental procedure is also presented. The temperature distribution, thermal efficiency and emission characteristics of PRB burners at different powers (Appendix-I) are also presented.

3.1 Experimental setup for conventional medium-scale LPG cooking stove

Fig. 3.1 illustrates the pictorial view of the medium scale CB. Here combustion takes place over the surface of the burner which is exactly above the head of the burner. Fig. 3.2 shows the different types of for conventional medium-scale LPG cooking stove's heads and burner assemblies available in the Indian market for the power range of 5-15 kW.

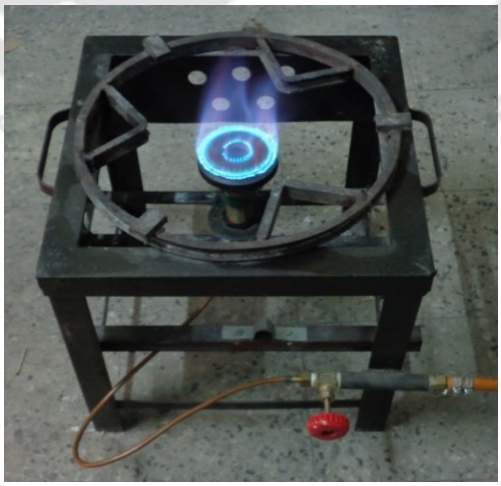

Fig. 3.1 Medium-scale conventional LPG cooking stove

a. Ring-type

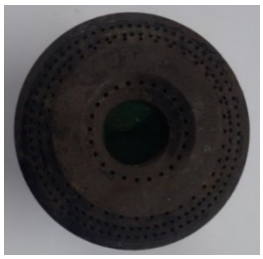

b. G-type

c. Torch-type

d. Burner assembly

Fig. 3.2. Different types of conventional medium-scale LPG cooking stove's burner head (a, b, c) and burner assembly (d) available in the Indian market conventional medium-scale LPG cooking stoves

The medium-scale conventional LPG cooking stove works on the same principle as conventional domestic cooking stove which is explained in chapter 1. The only difference is the orifice design, instead of single orifice in the case of small scale domestic stoves, multi orifices (4) have been used in medium-scale LPG stoves for LPG supply. As shown in Fig.3.2d, the air entrainment is taking place through the slots and then mixture is going to the burner via a mixing chamber and then combustion takes place on the burner head.

3.2 Experimental procedure

Thermal efficiencies of both types (CB and PRB) of the LPG cooking stoves were estimated by conducting the water boiling test as per the guidelines prescribed in the Bureau of Indian Standard (BIS):4246:2002. The procedure followed is briefly described in the following.

A LPG supply pipe line which is connected to a 19.5 kg cylinder fitted with a regulator, delivers LPG to the burner via a Coriolis mass flow meter (accuracy ± 0.001 g). The Coriolis mass flow meter is connected to the supply line for the measurement of LPG consumption. Aluminum vessel along with lid and stirrer for the experiment are selected and filled with known amount of water (10 kg) at room temperature (~30 °C). Weight of the vessel with water is noted with the help of a weighing balance (accuracy ± 0.5 g). Initial temperature (T_1) of water is measured using glass-in-mercury thermometer (accuracy ± 0.5 °C). After stabilizing the flame, the vessel is kept above the burner. Water is heated up to 80 °C, and for uniformity in temperature, stirring is started and continued until the end of the test when the temperature of water has reached (T_2) 90 ± 0.5°C. At this stage, the burner is switched off. The time taken to raise the temperature of the water from initial temperature (T_1) to 90 °C is noted. In every case, experiments were repeated at least three times, and the average of three was taken for the analysis. The percentage of thermal efficiency η_{th} $\left(\eta_{th} = \frac{\text{Heat output}}{\text{Heat input}}\right)$ of the stove is calculated based on (BIS): 4246:2002 prescribed formula:

$$\eta_{th} = \frac{\left(m_w \cdot C_w + m_p \cdot C_p\right)\left(T_2 - T_1\right)}{m_f \cdot \text{CV}} \tag{3.1}$$

where m_w is the mass of water, C_w is the specific heat of water, m_p is mass of pan along with the lid and stirrer and C_p is the specific heat of the pan, m_f is the mass of the LPG consumed and CV is the lower calorific value (44160 kJ/kg) of LPG. Properties of the LPG is presented in Appendix – I. The uncertainty in the efficiency was found to be ± 1.5% (detailed uncertainty analysis is presented in Appendix – III). To compare the thermal efficiencies and emissions of the burners with porous media with those of the conventional medium-scale LPG cooking stoves, a market survey was carried out to get the various types of burners used in conventional medium-scale cooking stoves. Three types of burners were

selected from the Indian market (shown in Fig. 3.2). The thermal efficiencies of these CB were in the range of 30 - 45%. For different powers, the measured efficiencies of the conventional medium-scale cooking burners are shown in Fig. 3.3. The height of the flame increases with increase in the power input, and this causes enhanced heat loss by convection, and hence is the observed trend in reduction of the thermal efficiency.

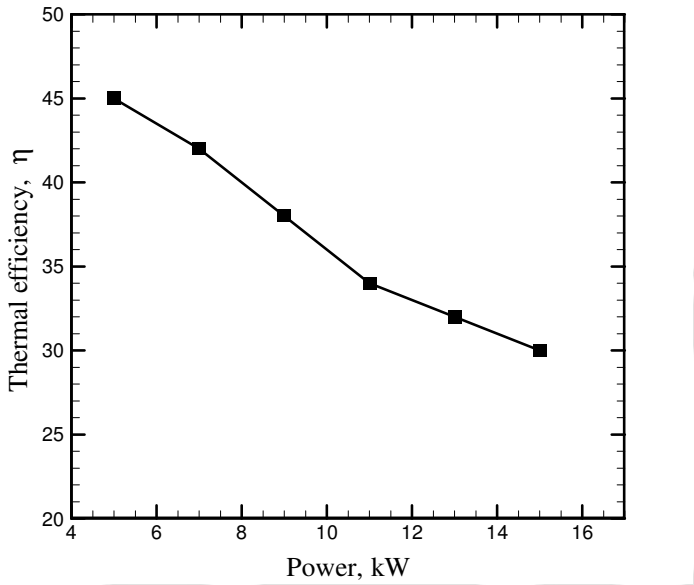

Fig. 3.3 Effect of power intensity on thermal efficiency of the conventional medium-scale LPG cooking stove

For the emission measurements, the flue gas sampling was done according to the IS: 4246. A hood shown in Fig. 3.4, was fabricated according to the dimensions mentioned in IS: 4246. The hood was placed above the burner along with the vessel and the portable flue gas analyser probe was placed in the first sampling hole. The main purpose of the hood is to isolate the flue gases from the atmospheric air. A portable flue gas analyser is used (Greenline 8000) for recording CO and NO_x emissions. The detailed specifications of the instrumentation/equipment used in the experiments are given in Appendix - IV.

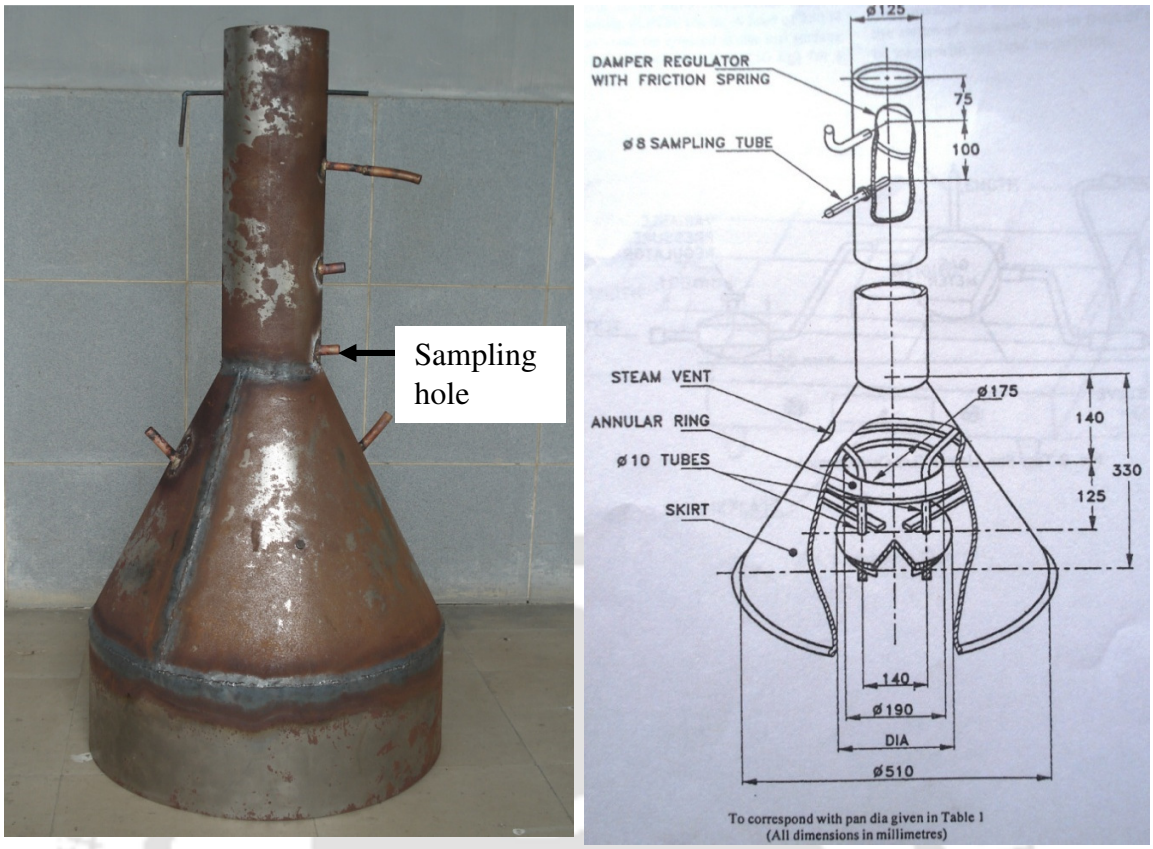

a. Hood for flue gas sampling

b. Schematic of the hood for flues gas sampling (imported from IS: 4246)

Fig. 3.4. Pictorial view and schematic of the hood for flues gas sampling

The typical measured emission levels of the conventional medium-scale cooking burner is shown in Fig. 3.5. From Fig. 3.5, it is observed that with increase in the input power, both CO and NOx emissions are found increase. Lower residence time combined with insufficient air, causes the incomplete combustion in the CB resulting in high CO emission. With increase in power input, the requirement of air increases. However, the design of the conventional stove does not permit increased air entrainment, and as a result, the air-fuel mixture is more fuel rich, and hence the increased amount of CO emission results. A similar trend with NOx emission is attributed to fuel rich combustion and high temperature in the reaction zone. Both the CO and NO_x emissions rise with the power and the maximum

values observed were much higher than the recommended values of World Health Organisation (WHO) [Kandpal *et al.*, 2002].

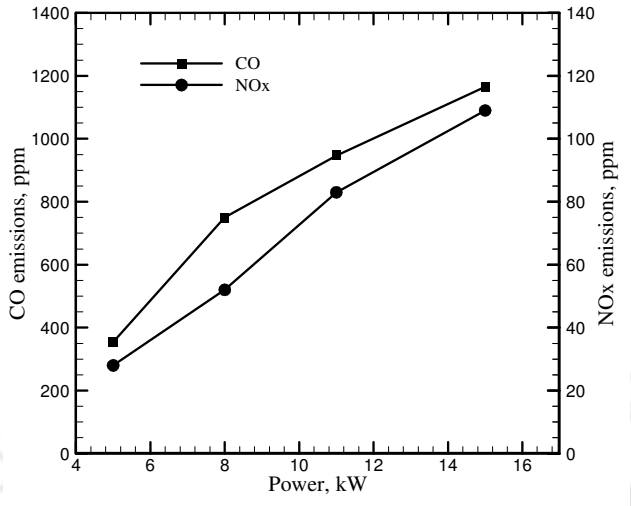

Fig. 3.5. Typical emissions characteristics of a conventional medium-scale LPG cooking stove

3.3 Experimental set-up of medium-scale LPG cooking stove with PRB

The experimental set-up used for testing the performance of the medium-scale LPG cooking stove with PRB is shown in Fig. 3.6. The fuel and air flow rates are monitored using the Coriolis mass flow meters with suitable valves. Air-fuel mixture reaches the burner through a mixing chamber made of Teflon. To minimize the radiation loss, an adjustable stand with radiation shield is attached.

3.3.1 Material and specifications

The two-layer PRB consists of a combustion zone and a preheating zone as shown in Fig. 3.7. Combustion zone is formed with high porosity (90%), average pore size (10 ppi), highly radiating SiC porous matrix of thickness 20 mm and diameter 120 mm, and the preheating zone consists of low porosity (pore size 2 mm and number of pores 463) alumina ceramic matrix of thickness 10 mm diameter 120 mm. The burner casing is fabricated

employing castable cement. The schematic of the burner casing assembly is shown in Fig. 3.8. The photographic view of the experimental setup is shown in Fig. 3.9.

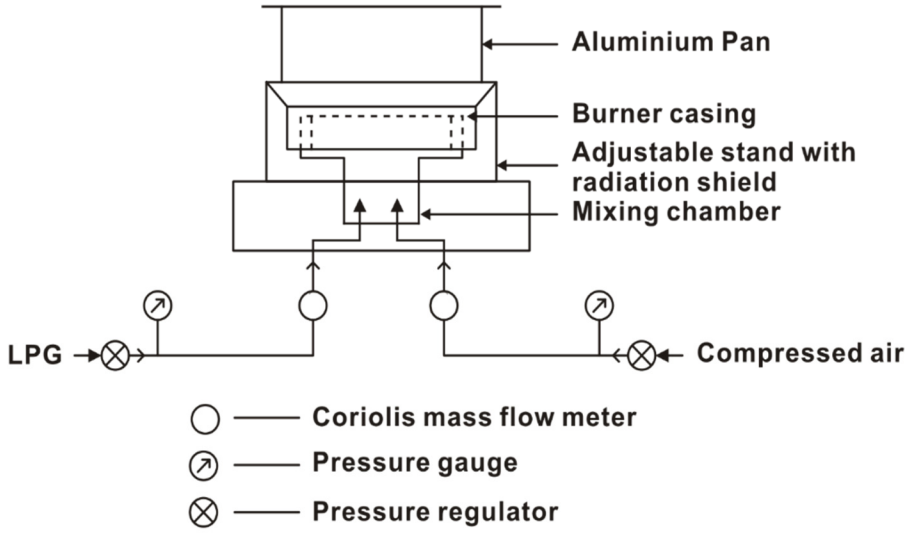

Fig. 3.6. Schematic of the experimental set-up of medium-scale PRB.

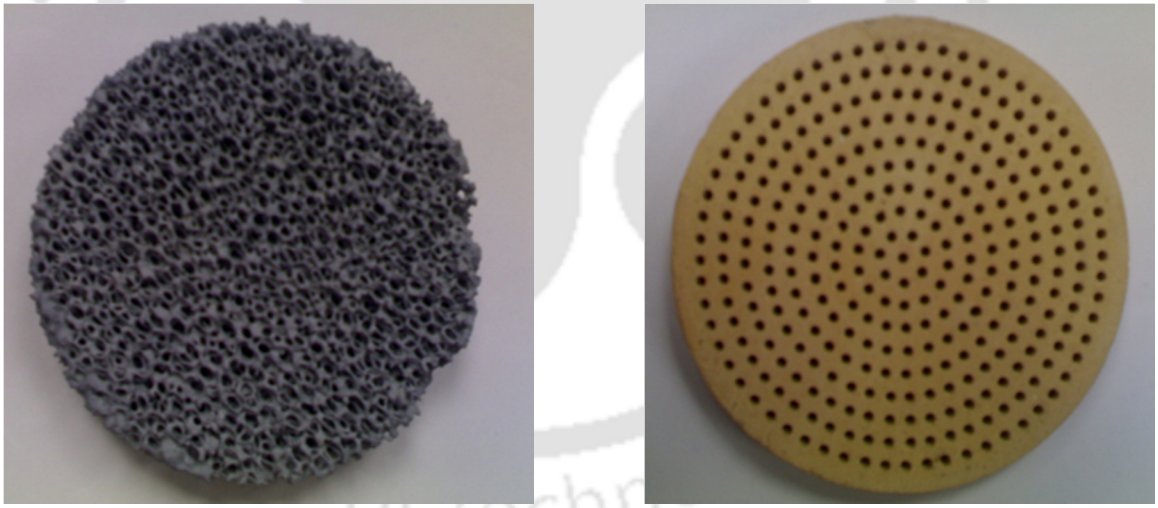

a. SiC matrix b. Alumina matrix

Fig. 3.7. Pictorial views of (a) combustion zone (SiC) and (b) preheating zone (alumina matrix)

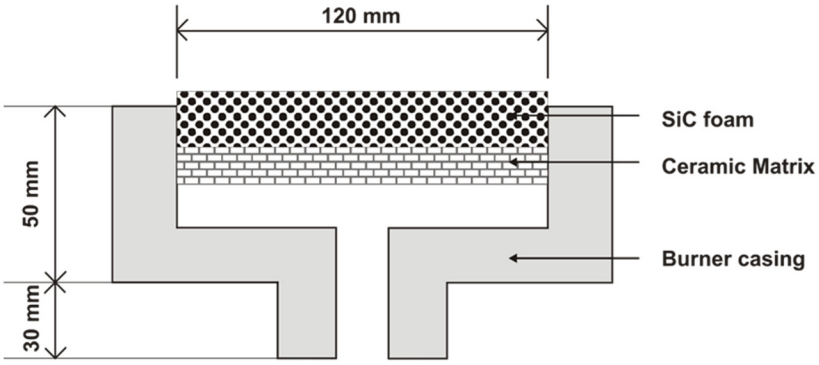

Fig. 3.8. Schematic of the PRB casing

Fig. 3.9 Photographic views of the experimental set up

3.3.2 Design of mixing chamber and base plate

The mixing chamber of the experimental setup is a part in which both LPG gas and air gets mixed, and the mixture is then forced to travel through the preheating zone followed by combustion zone. The mixing chamber is made of Teflon, which is a thermoplastic polymer whose melting point is 326 ºC. Basically the mixing chamber is mounted on the base plate. The mixing chamber is like a cylindrical hollow chamber. The height of the pipe is 200 mm, the inner diameter at the top is 80 mm, and the bottom diameter of the hole is 85 mm. And the rests of the pipe has 40 mm diameter. The outer diameter of the pipe is 90 mm. The entry of the mixing chamber was designed in a way that the casing of PRB fits in to the groove made inside the pipe on the upper side of mixing chamber. From the groove to

the bottom part of the mixing chamber the hole of same diameter is maintained. But, later on it was found that there was no enough space for the gas and the air to get mixed inside the mixing chamber. So keeping this in mind, the hole size at the bottom was made larger and gradually it was made decreasing towards the bottom part of the groove, to ensure the proper mixing of gas and air. Photographic view of mixing chamber is shown in Fig. 3.10 a.

(a) Mixing chamber (b) Base plate

Fig. 3.10 Different parts of experimental setup (a) Mixing chamber and (b) Base plate

The base plate assembly consists of two pipes. From one pipe air comes in and another pipe, LPG reaches to the mixing chamber through a centrally placed orifice in the base plate. The air which comes out through the pipe is supplied to the mixing chamber in three air distributor system for getting proper mixing. The photographic view of base plate assembly is shown in Fig. 3.10 b.

3.3.3 Start-up procedure and stability analysis

The start-up of the burner should be followed in a specified manner. Initially, the burner was started at a high equivalence ratio with a specified power input and then gradually increased the air flow rate to achieve a specified equivalence ratio. Once the burner stabilizes, then the equivalence ratio can be increased or decreased for that particular power input. The experiments were conducted at different power ranges (5 to 15 kW) and

equivalence ratios. The ratio of air fuel ratio (A/F) at stoichiometric condition to actual A/F is the equivalence ratio (Φ). Appendix – II provided the details of equivalence ratio. The formula for equivalence ratio is given by:

$$\Phi = AF_{Stioch} / AF_{actual} \quad (3.2)$$

The equivalence ratio (Φ) is a measure of how far the actual mixture is from the stoichiometry. Φ = 1.0 means the mixture is at stoichiometry. For rich mixtures, Φ is greater than 1 and lean mixtures Φ is less than 1. But the stable operation in the power range of 5 to 10 kW was found in equivalence ratio range of 0.54 to 0.72. Here, stability signifies the absence of lift-off and flashback. Within stability range, the PRB shows almost flameless combustion. The range of stability depends upon the thickness of combustion zone, the pore size of preheating zone and the velocity of air-fuel mixture. With increase in thickness and reduction in pore size of the preheater, the power rating of the burner can be increased. In the later part of Chapter 5, the power rating has been changed (5-15 kW) with the above mentioned modifications in the two-layer burner.

3.4 Results and discussion

In the following section, the temperature distributions (both axial and radial) of PRB, the effects of equivalence ratio on thermal efficiencies and CO and NOx emissions of the PRB in the power range of 5 to 10 kW are presented.

3.4.1 Temperature distribution

In the PRB, temperature was measured in both radial (Fig. 3.11a) and axial (3.11b) directions. For comparison, the temperature measurement has also been done in axial direction for CB. K-type metal sheathed thermocouples were used for temperature measurements in radial locations. For the measurement of the axial (Fig. 3.11c) temperature

distribution, in the CB, K – type thermocouples were used. The radial and axial locations of the thermocouples positions are shown in Figs. 3.11a and 3.11b, respectively. Outputs of the thermocouples were acquired through a data acquisition system.

Temperature distributions for the CB and PRB are shown in Figs. 3.12-3.14. Temperature measurements were carried out in the input power range of 5 – 10 kW. Axial temperature distributions in the CB and the PRB are shown in Figs. 3.12a and 3.12b, respectively. It is observed that in the CB, the temperature rise is very sharp, and temperature in the range 1000 – 1400 °C was observed close to the burner base. The maximum flame temperature was found in the reaction zone. In the CB, positions of the thermocouple along the axial direction (Fig. 3.11c) have been measured from the surface of the mixing chamber of the burner as shown in Fig. 3.11c, and except the first two positions, the remaining ones are within the flame. Temperature (80°C) of the thermocouple at the first position (Fig. 3.11c) shows the temperature of the mixing chamber, while the same second position is the surface temperature (210°C) of the burner head. The maximum flame temperature at 10 kW thermal load was found to be 1400°C at a distance of 1.5 cm from the burner head. It is observed that over a distance of 1.5 cm, the temperature rise is approx. 1200°C. This sharp rise in temperature is typical of the FF combustion.

With equivalence ratio 0.6, the axial temperature distributions measured in the PRB are shown in Fig. 3.12b. Temperatures at locations T0, T1, T2 and T3 (Fig. 3.11b) corresponding to the temperatures of the mixing chamber, the preheating zone, the reaction zone and the combustion zone. Radially 2 cm from the circumference of the burner, these axial positions of thermocouples are at 0.0, 0.8, 1.3, and 2.3 cm, respectively from the base of the ceramic matrix. Temperature distributions are shown in Fig. 3.12b. In the mixing

chamber (location T0), temperature in the range of 60 to 80 °C is well below the ignition temperature of LPG (≈500°C). This ensures no flash-back from the PRB. In the preheating zone at location T1, temperature is found in the range of 510 to 570 °C. Because of conduction and radiation, a significant preheating of air-fuel mixture is observed. The maximum temperature in the reaction zone at location T2 ranges between 1175 to 1300 °C. At any location, with increase in the input power, temperature increases. A comparison of temperature distributions in Figs. 3.12a and 3.12b, at any input power, in the PRB, temperature rise is less sharper than that in the CB. Radiation and conduction in the PRB, in one hand preheats the incoming air-fuel mixture, and on the other, helps faster transfer of heat from the reaction zone in the downward direction, and as a result, the temperature rise is lower.

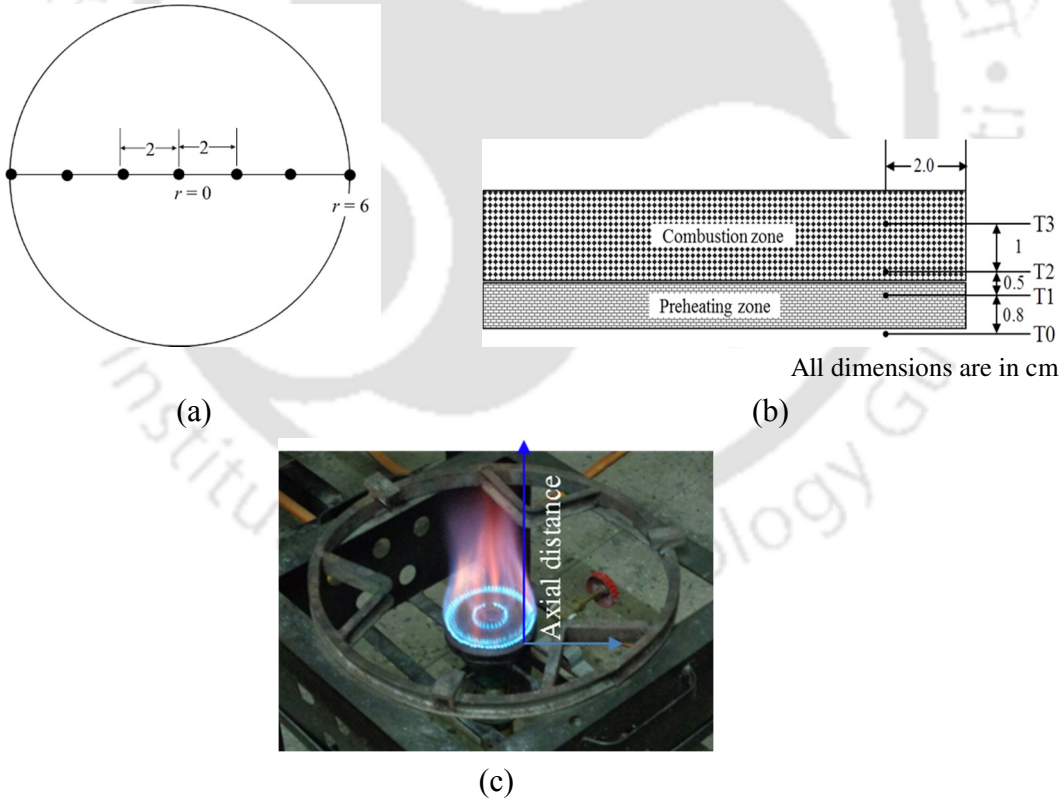

Fig. 3.11. (a) Radial positions of thermocouples on top surface of the PRB, (b) axial positions of thermocouple in the PRB, and (c) axial distance along which temperature was measured in CB.

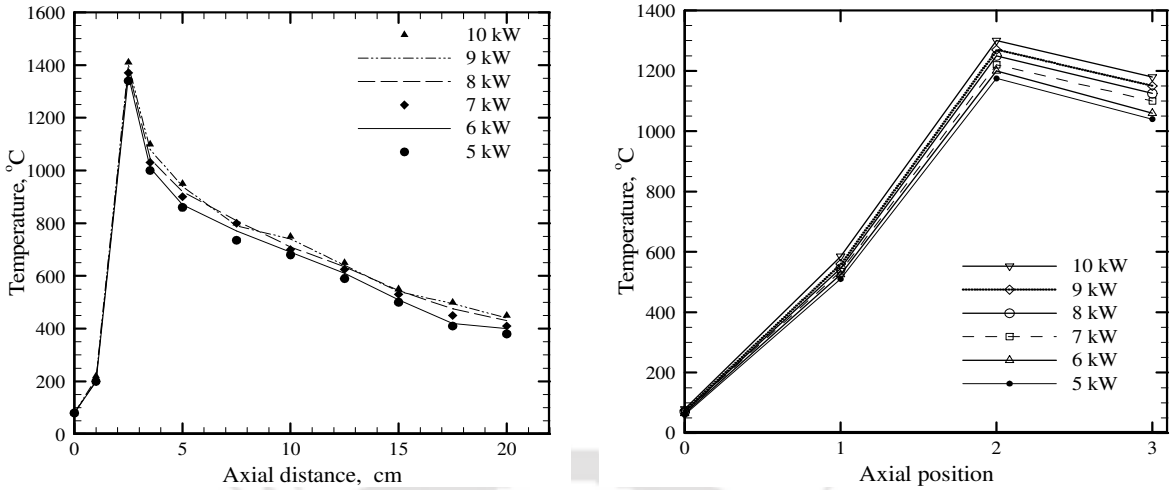

(a) (b)

Fig. 3.12. Axial temperature distributions in (a) CB and (b) PRB, Φ = 0.6; power inputs in the range 5 – 10 kW.

Radial temperature distributions in the PRB for different thermal loads in the range 5 – 10 kW at different equivalence ratios are shown in the Figs. 3.13a-c. For measurement of the radial temperature distribution, thermocouple measuring point was located 2.0 mm from the top surface. In Figs. 3.13a-c, radial temperature distributions are shown for the equivalence ratio 0.55, 0.6 and 0.7, respectively. It is to be noted that in the present work, flameless combustion was observed in equivalence ratio range of 0.54 – 0.72. The maximum temperature difference between centers to periphery is found to be 180°C for equivalence ratio 0.7.

It is to be noted that the maximum difference (180°C) in the radial temperature at equivalence ratio 0.7 is attributed to less supply of air and relatively more supply of fuel than that for the lower equivalence ratios (0.55 and 0.6). For 10 kW thermal load, the maximum temperature of PRB was around 1200°C at equivalence ratio 0.7 (Fig. 3.13c), which is 200°C lower than the CB (Fig. 3.12a). This is due to the lean combustion of LPG

in the PRB. An observation from Figs. 3.13a-c shows that at a given thermal load, higher is the equivalence ratio, higher is the peak temperature.

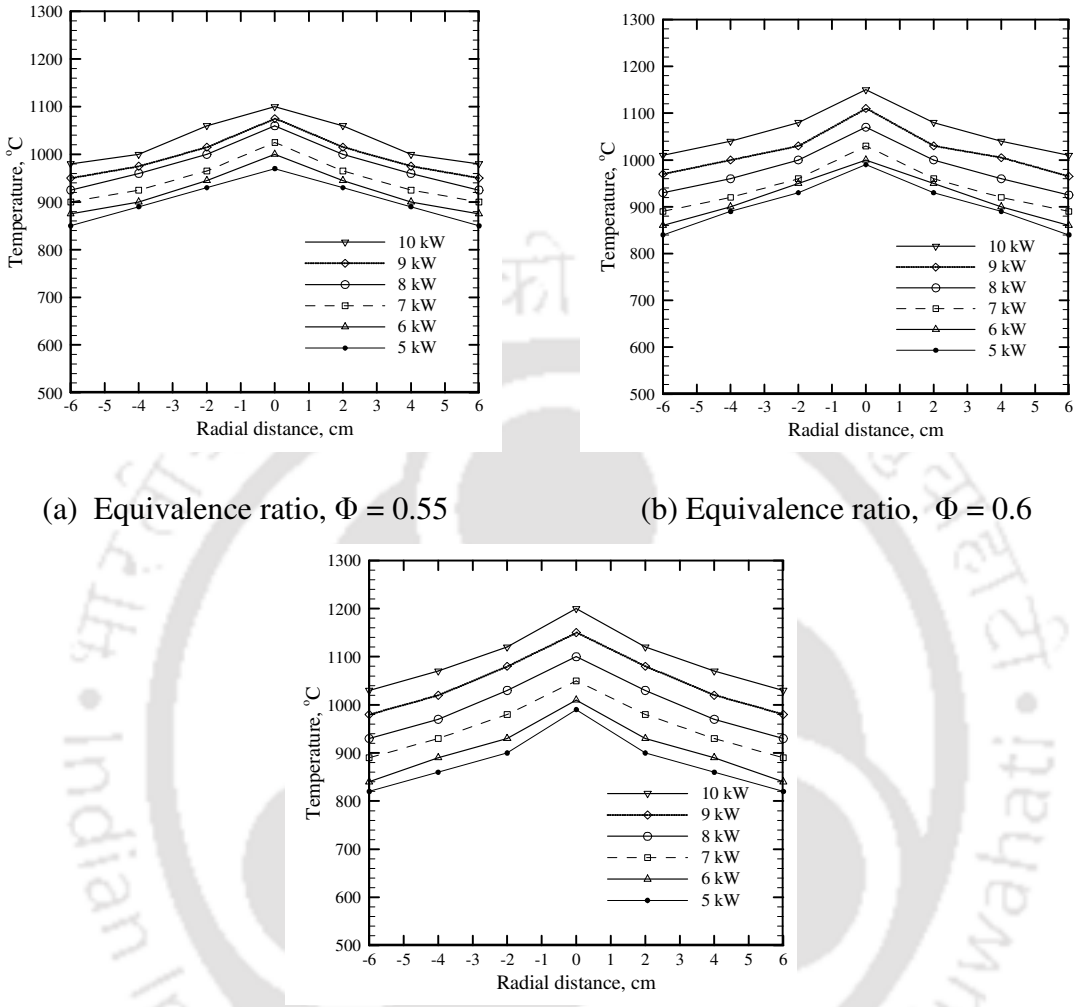

(a) Equivalence ratio, Φ = 0.55 (b) Equivalence ratio, Φ = 0.6

(c) Equivalence ratio, Φ = 0.7

Fig. 3.13. Radial temperature distribution of PRB at equivalence ratio, Φ (a) = 0.55, (b) = 0.6 and = 0.7.

In addition to thermocouples, surface temperatures of the PRB, can also be measured using an IR Camera. At equivalence ratio Φ = 0.6, the maximum and the minimum surface temperatures of the PRB measured by IR thermo-camera (InfraTec-VarioCAM hr) and thermocouple are compared in Fig. 3.14. The measured temperature through IR thermo-camera was found higher than the thermocouple. The difference ranged between 21°C to

30°C. The lower temperature recorded by the thermocouple is attributed to radiation and conduction losses.

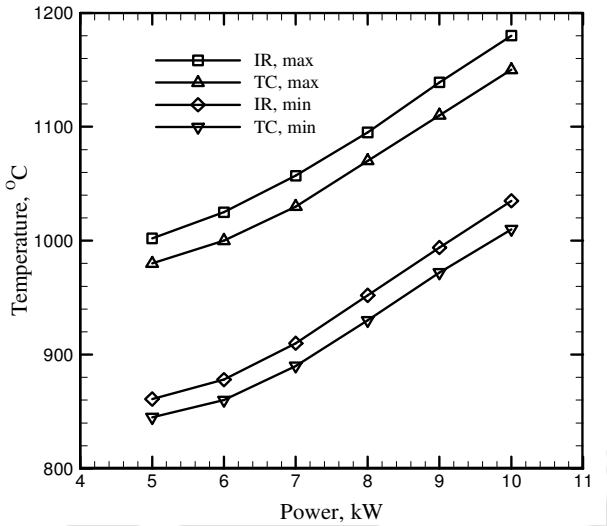

Fig. 3.14. Maximum and minimum temperature of PRB measured by IR Camera and thermocouple at Φ = 0.6

3.4.2 Thermal efficiency

Fig. 3.15 shows thermal efficiencies of the PRB measured at different thermal loads and equivalence ratios. In the PRB, because of conduction and radiation, the combustion is nearly complete. This leads to higher thermal efficiency. It is seen from Fig. 3.15 that at a given equivalence ratio, with increase in the power input, thermal efficiency decreases, and for a given power input, with increase in the equivalence ratio, thermal efficiency also decreases. At the lower equivalence ratio, the air supplied is more and this leads to better combustion and hence the higher thermal efficiency. Further at lower equivalence ratio, the downward shifting of the reaction zone takes place, and this augments the volumetric heat release. It can be seen that the maximum thermal efficiency of the PRB is 58% at equivalence ratio 0.56 for thermal load 5 kW.

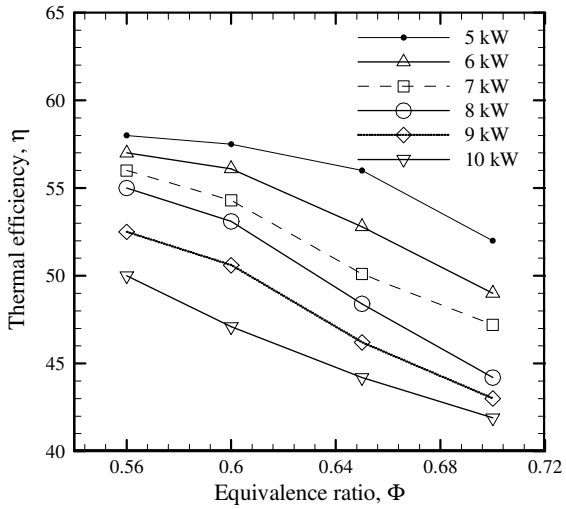

Fig. 3.15. Effects of power inputs and equivalence ratio on the thermal efficiency of PRB.

Thermal efficiency also depends on the loading height, viz., the distance between the top surface of the PRB and the vessel. For power input of 5 kW, equivalence ratio $\Phi = 0.56$, this variation is shown in Fig. 3.16. When the vessel is placed at a distance of 20 mm, thermal efficiency is 56%. While, when it is placed at a distance of 30 mm, the efficiency is 58%. With further increase in the distance, thermal efficiency is found to decrease. Above observation is owing to the fact that when the distance is 20 mm, the amount of diffusion air needed for the combustion is partially curtailed. At a distance of 30 mm, it is optimum, and hence this results in the maximum thermal efficiency. Beyond this distance, the radiation as well as convection losses through the gap between the radiation shield and the bottom surface of the vessel increases.

Thermal efficiency also depends on the ambient temperature. In order to study the influence of ambient temperature on the thermal efficiency of the PRB, the power intensity and equivalence ratio were kept constant at 5 kW and equivalence ratio 0.56, respectively. A series of experiments were carried out to cover a wide range of ambient temperatures from 10°C to 30°C (from July to December, 2014). Fig. 3.17 shows the influence of ambient

temperature on the thermal efficiency of the porous burner. As illustrated in Fig.3.17, the thermal efficiency of the porous burner is found to be directly proportional to ambient temperature. The maximum thermal efficiency for 5 kW, 0.56 equivalence ratio was found to be 58 % at 30°C and 52.5% at 10°C. As the ambient temperature decreases, the temperature gradient between the surface of vessel and the ambient increases, and hence the convective heat loss from the surface of the vessel increases significantly, resulting in lower thermal efficiency.

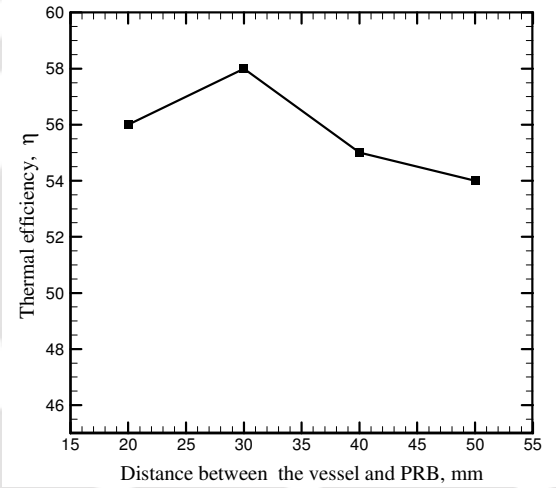

Fig.3.16. Effect of loading height on thermal efficiency for PRB

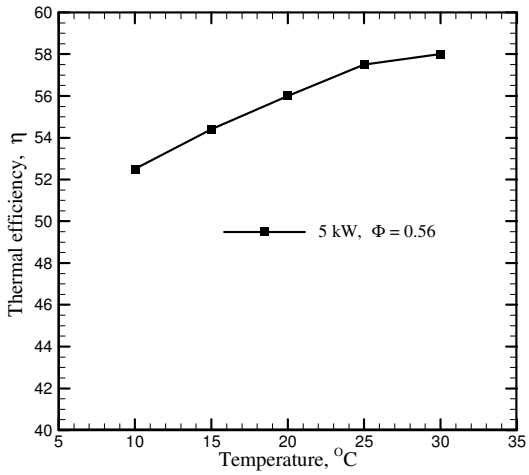

Fig.3.17. Effect of ambient temperature on the thermal efficiency of PRB

3.4.3 Emissions

In present study, the CO and NOx emissions were measured using Greenline 8000 portable flue gas analyzer. The sampling was done as recommended in the BIS: 4246:2002. The CO and NOx emissions measured for CB for different power inputs are shown in Fig. 3.5. It is to be noted that in the CB, with lean combustion, the undesirable feature of the flame lift-off occurs. To avoid this, conventional LPG cooking stove is designed for a fuel rich combustion.

With input power in the range 5 – 10 kW, in the PRB, CO and NOx variations with equivalence ratio are shown in Figs. 3.18a and Fig. 3.18b, respectively. For a given thermal load, the CO emission is found to increase with increase in equivalence ratio Φ. In case of a leaner mixture (lower value of Φ), fuel gets sufficient air to combust, so the CO emission is less. In the PRB, due to the lower global temperature (surface temperature of the burner), the NO_X emission is also found to be much lower than that of the CB.

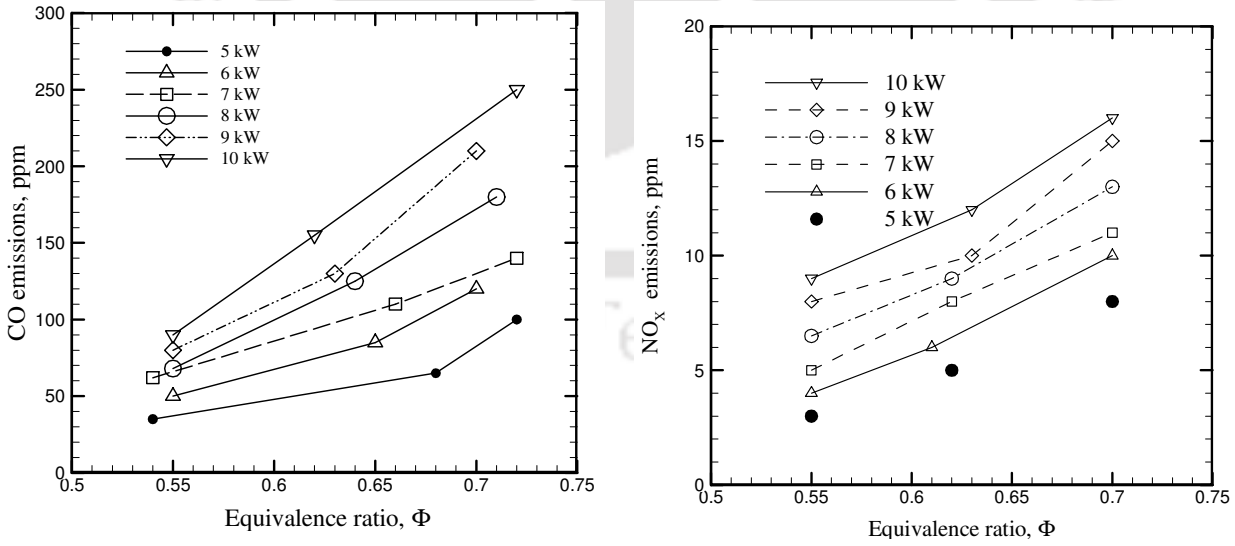

(a) (b)

Fig. 3.18. Effects of power input and equivalence ratio on (a) CO (b) NO_X emission for PRB

3.5 Summary

Performance in terms of temperature distributions, thermal efficiency and CO and NOx emissions of a two-layer medium scale (5 – 10 kW) LPG cooking stove with a PRB was experimentally investigated. For the purpose of comparison, the same parametric study was carried out with CB working in the FF combustion mode. The maximum axial temperature in the PRB was about 200 °C lower than that of the CB. The radial temperature distribution of the PRB was almost uniform. If the radial temperature distribution is uniform, the radiant heat flux can be achieved by the burner is near uniform and the heat loss in radial direction of the burner can be negligible. Axial temperature shows significance of pre-heating effect of air-fuel mixture and hence the combustion is improved. Preheating effect is responsible for excess enthalpy combustion for any combustion devices. In present work, measurement of axial temperature reveals that the preheating effect is significant in the developed PRB. At 5 kW power input, thermal efficiency of the PRB at equivalence ratio 0.56 was found to be 58%, while it was 45% for the CB for the same power input. CO and NOx emissions in the PRB were much lower than that with the CB. The recommended equivalence ratio for PRB in the range of 5-10 kW is 0.56.

Significant amount of LPG can be saved by using PRB. But the main problem is the requirement of external air. For this, there is need of a compressor or a blower. For cooking application, it is not economical to purchase a compressor. So further research is needed to re-design the cooking stove which can be operated through natural draught.

Chapter 4

Self-aspirated Domestic LPG Cooking Stove with Porous Radiant Burner

In this chapter, the performance investigations of a domestic LPG cooking stove and a self-aspirated LPG cooking stove with PRB are discussed. Details about the experimental set up and procedure are presented. The thermal efficiency and emission characteristics of both the burners at different powers are also presented.

4.1 Performance analysis of domestic LPG cooking stove

The vital part of this LPG stove is the design of mixing chamber and burner (Fig. 4.1). It works on the venturi effect. The working principle of (CB) is already discussed in Chapter 1. Combustion takes place on top of the burner head as shown in Fig. 4.2. The different types of burner heads available in the Indian market for conventional domestic LPG cooking stoves are shown in Fig. 4.3.

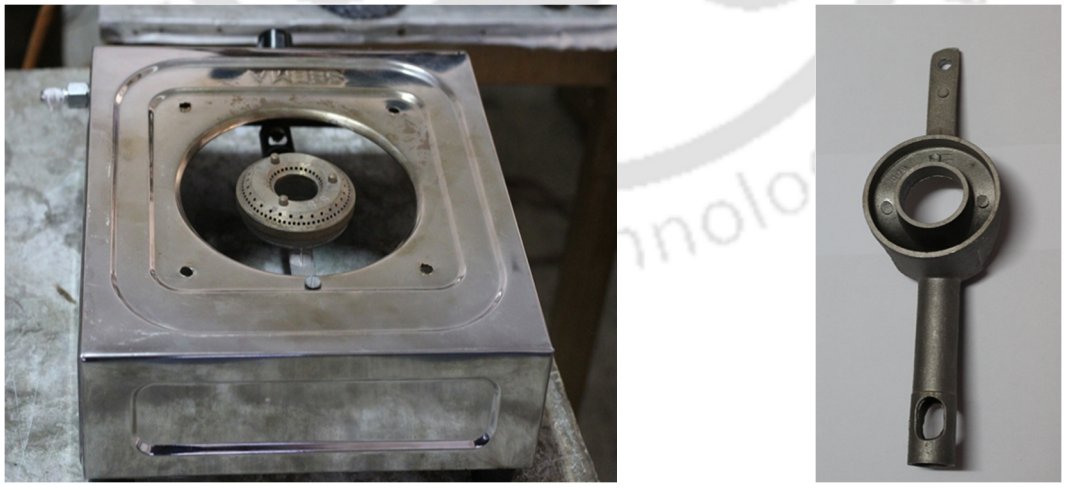

a. Conventional domestic LPG stove b. Mixing chamber

Fig. 4.1. Conventional domestic LPG stove with mixing chamber

Fig. 4.2. Pictorial views of the free flame in conventional domestic cooking stove.

a. Regular Burner

b. Nikitsa Burner

c. Aluminium Base Burner

Fig. 4.3. Pictorial views of the different conventional burners heads available in the market chosen for comparison

4.2 Experimental procedure

In India, Bureau of Indian Standards (BIS) sets guidelines for testing the thermal efficiencies for all types of cooking stoves. The thermal efficiencies are determined according to Indian Standards (IS) 4246:2002.

Following the guidelines of IS 4246:2002, thermal efficiencies of cooking stoves in the present work were estimated by conducting the water boiling test and the procedure is already briefly described in Chapter 3. The typical thermal efficiency variation of the conventional domestic cooking burner at different power inputs is shown in Fig. 4.4.

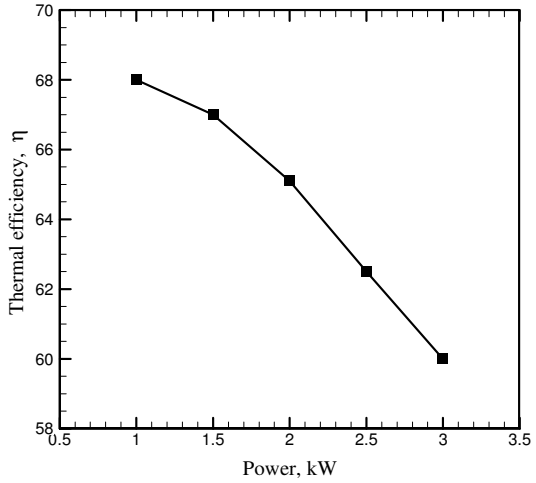

Fig. 4.4 Thermal efficiency variation of the domestic CB at different power inputs

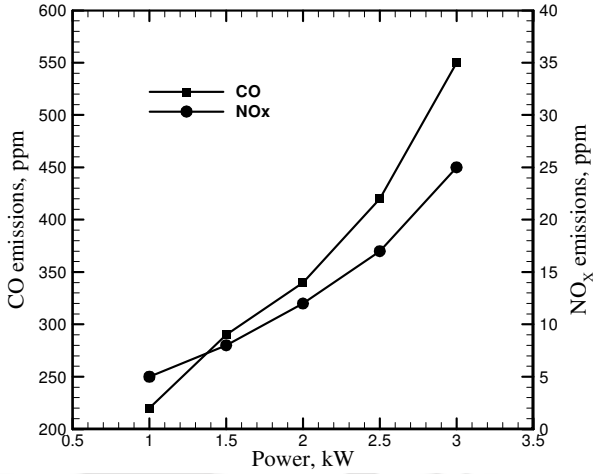

Fig. 4.5 Emissions characteristics of a domestic CB

In present study, the CO and NOx emissions were measured by Greenline 8000 portable flue gas analyser. The sampling was done as recommended in the BIS: 4246:2002. The detailed specifications of the hood for collecting flue gas through burner has been presented in Chapter 3. The typical measured emission levels of the domestic cooking burner is shown in Fig. 3.5. Both the CO and NO_x emissions rise with the power and the maximum values observed were much higher than the recommended values [Kandpal *et al.*, 2002] of WHO. Due to high emissions and lower thermal efficiency the domestic CB is not desirable. As discussed in Chapter 3, the thermal efficiency can be improved by the use of PRB. A significant amount of LPG can be saved by using PRB. But the main problem is the requirement of external air. For domestic cooking application, it is difficult to provide compressed air. Therefore, further research is needed to re-design the cooking stove which can be operated through natural draught. This chapter discusses the comprehensive efforts

have been made for the use of PRB in domestic cooking application, without external air supply. The prototype PRBs assembly mounted on existing CB.

4.3 Necessary modifications in conventional LPG stove with PRB

4.3.1 Arrangement of PRB with PZ with secondary air opening

As illustrated in Fig. 4.6, a hole has been made at the center of the both combustion and preheating zones for the secondary air entrainment. PZ was placed on top of mixing chamber and combustion zone was kept above it. Partial red hot condition was achieved but effective radiating area got decreased because of the hole at center. Preheating effect was found in the mixing chamber. But the flame formed at the hole region. Flame color was found to be yellow, which means that the combustion was incomplete.

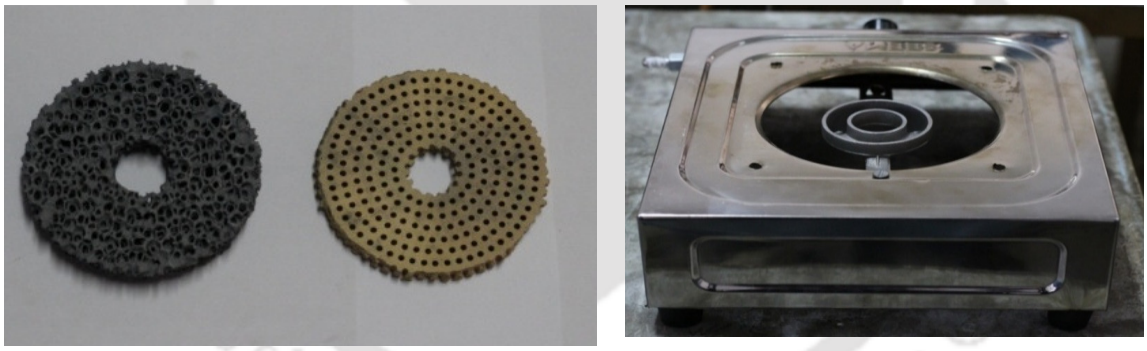

Fig.4.6. PRB with PZ with secondary air opening

4.3.2 Arrangement of two layer PRB in flat mixing chamber without secondary air opening

LPG cooking stove manufactured by M/s. Sunshine Company has been modified by incorporating PRB for the conventional domestic cooking purposes. This stove is having a flat mixing chamber without any secondary air opening, as shown in Fig.4.7c. Employing the same mixing chamber, necessary modifications were carried out with SiC matrix as a

CZ and alumina matrix as a PZ. The diameter of the CZ and PZ was 80 mm. whereas the thickness of CZ was 20 mm and for PZ, it was 10 mm. The major difference between the old designs of the stoves and the stove with PRB, is that the design of the mixing chamber. In the regular stoves, the mixing chamber has the hole at the center part for providing the necessary secondary air entertainment (shown in Fig.4.1b). While in the new stove with PRB, the hole at the center of the mixing chamber is not provided. The height of the mixing chamber is also increased by 20 mm which provides the required secondary air from its periphery. The operation of porous radiant burner instead of CB has been tried using the same mixing chamber as shown in Fig.4.8.

a. SiC matrix (combustion zone)

b. Alumina matrix (preheating zone)

c. Mixing chamber without secondary air opening

Fig.4.7. Two layer porous burner (a, b) and mixing chamber (c)

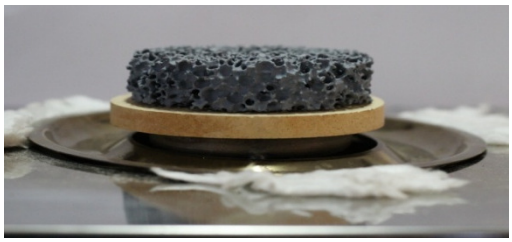

Fig.4.8. Cooking domestic stove with PZ and CZ

After that a combination of CZ and PZ formed and they were placed above the mixing chamber. Experiments were conducted with the above mentioned modifications and found that there hasn't been a problem of secondary air entrainment and the porous radiant burner turns out to be partially red hot in comparison with the previous arrangement. In the above experiment, after about 15 to 20 min operation flash back was observed. This was mainly due to the less mixture velocity and overheating of mixing chamber. From the above observation, it was concluded that the air–entrainment should be proper and the heat loss to the surrounding to be minimized.

4.3.3 Arrangement of a two-layer PRB with a high pressure regulator

Now the most challenging issue is that the velocity of air-fuel mixture is need to be increased and also more primary air entrainment is required. So for getting more air-entrainment, different types of high pressure regulators have been tried. If the LPG supply pressure will increase, then the LPG velocity at the orifice will be higher and hence due to venturi effect, more air-entrainment will take place. Different types of tried pressure regulators are shown in Fig. 4.9. The stability analysis has been done for PRB in terms of supply pressure. It was found that for obtaining full red hot condition, the required minimum supply pressure should be 1 bar gauge pressure. Where as in case of CB, the supply pressure is 30 mbar gauge. Now same cooking stove with a high pressure regulator, the PRB becomes stable and fully red hot condition was achieved (shown in Fig. 4.9).

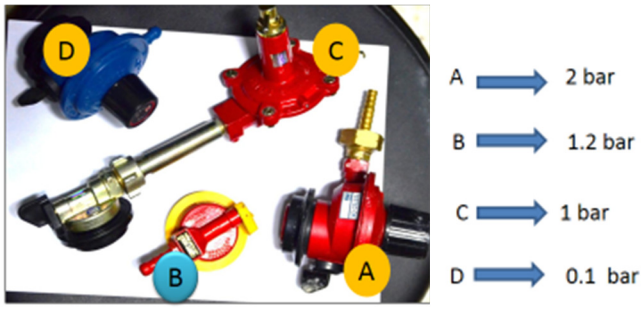

Fig. 4.9. Different types of high pressure regulators

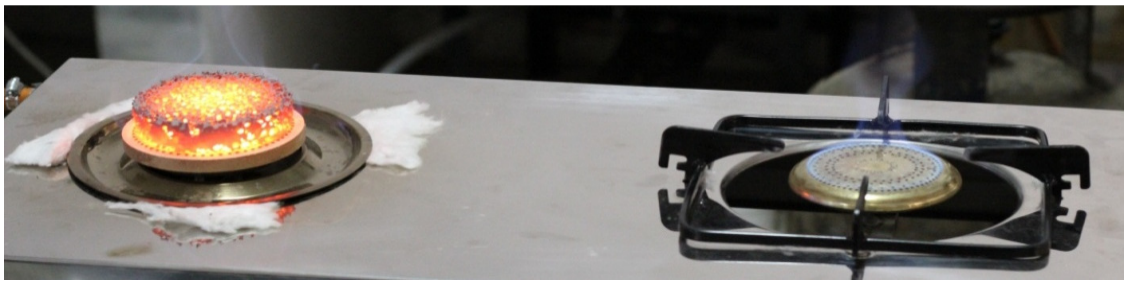

Fig.4.10. Combustion in conventional and PRB Burner

The thermal efficiency of the modified burner was 1 to 2 % less compared to the CB for same power rating. This is due to radiation heat loss through burner and conduction heat loss through mixing chamber. One more reason behind for the lower efficiency is that above mentioned cooking stove has been design for free flame combustion not for PRB.

Therefore, to achieve better thermal efficiency, the air-entrainment system is need to be redesigned. As discussed in Chapter 3, for getting higher thermal efficiency the leaner air-fuel mixture is required for the PRB. With above mentioned modification with PRB, it is observed that there was possibility of improving thermal efficiency of CB by replacing the existing metallic burner with PRB. Porous Burner is the only possible technology for the combustion of lean mixtures. A lean mixture can be obtained by a higher amount of air entrainment. The applications of PRB for cooking application were extensively studied employing compressed air [Pantangi et *al*; 2011, Muthukumar P and Shyamkumar P; 2013]. However, employing an external compressor is not a feasible option for domestic cooking applications. Therefore, an efforts have been made for making the PRB to work in self-aspiration mode. Further, to improve the thermal efficiency, the radiative heat loss should be minimized for providing a suitable shield.

4.4 Development of self–aspirated LPG cooking stove with PRB

Combustion process is characterized by the formation of flame. In conventional cooking stoves a flame front is formed on the surface of the burner. This flame is premixed flame because air and fuel are mixed before entering into combustion zone. Flameless combustion can be achieved with PRB. It is also known as surface combustion. This mode of combustion is well known for high burning velocities, extended limit of flammability, low emissions.

4.4.1 Basic design Considerations for air–entrainment

A lean mixture can be obtained by a great amount of air mixing. So mostly PRB is used with compressed air. In this work, self-aspiration mode in proposed. i.e. the creation of sufficient natural air entertainment. Prichard *et al.* [1977] provided e a correlation for rate of primary air entrainment from an orifice to the mixing tube.

$$R = -\frac{(1+\sigma)}{2} + \sqrt{\frac{\sigma D_P^2}{D_I{}^2\sqrt{1+C_L}}} \qquad (4.1)$$

where, R = ratio of air and gas entrainment; σ= relative density of gas (ratio of density of LPG and air); D_P = inlet burner port diameter ; C_L = loss coefficient ; D_I = inlet diameter of the orifice. Since most of the parameters are almost fixed, excluding the orifice diameter and burner port. Therefore, for getting more air entrainment, it is necessary to decrease the orifice diameter and increase the port diameter. In conventional domestic stoves 0.8 mm diameter orifice is used. So first approach towards this experiment, is to explore the various diameters of the orifice for providing sufficient air entertainment.

4.4.2 Orifices

If an orifice less than 0.8 mm diameter is used, then more velocity can be obtained at exit of the orifice which in turn create greater pressure difference. Hence, resulting in more air entrainment. Effect of air entrainment on the three different types of orifices, i.e., 0.25 mm, 0.35 mm, and 0.5 mm diameters are investigated. Fig. 4.11 shows the different types of orifices used in the experimental investigation.

a. Orifices used in present work b. Orifice for CB

Fig. 4.11 Orifices of 0.25 mm,0.35 mm,0.5 mm and 0.8 mm diameters

4.4.3 Burner port

In the CB, a horizontal type mixing tube shown Fig. 4.12.a is used. In this mixing tube, a bend is provided which causes slows down of the mixtures. Because the mixture couldn't overcome the flow resistance. So to overcome this problem vertical type of burner port which acts like mixing tube are designed as shown in Fig. 4.12.b. Three types of burner port of internal diameters of 17 mm, 19 mm and 21 mm and length of 90 mm with slot length of 30 mm and slot width of 10 mm for the air-entrainment were fabricated.

(a)

(b)

Fig. 4.12 (a) Mixing tube of conventional stove (b) Different burner ports used in the present work

4.4.4 Mixing chamber

Initially a mixing chamber of stainless steel (Fig. 4.13) was investigated for proper mixing of air-fuel mixture. To minimize the radiative heat loss, alumina insulation was provided on the outer periphery of the burner. The insulation is also acting like a burner casing. In this arrangement, flameless combustion was obtained, but after some interval of time, flashback was taking place. Flashback occurred due to the flow resistance of incoming fuel-air mixture. And this happens due to overheating of mixing chamber. Therefore, the stainless steel mixing chamber cannot be used with this arrangement. When stainless steel mixing chamber was used in conventional stove (shown in Fig. 4.13), during combustion, a significant part of heat was lost to ambient. To overcome this problem, Teflon mixing chambers shown in Fig. 4.14 were fabricated. These mixing chambers were of 4 cm, 5 cm, 7 cm, and 10 cm diameters. Height of 5 cm chamber was found to be suitable for proper mixing.

Fig. 4.13. PRB fitted on conventional stove with steel mixing chamber

Fig. 4.14. Different types of mixing chambers

4.4.5 Burner casing

As illustrated in Fig. 4.13, alumina paste was applied on the periphery of burner and preheater as casing, which acts as an insulator for heat transfer. Later this arrangement was found to not effective. As a first attempt, the burner casing was made with the cast iron (Fig. 4.15a) to have better mechanical strength. However, due to high thermal conductivity of cast iron, the conduction loss was found more and due to heating, the burner casing was getting red hot, which was undesirable. Later, the burner casing was fabricated with using fine alumina powder and sodium silicate as binder (shown in Fig. 4.15b). But after a long run, the alumina casing was found to develop thermal crack and therefore, it cannot be used for long term application. Finally, as shown in Fig. 4.15c, the burner casing was fabricated with castable cement with water. This special type of castable cement is having very good thermal shock resistance and low thermal conductivity. Since, the casing made of castable

cement was found to have best features and hence, all parametric analyses have been carried employing this casing.

a. Cast iron b. Alumina c. Castable cement

Fig. 4.15. Burner Casing of different materials

4.4.6 Working principle of self-aspirated domestic LPG cooking stove with PRB

A schematic of the experimental set-up used for testing the performance of PRB based self – aspirated LPG cooking stove is shown in Fig 4.16. A 19.5 kg LPG commercial cylinder was connected to a pressure regulator and then with a coriolis flow meter (accuracy± 0.001 g) between to the burner. The fuel flow rate was monitored using a suitable flow control valves. LPG passes through an orifice in the burner port. Due to the venturi effect, the high velocity LPG jet creates a low static pressure near the burner port and this causes suction of primary air through the two primary air slots. Air and gas moves via burner port through a mixing chamber it reacehs to the burner casing. Using an igniter, the combustion is ignited. The combustion is taking place inside the PRB. After some time, the PRB becomes the fully red hot (shown in Fig 4.17). Photographic view of experimental setup measuring emissions and thermal efficiency has been shown in Fig 4.18 and Fig 4.19 respectively. It was tested for more than 2 hours and no flashback was observed. To overcome the heat loss by radiation, a conical ring shown in Fig. 4.16 is provided, which is acting as a radiation shield. With different port diameters and orifice diameters, the parametric analyses have been carried out. The parametric analyses includes the estimation of thermal efficiency, CO and NOx emissions and measurement of temperature distributions.

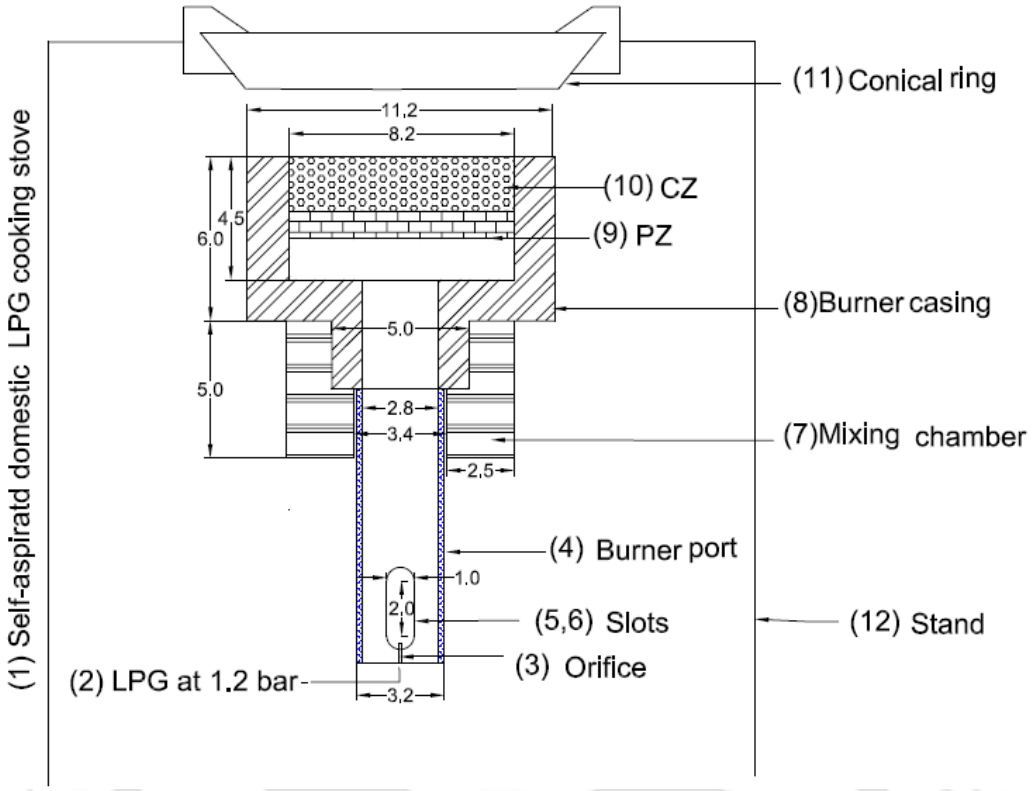

Fig. 4.16. Schematic of self-aspirated domestic LPG cooking stove with PRB

a. PRB stove b. Air-entrainment c. PRB with radiation shield

Fig. 4.17. Photographic views of different parts of the experimental setup

Fig. 4.18. Photographic view of experimental setup - for measuring emissions

Fig. 4.19. Photographic view of experimental setup – for measuring thermal efficiency

4.4.7 Specification of self-aspirated domestic LPG cooking stove with PRB

The complete assembly as shown in Fig. 4.16. Self-aspirated domestic LPG cooking stove with two-layer PRB (1) consisting of (2) pressure regulator that delivers LPG at 1.2 bar gauge pressure, (3) orifice of diameter = 0.35 mm and 0.50 mm, (4) burner ports of different internal diameter (viz. 17, 19, 21 mm), (5,6) slots length of 30 mm and slot width of 10 mm, The mixing chamber (7) made of Teflon length 50 mm and outer diameter 75 mm is made in two sections each of length 25 mm. The burner casing (8) of castable cement is of total length 85 mm is made in two sections. The bottom section of length 30 mm has inner diameter 28 mm and outer diameter 50 mm. The top section of length 55 mm is of inner diameter 82 mm and outer diameter 112 mm. Up to length 25 mm of the bottom section of the casing is inserted in the mixing chamber. The preheating zone (9) made of alumina porous matrix of diameter 80 mm and thickness 10 mm with through holes (1.5 mm diameter 204 holes) is fixed at 10 mm from the bottom of the upper section of the burner casing. The combustion zone (10) made of silicon carbide with diameter 80 mm and thickness 20 mm is placed over the preheating zone.

4.4.8 Stability of PRB based on experimental analysis

It has been found that by decreasing the orifice diameter, the amount of air entrained can be increased and hence the air-fuel mixture velocity increases. There are two phenomena occurring in burner, one is flash-back (FB) another is flame lift-off (FL). When the burning velocity is higher than the incoming air-fuel mixture velocity, FB is taking place. And when the mixture velocity is higher than burning velocity, FL is occurring on the surface of the burner. Therefore, for stable operation for any PRB there should not be any FB and FL. So a comprehensive experimental analyses have been done to avoid these two effects. For each burner port and orifice diameter, the stability analyses have been done and same has been

presented in Table 4.1. For an orifice diameter of 0.25 mm, the FL was observed and hence, it was not suitable with any of port diameter. Orifice diameter 0.35 mm was best suitable. The stability analyses have also been carried out for different supply pressures. It has been observed that LPG regulator with supply pressure of 1.2 bar gauge was best suitable for present work.

Table 4.1 Stability analysis of PRB for different orifice diameters and port diameters

S.No.	Port internal diameter (D_P) in mm	Orifice diameter (D_I) in mm		
		0.25	0.35	0.50
1.	17	FL	Stable	FB
2.	19	FL	Stable	Stable
3.	21	FL	Stable	Stable

4.5 Results and discussions for self-aspirated Porous Radiant Burner

Thermal efficiency and emission tests have been carried out employing different orifice diameters and port diameters. The temperature distribution along axial and radial directions have also been measured.

4.5.1 Thermal efficiency

Fig. 4.20 shows thermal efficiencies of the PRB at different thermal loads for different port diameters and orifice diameters. In the PRB, because of conduction and radiation, the combustion is improved. This leads to higher thermal efficiency. It is seen from Fig. 4.20 that at the same power input due to improved air-entrainment the thermal efficiency was increasing with increasing port diameter. Because the air supplied is more and this leads to better combustion and hence the higher thermal efficiency.

For higher input, the thermal efficiency is decreasing due to net heat output is decreasing sharply (due to heat loss) as comparison to power input. Further, at smaller orifice diameter (0.35 mm), the downward shifting of the reaction zone takes place, and this augments the volumetric heat release. It can be seen that the maximum thermal efficiency of the PRB is 75.1% for port diameter 21 mm and orifice diameter 0.35 mm at thermal load 1 kW.

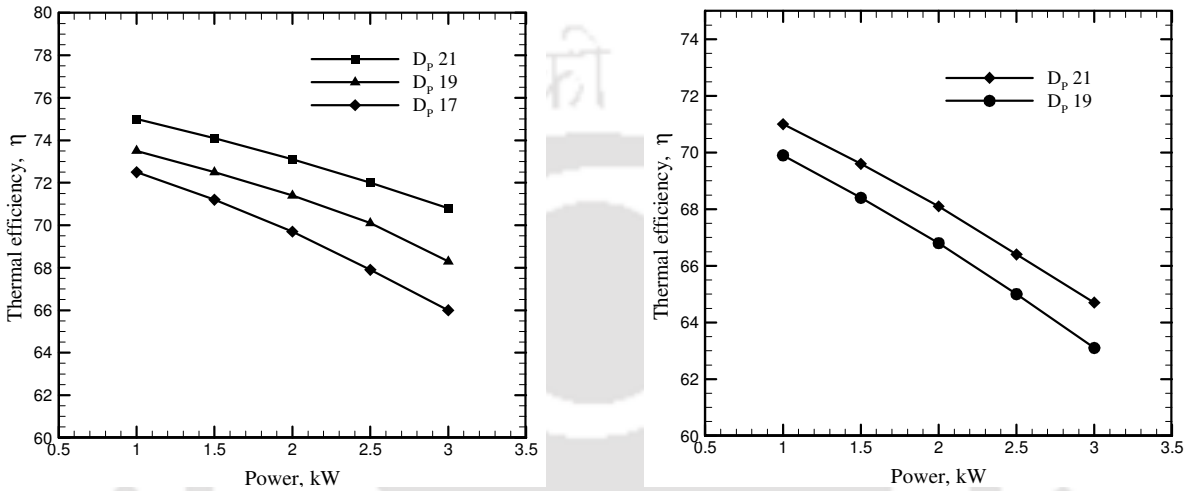

a. Orifice diameter(D_I) = 0.35 mm b. Orifice diameter(D_I) = 0.50 mm

Fig. 4.20. Thermal efficiency for different orifice diameters and port diameter (D_P)

4.5.2 Emissions analysis

In this study, the CO and NOx emissions were measured by using Greenline 8000 portable flue gas analyzer. The sampling was done as prescribed in the BIS: 4246:2002. The CO and NOx emissions measured for CB at different power inputs (1-3 kW) was shown in Fig. 4.5. It is to be noted that in the CB, with lean combustion, the undesirable feature of the flame lift-off occurs. To avoid this, conventional LPG cooking stove is designed for a fuel rich combustion and hence the emissions are high.

With input power in the range 1-3 kW, the CO and NOx variations of PRB with different ports and orifice diameters are shown in Figs. 4.21 and Fig. 4.22, respectively. For a given

thermal load, the CO emission is found to increase with decrease in port diameter. With increasing port diameter and reducing orifice diameter, due to improved air-entrainment, fuel gets sufficient air to combust, so the CO emission is found less.

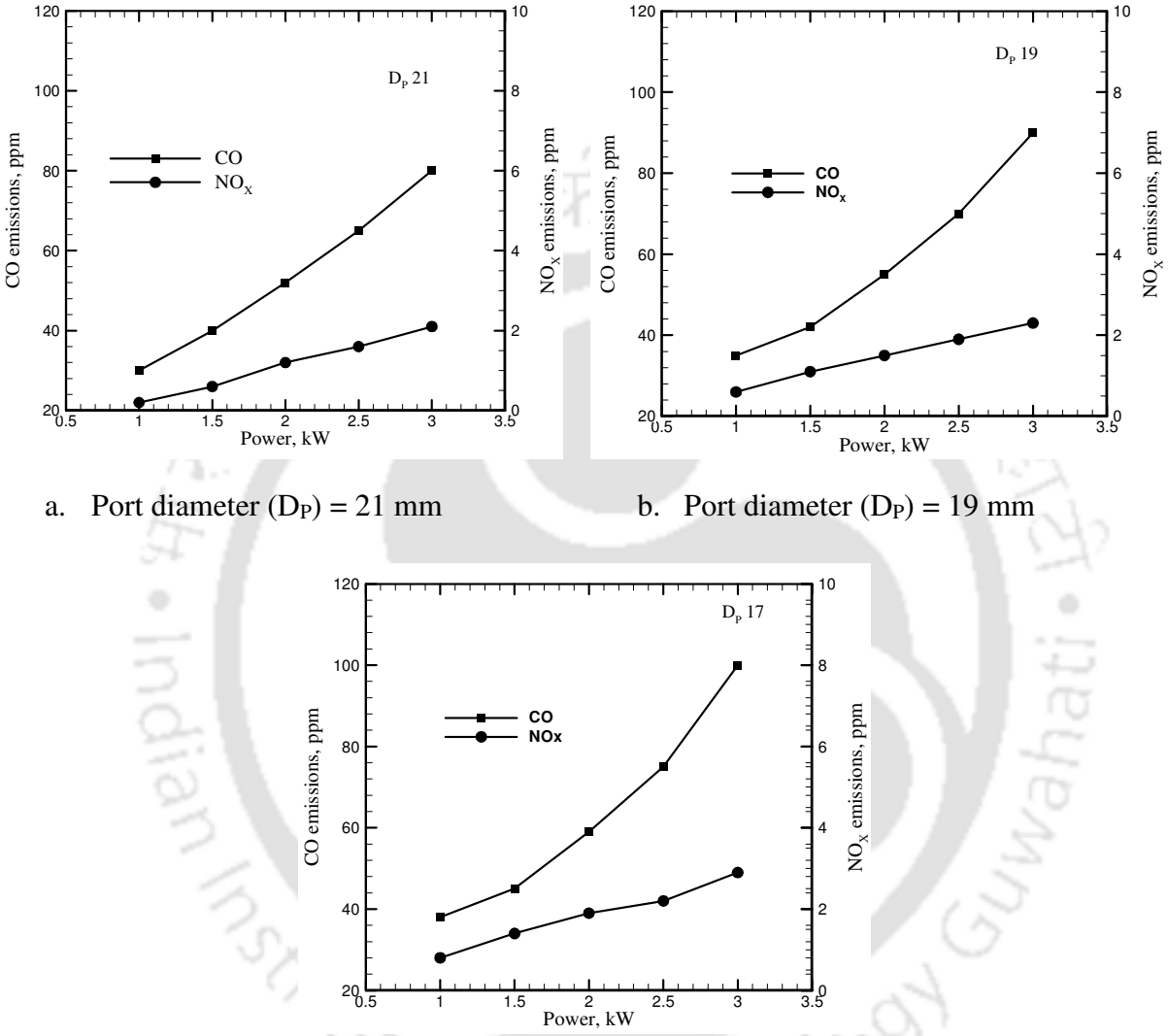

a. Port diameter (D_P) = 21 mm

b. Port diameter (D_P) = 19 mm

c. Port diameter (D_P) = 17 mm

Fig. 4.21. Emissions characteristics of PRB with an orifice diameter (D_I) 0.35 mm and different port diameters (D_P)

The measured emissions are lower than the CB, due to improved combustion and increase in residence time. In the PRB, due to the lower global temperature (surface temperature of the burner), the NO_X emission is also found to be much lower than that of the CB.

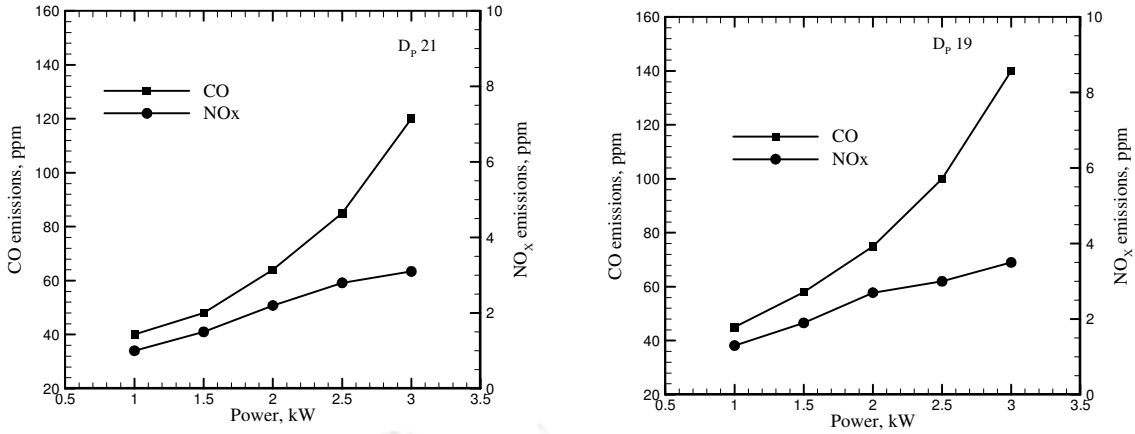

a. Port diameter (D_P) = 21 mm b. Port diameter (D_P) = 19 mm

Fig. 4.22. Emissions characteristics of PRB with an orifice diameter 0.50 mm and different port diameters

4.5.3 Temperature distributions

In the PRB, temperature distributions were measured in both axial (Fig. 4.23) and radial (Fig. 4.24) directions. K-type thermocouples were employed in axial and radial directions and the respective thermocouple positions are shown in Figs. 4.23a and 4.24a, respectively. Outputs of the thermocouples were acquired through a data acquisition system.

With port diameter 21 mm and orifice diameter 0.35 mm, the axial temperature distributions in the PRB are shown in Fig. 4.23b. Temperatures at locations T0, T1, T2 and T3 (Fig. 4.23a) are corresponding to the temperatures of the mixing chamber, the preheating zone, the reaction zone and the combustion zone. Radially 1.0 cm from the circumference of the burner, these axial positions of thermocouples are at 0.0, 0.8, 1.3, and 2.3 cm, respectively from the base of the ceramic matrix. In the mixing chamber (location T0), temperature in the range of 60 to 80 °C is well below the ignition temperature of LPG. This ensures no flash-back from the PRB. In the preheating zone at location T1, temperature is found in the range of 540 to 560°C. Because of conduction and radiation, a significant preheating of air-fuel mixture is observed. The maximum temperature in the reaction zone

at location T2 ranges between 980 to 1010°C. At any location, with increase in the input power, temperature increases. Radiation and conduction in the PRB, in one hand preheats the incoming air-fuel mixture, and on the other, helps faster transfer of heat from the reaction zone in the downward direction, and as a result, the temperature rise is lower.

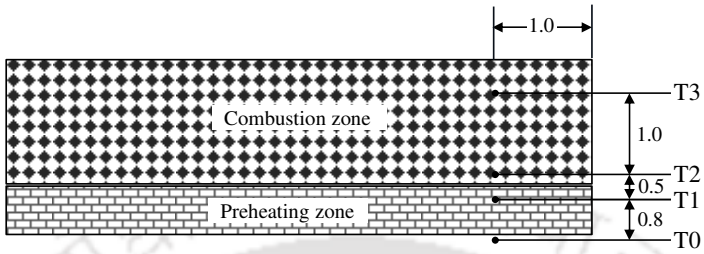

All dimensions are in cm

a. Axial positions of thermocouple in the PRB

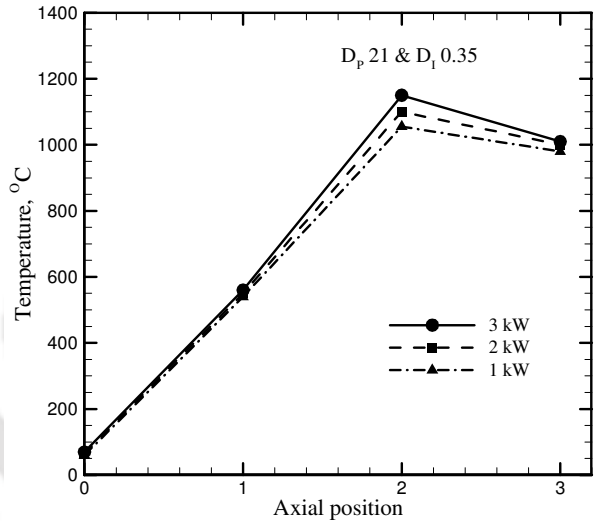

b. Axial temperature distributions in PRB

Fig. 4.23. Axial positions of thermocouple and temperature distribution

Radial temperature distributions in the PRB for different thermal loads in the range 1-3 kW with port diameter 21 mm and orifice diameter 0.35 mm are shown in the Fig. 4.24b. For measurement of the radial temperature distribution, thermocouple measuring point was located 2.0 mm from the top surface as shown in Fig. 4.24a. The maximum temperature

difference between centres to periphery is found to be 115°C which showed the radial temperature distribution of the PRB was almost uniform.

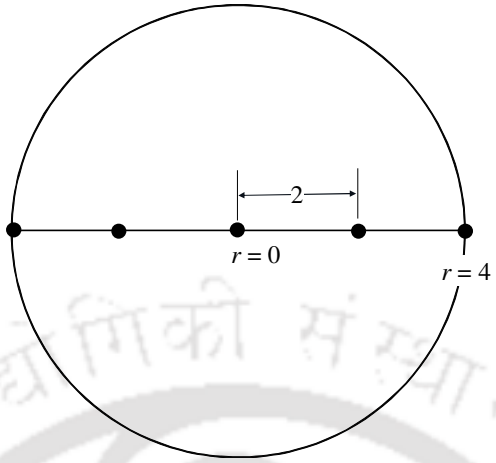

a. Radial positions of thermocouples on top surface of the PRB

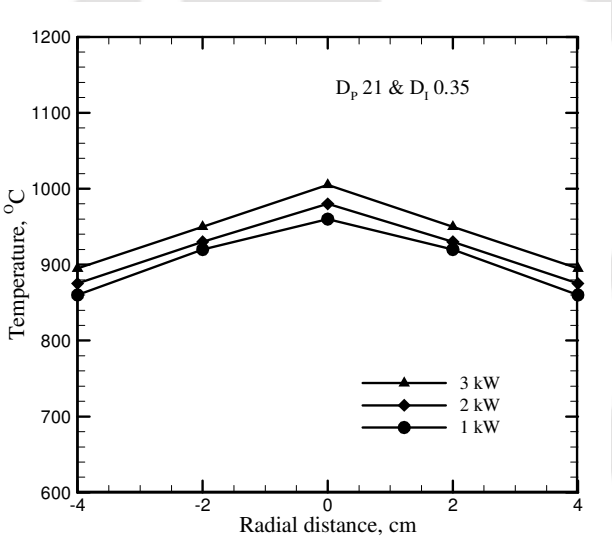

b. Radial temperature distribution

Fig. 4.24. Radial positions of thermocouple and temperature distribution

4.6 Summary

Performances analyses of a self-aspirated domestic LPG cooking stove (1-3 kW) with a two-layer PRB have been carried out in terms of thermal efficiency, CO and NOx emissions characteristics. It was found that the maximum thermal efficiency of the PRB was 75.1% for a port diameter 21 mm and an orifice diameter 0.35 mm at thermal load 1 kW, whereas

for same power input the maximum thermal efficiency of CB was found 68%. Therefore, a substantial amount of LPG can be saved by using self-aspirated domestic LPG cooking stove with a two-layer PRB. The measured CO and NOx emissions of the presently developed PRB stove were found in the ranges 30-140 ppm and 0.2-3.5 ppm respectively. Whereas CO and NOx emissions from conventional domestic LPG cooking stoves (1 – 3 kW) are in the range of 220 ppm to 550 ppm and 5 ppm to 25 ppm, respectively. As it is self-aspirated, it works on the natural draft. It perfectly suits for domestic LPG cooking applications.

Chapter 5

Self-aspirated Porous Radiant Burner for Medium-scale LPG Cooking Applications

In this chapter, the design and fabrication details of self-aspirated PRB for medium-scale LPG cooking stove and their performance parameters such as thermal efficiency and emission characteristics at different input powers (5-15 kW) are presented. Temperature distributions measured both in radial and axial directions of the PRB are also presented.

5.1 Proto-type of conventional medium-scale LPG stove with PRB

Fig. 5.1a shows the pictorial view of the medium scale conventional LPG stove. The medium-scale conventional LPG cooking stove works on the same principle as conventional domestic cooking stove which is already explained in Chapter 1. For medium-scale LPG stove multi orifices (four) are used instead of a single orifice. As shown in Fig.5.1b, the air entrainment is taking place through the slots and then mixture is going to the burner via a mixing chamber and then combustion takes place over the burner head.

As shown in Fig. 5.2, by using the same mixing chamber with SiC matrix as a CZ placed over the mixing chamber, the initial trial of PRB concept was tested. While performing the tests with above arrangements, it was found that there hasn't been a problem of secondary air entrainment. But, the porous radiant burner was not getting fully red hot. With the above arrangements, after 10 - 15 min operation, flash back was found to occur. This was mainly due to less air-fuel mixture (lack of sufficient air entrainment) velocity and overheating of

mixing chamber. As illustrated in Fig. 5.1b and 5.1c, in the CB, LPG is passing through four orifices, which are welded in the same base plate (Fig. 1c). It was observed that with this arrangement, the venturi effect was not effective for all the orifices. Thus, there must be proper air–entrainment system.

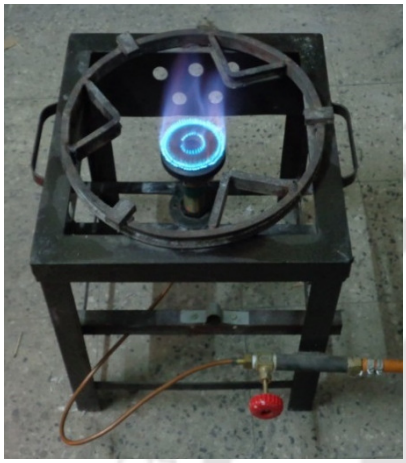

a. Medium-scale conventional LPG cooking stove

b. Mixing chamber with base plate

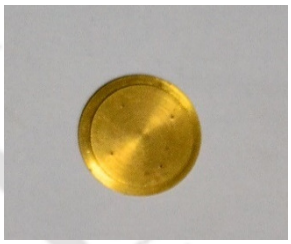

c. Base plate

Fig. 5.1. Different parts of the medium-scale conventional LPG cooking stove

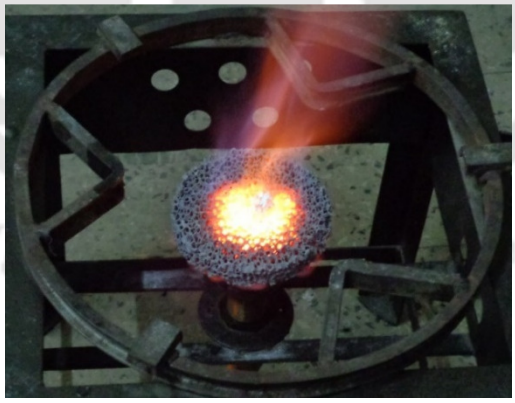

Fig. 5.2. Pictorial view of the SiC matrix as a burner in conventional stove

Therefore, proper air-entrainment system is need to be redesigned for getting lean and improved combustion. As concluded in Chapter 3, for getting higher thermal efficiency,

the leaner air-fuel mixture is necessary for the PRB. A lean mixture can be obtained by a higher amount of air entrainment.

5.2 Development of self–aspirated medium-scale LPG cooking stove with PRB

As discussed in Chapter 4, the best thermal performance was achieved with a port diameter of 21 mm and an orifice diameter of 0.35 mm. So for the development of PRB for medium scale application, the same dimensions have been chosen. For getting more air-entrainment, the four orifices were connected to four different LPG pipe lines. So that more air-entrainment can take place with all four burner ports separately. All four pipe line were connected to a single main LPG supply with three metallic T joints. The four orifices were fitted with a common base plate (Fig.5.3a). As shown in Fig.5.3 b, the four ports were welded with a connector, which connect the four ports with a mixing chamber. When the high velocity LPG is passed through these orifices, due to venturi effect, the air is getting entrained through slots made in ports. Then via connector, the air-fuel mixture passes through a mixing chamber. The air-fuel mixture passes through a mixing chamber and reaches the burner casing.

a. Base plate with four orifices b. Burner ports with connector

Fig. 5.3. Pictorial view of base-plate and burner ports assembly

5.2.1 Specification of self-aspirated medium-scale LPG cooking stove with PRB

The complete assembly has been shown in Fig. 5.4. Self-aspirated medium-scale LPG cooking stove with two-layer PRB (1)The complete assembly consisting of (2) pressure regulator that delivers LPG at 1.5 bar gauge pressure, (3) orifice of diameter = 0.25 mm and 0.35 mm, (4) slots (10 ×30), (5) four burner ports (ID = 21 mm, OD = 23 mm, vertical length = 90 mm) made of copper, (6) connector made of mild steel (length = 60 mm, thickness = 2 mm, length of the bottom portion = 30 mm, OD of the bottom portion = 60 mm, ID of the top portion = 30 mm, (7) mixing chamber of Teflon (bottom portion: length = 30 mm, ID = 25 mm; middle portion: length = 30 mm, ID = 25 mm, OD = 75 mm; top portion: length = 30 mm, ID = 45 mm, OD = 75); (8) casing made of castable cement (bottom portion: length = 30 mm, ID = 25 mm; top portion: length = 70 mm, ID = 122 mm, OD = 152 mm), (9) preheating zone made of alumina porous matrix (pore diameter: 1.5 mm, number of pores: 463; diameter: 120 mm, thickness: 10 mm) and (10) combustion zone made of silicon carbide porous matrix (porosity: 90%, diameter: 120 mm, thickness: 25 mm).

5.3 Stability analysis of PRB

A comprehensive experimental analysis has been carried out for investigation the stability of PRB based medium-scale LPG cooking stove. As discussed in Chapter 4, the best thermal performance was achieved with port diameter of 21 mm. Therefore, the port diameter of 21 mm was fixed in present analysis. But the orifice diameters was varied (viz, 0.25, 0.35, 050 mm) and the stability analysis has been carried out. With orifice diameters of 0.25 and 0.35 mm burner were found stable, whereas in case of 0.50 mm orifice diameter the flash back was found to occur. It was observed that an orifice diameter of 0.25 mm and 0.35 mm showed stable operation. The stability analysis has also been carried out by

varying the supply pressure. It has been observed that LPG regulator with supply pressure 1.5 bar gauge was showing stable operation for present work.

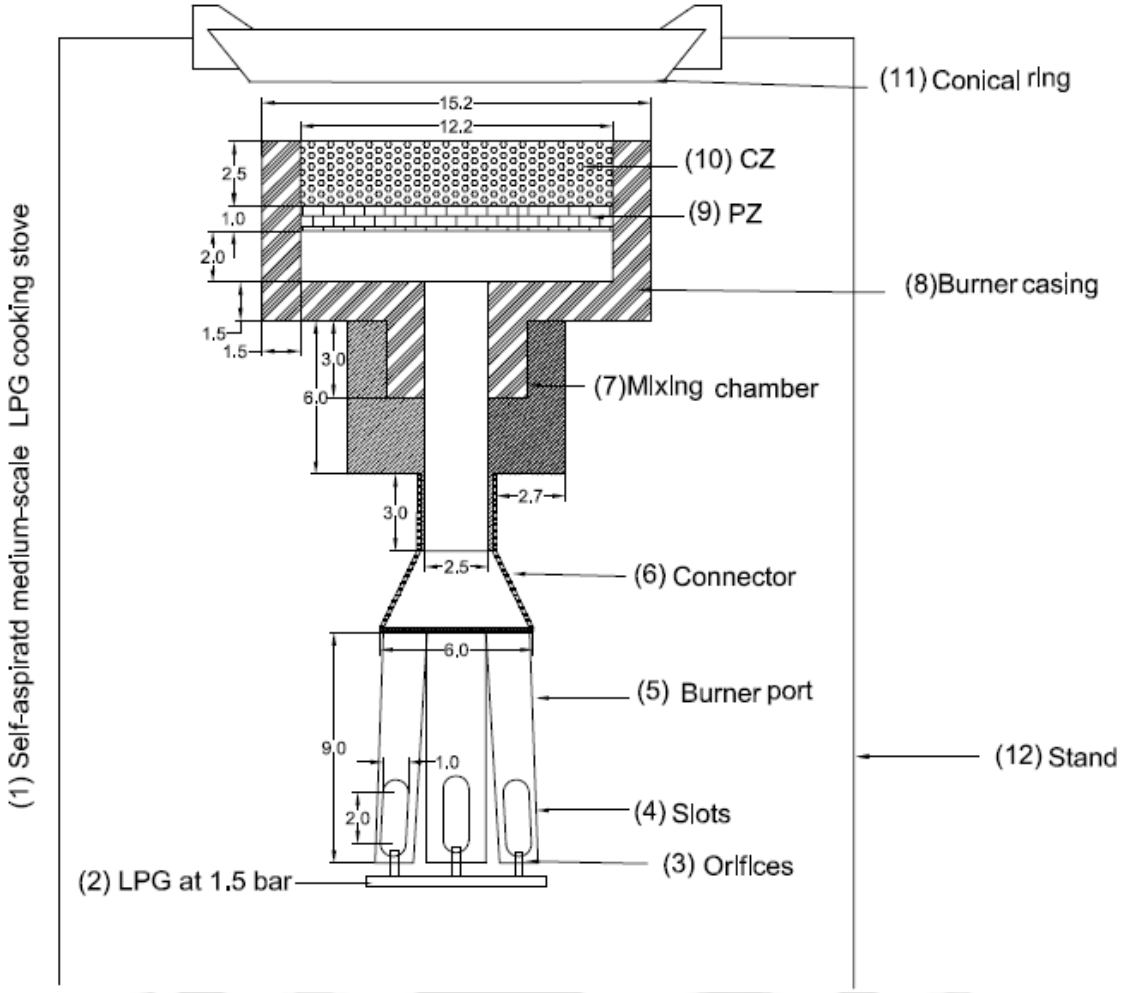

All dimensions are in cm

Fig. 5.4. Schematic of self-aspirated medium-scale LPG cooking stove with PRB

As discussed in Chapter 3, with increase in thickness of combustion zone and reduction in pore size of the preheater, the power rating of the burner can be increased. For getting higher power rating 5-15 kW, the pore size of alumina matrix was reduced and thickness was increased. Combustion zone is of high porosity of thickness 25 mm and diameter 120 mm, and the preheating zone consists of low porosity (pore size 1.5 mm) alumina ceramic matrix of thickness 10 mm diameter 120 mm are used for present work as shown in Fig.5.5.

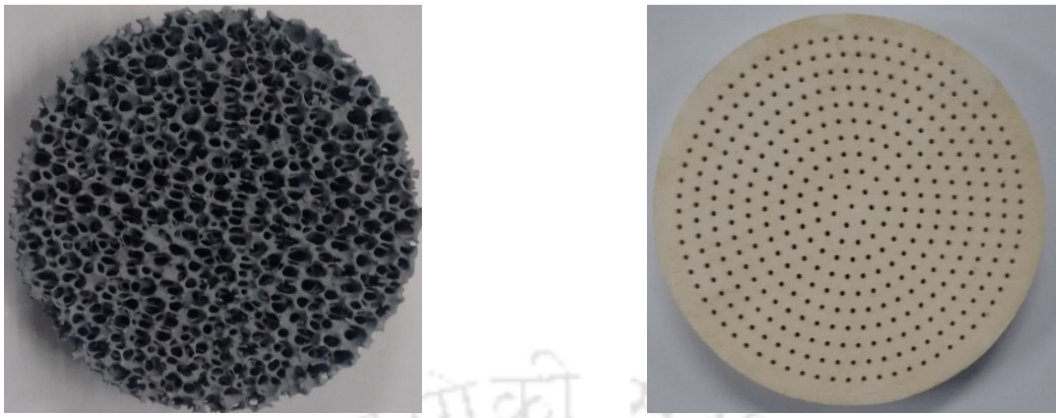

a. SiC matrix **b.** Alumina matrix

Fig. 5.5. Pictorial views of (a) combustion zone(SiC) and (b) preheating zone (alumina matrix)

5.4 Working principle of self-aspirated medium-scale LPG cooking stove with PRB

A schematic of the experimental set-up used for testing the performance of PRB based self–aspirated LPG medium-scale cooking stove is shown in Fig 5.4. A 19.5 kg LPG commercial cylinder was connected to a high pressure regulator and then with a coriolis flow meter (accuracy ± 0.001 g) between to the burner. The fuel flow rate was monitored with suitable flow control valves. The fuel is supplied in single main supply line which is connected through all four pipes line by metallic T joints. Each of pipe line connected with an orifice. LPG reaches the burner ports through their respective orifice. Due to venturi effect, the high velocity LPG jet creates a low static pressure near the burner ports and this causes the suction of primary air through the two primary air slots. Air and LPG mixes in the burner ports and through connector and mixing chamber it reches to the burner casing. Through igniter the combustion is initiated. The combustion is taking place inside the PRB. After some time the PRB becomes the fully red hot (Fig 5.6c), experiments were performed for more than two hr and no flashback was reported.

In order to overcome the heat loss by radiation, a conical ring was provided, which acted as a radiation shield. With different orifice diameters, the parametric analyses have been carried out. The parametric analyses includes estimation of thermal efficiency, and measurements of CO and NOx emissions and axial and radial temperature distributions. Thermal efficiencies of the self-aspirated PRB stoves were estimated by conducting the water boiling test (discussed in Chapter 3). Pictorial view of the experimental set up is shown in Fig. 5.7. For the emission measurements, the flue gas sampling was done according to the IS: 4246. The details of the emission measurement has been already presented in Chapter 3. Pictorial view of the experimental set up used for measuring emission is shown in Fig. 5.8.

(a) PRB stove

(b) Air-entrainment

(c) Red hot PRB with radiation shield

Fig. 5.6. Different parts of experimental setup

Fig. 5.7. Pictorial view of the experimental set up- for measuring thermal efficiency

Fig. 5.8. Pictorial view of the experimental set up- for measuring emissions

5.5 Results and discussions for self-aspirated Porous Radiant Burner

Thermal efficiency and emission tests were carried out employing different orifice diameters. The temperature distribution along axial and radial directions have also been measured.

5.5.1 Thermal efficiency

Fig. 5.9 shows thermal efficiencies of the PRB estimated for different thermal loads at different orifice diameters. In the PRB, because of conduction and radiation, the combustion is improved. This leads to higher thermal efficiency. It is seen from Fig. 5.9 that at the same power input, due to improved air-entrainment, the thermal efficiency is found to be higher at lower orifice diameters. Because of supplied air is more and this leads to better combustion and hence the higher thermal efficiency. For higher input, the thermal efficiency is decreasing due to net heat output is decreasing sharply as comparison to power input.

Further for smaller orifice diameter (0.25 mm), the downward shifting of the reaction zone takes place, and this enlarges the volumetric heat release. It can be seen that at a thermal load 5 kW, the maximum thermal efficiency of the PRB is 55% for port diameter 21 mm and orifice diameter 0.25 mm. lowest thermal efficiency reported was 44% at 15 kW with orifice diameter 0.35 mm. For same the power input, the thermal efficiency of conventional medium scale burner was found to be 30%. The details of thermal efficiency of conventional medium-scale stove have already been presented in Chapter 3.

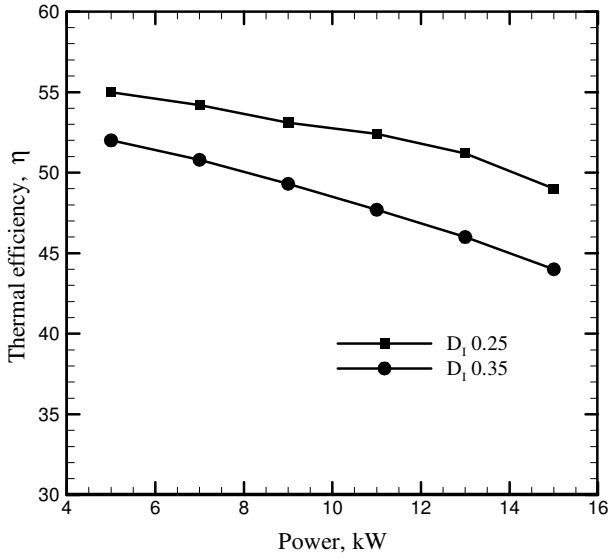

Fig. 5.9. Thermal efficiency of self-aspirated medium-scale LPG cooking stove with PRB for different power inputs

5.5.2 Emissions analysis

In present study, the CO and NOx emissions were measured by Greenline 8000 portable flue gas analyzer. The sampling was done as recommended in the BIS: 4246:2002. The CO and NOx emissions measured for medium-scale CB were discussed in Chapter 3. It is to be noted that in the CB, with lean combustion, the undesirable feature of the flame lift-off occurs. To avoid this, conventional LPG cooking stove is designed for a fuel rich combustion and hence the emissions are high. With input power in the range 5-15 kW, in the PRB, CO and NOx variations with different orifice diameters are shown in Figs. 5.10. With reducing orifice diameter, due to improved air-entrainment, fuel gets sufficient air to combust, so the CO emission is found less.

The measured emissions are lower than the CB, due to improved combustion and increase in residence time. In the PRB, due to the lower global temperature (surface temperature of the burner), the NO_X emission is also found to be much lower than that of the CB. The CO

emissions of PRB were found in the range 60 – 190 ppm and NOx emissions were in the range of 2 – 10 ppm.

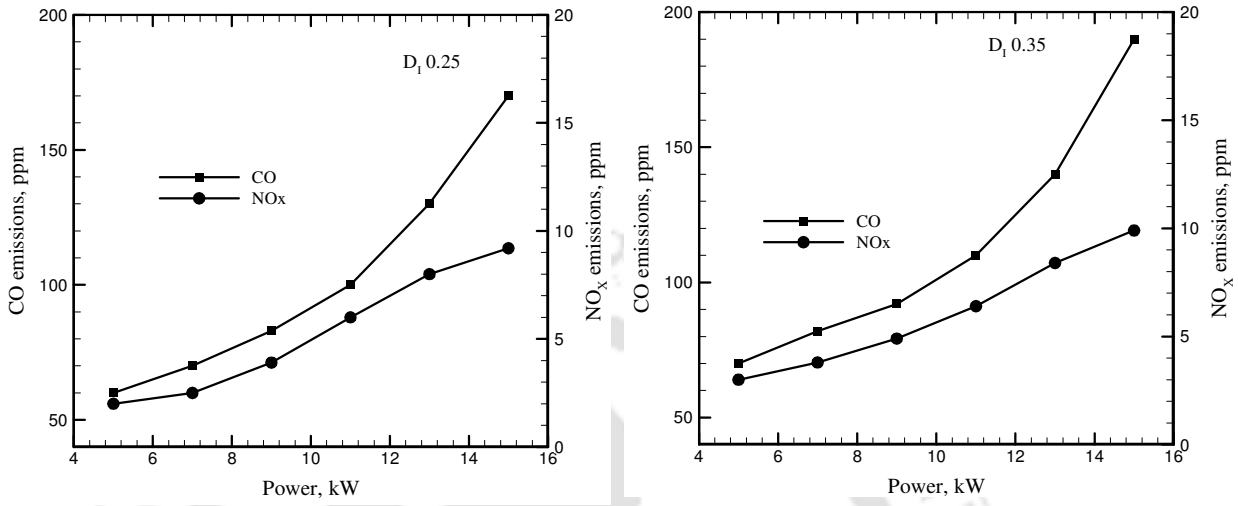

(a) (b)

Fig. 5.10. Emissions of self-aspirated medium-scale LPG cooking stove with PRB for different power inputs with orifice diameter (a) $D_I = 0.25$ and (a) $D_I = 0.35$.

5.5.3 Temperature distributions

In the PRB, temperature was measured in both axial (Fig. 5.11a) and radial (5.11b) directions. K-type thermocouples were used for both axial and radial directions temperature measurements and their respective positions are shown in Figs. 5.11a and 5.11b. Outputs of the thermocouples were acquired through a data acquisition system.

With port diameter 21 mm and orifice diameter 0.25 mm, the axial temperature distributions in the PRB are shown in Fig. 5.12a. Temperatures at locations T0, T1, T2 and T3 (Fig. 5.11a) are correspond to the temperatures of the mixing chamber, the preheating zone, the reaction zone and the combustion zone. Radially 2.0 cm from the circumference of the burner, these axial positions of thermocouples are at 0.0, 0.8, 1.3, and 3.0 cm, respectively from the base of the ceramic matrix. In the mixing chamber (location T0),

temperature in the range of 60 to 80 °C is well below the ignition temperature of LPG. This ensures no flash-back from the PRB. In the preheating zone at location T1, temperature is found in the range of 560 to 580 °C. Because of conduction and radiation, a significant preheating of air-fuel mixture is observed. The maximum temperature in the reaction zone at location T2 ranges between 1150 to 1370°C. This is owing to maximum heat release rate takes place at the reaction zone. At any location, with increase in the input power, temperature increases. Due to radiation and conduction in the PRB, in one hand preheats the incoming air-fuel mixture, and on the other, helps faster transfer of heat from the reaction zone in the downward direction, and as a result, the temperature rise is lower. Radial temperature distributions in the PRB for different thermal loads in the range 5-15 kW with port diameter 21 mm and orifice diameter 0.25 mm are shown in the Figs. 5.12b. For measurement of the radial temperature distribution, thermocouple measuring point was located 2.0 mm from the top surface (5.11b). The temperature difference between centres to periphery is found in between 130 to 230 °C.

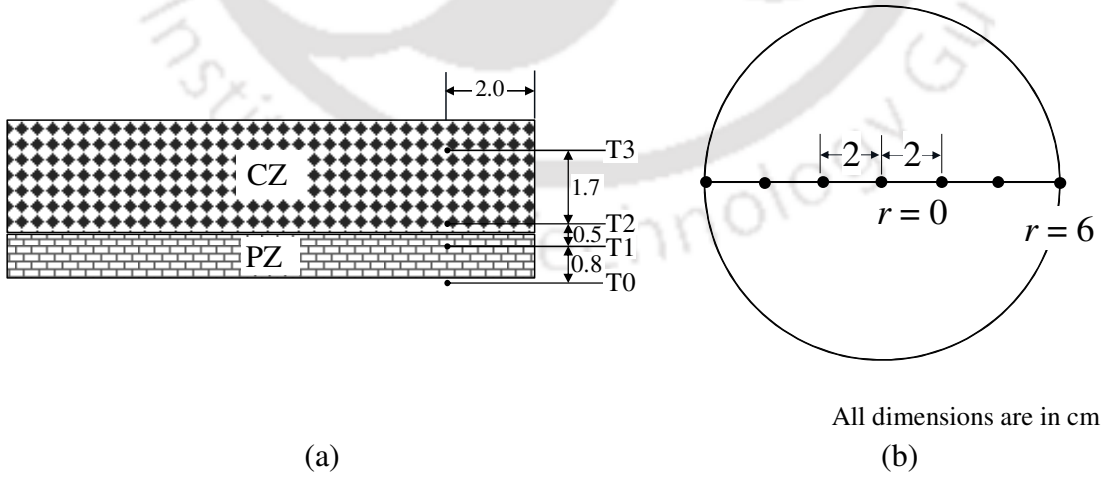

Fig. 5.11. Schematic of (a) Axial and (b) radial locations of thermocouples in the PRB

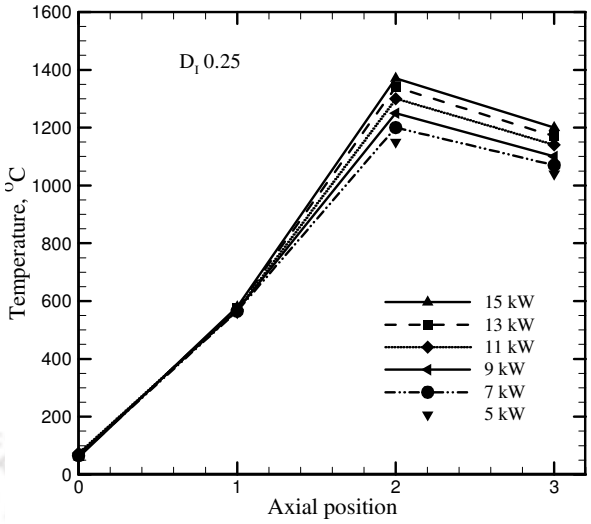

(a)

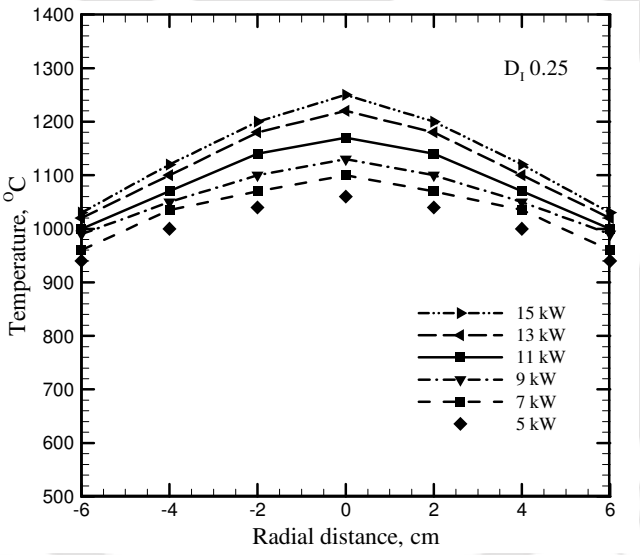

(b)

Fig. 5.12 (a) Axial and (b) Radial temperature distribution in PRB

5.6 Summary

Performances in terms of temperature distributions, thermal efficiency and CO and NOx emissions of a self-aspirated medium scale (5-15 kW) LPG cooking stove with a two-layer PRB were experimentally investigated. It was found that the maximum thermal efficiency

of the PRB was 55% for a port diameter 21 mm and an orifice diameter 0.25 mm at thermal load 5 kW. Significant amount of LPG can be saved by using self-aspirated medium scale LPG cooking stove with a two-layer PRB. The measured CO and NOx emissions of the presently developed PRB stove were found in the ranges 60-190 ppm and 2-10 ppm respectively. Whereas CO and NOx emissions from conventional medium-scale LPG cooking stoves are in the range of 355 ppm to 1165 ppm and 28 ppm to 110 ppm, respectively. As it is self-aspirated, it works on the natural draft, therefore it is perfectly suits for medium-scale LPG cooking applications.

Chapter 6

Conclusions and Future work

6.1 Conclusions

This chapter presents the important conclusions obtained from the various stages of self-aspirated porous radiant burner's development for domestic as well as medium-scale cooking applications. With an objective of improving the performance of the conventional LPG stove in terms of emissions and thermal efficiency, the concept of PMC was introduced. The geometrical parameters of the novel stoves were chosen on the basis of a series of parametric studies conducted to address some critical issues like air-entrainment (natural draft), combustion stability, etc.

In the Chapter3, the performances analyses have been carried out for the medium-scale LPG cooking stove with a porous radiant burner. With external air supply, the objective of the first study was to understand the stability range of the burner, and to fix the geometric and operating parameters. Performances in terms of temperature distributions, thermal efficiency and CO and NOx emissions of a two-layer medium scale (5 – 10 kW) LPG cooking stove with a PRB were experimentally investigated. For the purpose of comparison, the same parametric study was carried out with CB working in the FF combustion mode. The maximum axial temperature in the PRB was about 200 °C lower than that of the CB. The radial temperature distribution of the PRB was almost uniform. The temperature measurement has been done using both thermocouple and IR camera. Temperature measured by IR camera was found 21°C to 30°C higher than the K – type

thermocouple readings. At 5 kW power input, thermal efficiency of the PRB at equivalence ratio 0.56 was found to be 58 %, while it was 45% for the CB. CO and NOx emissions in the PRB were much lower than that with the CB. Improvements in efficiency leads to reduce fuel consumption and then which in turn implies reduced emission of CO_2.

It was concluded from the Chapter 3 of thesis work that significant amount of LPG can be saved by using PRB. But the main problem is the requirement of external air and which demand an external compressor or blower. This is not economical for domestic application. So, further research was needed to re-design the cooking stove which can be operated through natural draught.

The Chapter 4 of the study was devoted to the development of self-aspirated domestic LPG cooking stove with a porous radiant burner (PRB). Placement of porous matrix in the flow path adds to the flow resistance, and to overcome flow resistance, in previous studies, researchers have used the compressed air. This has been one of the major limitations in using the PRB in LPG cooking stoves. To overcome this limitation, the design modifications in terms of LPG supply pressure and dimensions of orifice, burner port, mixing chamber and burner casing were done. For power input 1-3 kW, LPG cooking stove with a PRB, for air entrainment, two slots in the burner port was introduced. The orifice diameter too was re-designed. The LPG supply pressure was increased to 1.2 bar (gauge). With the improved design of the burner assembly, thermal efficiency, emission characteristics and temperature distribution were measured for the power input in the range of 1 - 3 kW. Maximum thermal efficiency of self-aspirated domestic cooking stove with PRB, with port diameter 21 mm with orifice diameter 0.35 mm was 75% at 1 kW power input, which is 10 % higher than the best available CB. A significant improvement in thermal efficiency and a large reduction in emissions were observed.

The development of self-aspirated medium-scale PRB for LPG cooking stoves is the Chapter 5 of the study. For the medium scale (5 – 15 kW) LPG cooking stove with PRB, the design of the burner is completely different from the one with 1-3 kW considered in the second study, and also of the conventional ones of the same input power range (5 – 15 kW). Instead of one burner port in the previous one (1 -3 kW), to meet the requirement of large volume of air, four burner ports with four orifices were incorporated. Each of the four burner port was fitted with an orifice. All the four orifices were connected to the same LPG supply line. Performances in terms of temperature distributions, thermal efficiency and CO and NOx emissions of a self-aspirated medium scale (5-15 kW) LPG cooking stove with a two-layer PRB were experimentally investigated. It was found that the maximum thermal efficiency of the PRB was 55% for a port diameter 21 mm, an orifice diameter 0.25 mm and at thermal load 5 kW. For the same power input the thermal efficiency of conventional medium-scale burner was found 45%. Significant amount of LPG can be saved by using self-aspirated medium scale LPG cooking stove with a two-layer PRB. The measured CO and NOx emissions of the present developed stove were much lower than the CB.

For both self-aspirated domestic as well as medium-scale cooking stoves with PRB, the measured emissions were found lower than the CB. Significant amount of LPG can be saved by using developed LPG cooking stove with a two-layer PRB. Newly developed burners with PRB showed a steady-state operation without any flashback and blow-off. It was observed that the radial temperature distribution of the PRB was almost uniform. As both developed stoves are self-aspirated, they can be used for any type of LPG cooking applications. The significant amount of fuel can be saved by commercializing this product. For domestic application, the amount of fuel saving can be possible up to 10 % whereas for medium-scale, it can save up to 22 %.

6.2 Scopes for future work

The following are the scope for the future research work in the development of porous burners for domestic cooking applications.

- The newly developed PRB can be tested with biogas and also natural gas.
- For the further improvement in thermal efficiency of newly developed burner, the optical parameters need to be optimized.
- The PRBs need to be tested further to understand the effect of different burner materials and geometry of matrix.
- A numeral tool can be developed for investigating the combustion behaviour of PRB.

References

Abdelaal MM, Riedy MK and Nahas AM (2013), Effect of oxygen enriched air on porous radiant burner performance and NO emissions, *Exp. Therm Fluid Sci*, 45, 163–168.

Alexander M (2012), Radiant Burner, Patent No. US20120164590 A1.

Andersen F (1992), Heat transport model for fiber burners, *Prog. Energy Combust, Sci.* 18, 1-12.

Antonette D'Sa and Narasimha M KV (2004), Report on the use of LPG as a domestic cooking fuel option in India, *Int. Energy Initiative*, June.

Arai N, Shinoda M and Churchill SW (1999), The characteristics of heat recirculating burner, *Trans. CSME*, 23 (1B), 147-58.

Assmann M, Falkenreck U, Hecken HJ, Schlüter J and Weischedel W (2010), Burner arrangement, Patent No. US 20100104989A1

Avdic F (2004), Application of the porous medium gas combustion technique to household heating systems with additional energy sources, *Ph.D thesis*, Universität Erlangen-Nürnberg, Germany.

Babkin VS, Korzhavin AA and Bunaev VA (1991), Propagation of premixed gaseous explosion flames in porous media, *Combust. Flame*, 87, 182-90.

Baek SW (1989), The premixed flame in a radiatively active porous medium, *Combust. Sci. Technol.*, 64, 277-87.

Barra AJ, Diepvens G, Ellzey JL and Henneke MR (2003), Numerical study of the effects of material properties on flame stabilization in a porous burner, *Combust. Flame*, 134, 369-79.

Barra AJ and Ellzey JL (2004), Heat recirculation and heat transfer in porous burners, *Combust. Flame*, 137, 230-41.

Basic Statistics on Indian Petroleum & Natural Gas, Annual Report (2013-2014), Ministry of Petroleum & Natural Gas, Government of India.

Basu D, Saha R, Ganguly R and Datta A (2008). Performance improvement of LPG cook stoves through burner and nozzle modifications. J. Energy Institute, 81, 218-222.

Basu P, Kefa C and Jestin L (2000), Boilers and Burners: Design and Theory, Springer, New York, 563.

Bellucci V, Meili F, Paschereit OC and Schuermans B (2006), Premixburner, Patent No. US 20060101825.

Bingue JP, Saveliev AV, Fridman AA, and Kennedy LA (2002), Hydrogen production in ultra-rich filtration combustion of methane and hydrogen sulfide, *Int. J. Hydrogen Energy*, 27, 643-49.

Bingue JP, Saveliev AV and Kennedy LA (2004), Optimization of hydrogen production by filtration combustion of methane by oxygen enrichment and depletion, *Int. J. Hydrogen Energy*, 29, 1365-70.

Boggavarapu P, Ray B and Ravikrishna RV(2014). Thermal Efficiency of LPG and PNG-fired burners: Experimental and numerical studies. *Fuel,* 116, 709–715.

Bone WA (1912), Surface combustion, *J. Franklin Inst.*, 173, 101-31.

Bouma PH and De Goey LPH (1999), Premixed Combustion on ceramic foam burners, *Combust. Flame,* 119, 133-43.

Bouma PH, Eggels RL, DE Goey LPH, Nieuwenhuizen JK and Vander Drift AA (1995), Numerical and experimental study of the NO-emission of ceramic foam surface burners, *Combust. Sci. Technol*., 108, 193-203.

Bowman CT (1975), Kinetics of Pollutant Formation and Destruction in Combustion, *Prog. Energy Combust. Sci.*, 1, 33-45.

Brenner G, Pickenacker K, Pickenacker O, Trimis D, Wawrzinek K and Weber T (2002), Numerical and experimental investigation of matrix-stabilized methane/air combustion in porous inert media, *Combust. Flame,* 123, 201-13.

Bubnovich V and Toledo M (2007), Analytical modelling of filtration combustion in inert porous media, *Appl. Therm. En*, 27, 1144-49.

Buckmaster J and Takeno T (1981), Blow off and flashback of an excess enthalpy flame, *Combust. Sci. Technol*, 1981, 25, 153-58.

Byeonghun Y, Kum SM, Lee CE, Lee S (2013), Combustion characteristics and thermal efficiency for premixed porous-media types of burners, Energy, 53, 343-350

Chandra A, Presentation at World LPG Forum 2010, Madrid: http://www.petrofed.winwinhosting.net/upload/Apurva_Chandra.pdf retrieved on November 3, 2012.

Chen YK, Hsu PF, Lim IG, Lu ZH, Matthews RD, Howell JR and Nicholas SP (1988), Experimental and theoretical investigation of combustion within porous media, *22nd Int. Symp. on Combust.*, *The Combust. Inst.*, Seattle, U.S.A, Aug 14 -19 Poster Paper: 22, 207.

Chen YK, Matthews RD and Howell JR (1987), The effect of radiation on the structure of a premixed flame within a highly porous inert medium, *Radiation, Phase Change Heat Transfer and Thermal Systems,* ASME-HTD, 81, 35-42.

Cho KW, Han K, Lee YK, Noh DS, Yoon HM, Riu KJ and Lee KH (2001), Premixed combustion of coke oven gas in a metallic fibre mat, *Fuel*, 80, 1033-36.

Churchill SW (1989), Thermally stabilized combustion, *Chem. Eng. Technol.*, 12, 249-54.

Claerbout K, Dumortier G and Olalde V (2012), Improved radiant burner, Patent No. US 20110111356 A1.

Cookson EJ and Floyd II DE (2005), Application of reticulated metal foam to gas fired infrared burners, *4th Int. Conf. Porous Metals and Metal Foaming Technol. (JIMIC-4)*, Tokyo, Japan, September 21-23, 69-72.

Delalic N, Mulahasanovic Dz and Ganic EN (2004), Porous media compact heat exchanger unit–experiment and analysis, *Exp. Therm Fluid Sci.*, 28, 185-92.

Dillon J (1999), Combustion in porous media, LA-SUB-99-56 Final report. California Institute of Technology, Los Alamos National Lab, 1-27.

Dobrego KV, Gnezdilov NN, Kozlov IM, Bubnovich VI and Gonzalez HA (2005), Numerical investigation of the new regenerator–recuperator scheme of VOC oxidizer, *Int. J. Heat Mass Transfer*, 48, 4695-703.

Dobrego KV, Gnezdilov NN, Kozlov IM and Shmelev ES (2006), Numerical study and optimization of the porous media VOC oxidizer with electric heating elements, *Int. J. Heat Mass Transfer*, 6, 1-10.

Dobrego KV, Gnezdilov NN and Kozlov IM (2007), Parametric study of recuperative VOC oxidation reactor with porous media, *Int. J. Heat Mass Transfer*, 50, 2787–94.

Durst F, Trimis D, and Dimaczek G (1996a), Burner having material of varying porosity, *United States Patent*, No: 5522723.

Durst F and Trimis D (1996b), Compact porous medium burner and heat exchanger for household applications, *E C project report* (contract no. JOE3-CT95-0019).

Durst F and Weclas M (2001), A new type of internal combustion engine based on the porous-medium combustion technique, *J. Automobile Eng. IMechE Part D*, 215, 63-81.

Durst F and Trimis D, (2002), Combustion by free flames versus combustion reactors, *16th Int. Clean Air and Environ Conf. (Clean Air 2002)*, Christchurch, Newzland, August 19-22, 3, 1-20.

Echigo R (1982), Effective energy conversion method between gas enthalpy and thermal radiation and application to industrial furnaces, *Proc. 7th Int. Heat Transfer Conf.*, Munich, Germany, September 6-10, VI, 361-66.

Echigo R (1984), Method and device for combustion, Application No. 57-160456, Int. CI. F23C11/00, 8, 154.

Echigo R, Yoshizawa Y, Hanamura K and Tomimura T (1986), Analytical and experimental studies on radiative propagation in porous media with internal heat generation. *Proc. 8th Int) Heat Transfer Conf.*, San Francisco, U.S.A, March 16-20, II, 827-32.

Echigo R, Kurusu M, Ichimiya K and Yoshizawa Y (1987), Combustion augmentation of extremely low calorific gases, *Proc. of ASME/JSME Therm. Eng. Joint Conf.*, Honolulu, U.S.A., March 22-27, 99-103.

Echigo R. (1991), Radiation enhanced/controlled phenomena of heat and mass transfer in porous media, *Proc. ASME/JSME Thermal Eng. Joint Conf.*, Reno, U.S.A., September 30-October 2, 21-32.

Echigo R, Yoshida H, Tawata, H and Tada S (1993), *12th Int. Conf. on Thermoelectrics*, Yokohama, Japan, November 9-11.

Echigo R, Yoshida H, Tawata K, Koda M and Hanamura K (1994), Transient heat and mass transfer with condensable vapor in porous media, *Proc. 10th Int. Heat Transfer Conf.*, Brighton, UK, August 14-18, 5, 231-236.

Echigo R, Yoshida H, Tawata K and Tada S. (1995), Effective heating/cooling method for porous thermoelectric device in reciprocating flow combustion system, *Proc. 4th ASME/JSME Therm. Eng. Joint Conf.*, Lahaina, U.S.A, March 19-24, 4, 389-96.

Ellzey JL ad William JM (2004), Porous burner for gas turbine applications, Patent No. US2003024655.

Ellzey JL and Schoegl IM (2009), System and method for super adiabatic counter flow reactor, Patent No. WO2007121004A2

Escobedo F and Viljoen HJ (1994), Modeling of porous radiant burners with large extinction coefficients, *Canadian J. Chem. Eng.*, 72, 805-14.

Fabrice G and Beatrice F (2008), Compact exchanger reactor using a plurality of porous burners, Patent No. WO2008132313 A2

Fleming DK (1987), Non-catalytic porous-phase combustor, Patent No. US4643667.

Franz M and Götz S (2010), Device for burning a fuel/oxidant mixture, Patent No. WO2010031869 A3

Fu X, Viskanta R and Gore JP (1998a), Measurement and correlation of volumetric heat transfer coefficients of cellular ceramics, *Exp. Therm Fluid Sci.*, 17, 285-93.

Gao HB, Qu ZG, He YL, and Tao WQ, (2012), Experimental study of combustion in a double-layer burner packed with alumina pellets of different diameters, Appl. Energy, 100, 295–302.

Goeckner BA, Helmich DR, McCarthy TA, Arinez JM, Peard TE, Peters JE, Brewster MQ and Buckvis RO (1992), Radiative heat transfer augmentation of natural gas flames in radiant tube burners with porous ceramic inserts, *Exp. Therm Fluid Sci.*, 5, 848-60.

Hackert CL, Ellzey JL and Ezekoye OA (1999), Combustion and heat transfer in 2-D model porous burners. *Combust. Flame*, 116, 177-91.

Hale MJ and Bohn MS (1992), Measurement of the radiative transport properties of reticulated alumina foams, *ASME/ASES Joint Solar Eng. Conf.*, Washington D.C., U.S.A., April 4-8, Paper 92-v-842.

Hanamura K and Echigo R (1991), An analysis of flame stabilization mechanism in radiation burners, *Heat Mass Transfer*, 26, 377-83.

Hanamura K, Echigo R and Zhdanok SA (1993), Superadiabatic combustion in a porous medium, *Int. J. Heat Mass Transfer*, 36, 3201-09.

Hardesty DR and Weinberg FJ (1974), Burners producing large excess enthalpies, *Combust. Science Technol.*, 8, 201-14.

Hayashi TC, Malico I and Pereira JCF (2004), Three-dimensional modeling of a two-layer porous burner for household applications, *Comput. Struct.*, 82, 1543-50.

Hays JW (1933), Surface combustion process, *United States Patent,* No. 2095065.

Hoetger M and Thiele W (2006), Pore-type burner with silicon-carbide porous body, *United States Patent* No. 20060035190.

Hoffmann JG, Echigo R, Tada S and Yoshida H (1995),, Analytical study on flammable limits of reciprocating superadiabatic combustion in porous media, *Proc. 8th Int. Symp. Transport Phenomena in Combust.*, San Francisco, U.S.A, July 16-20. 2, 1430-40.

Hoffman JG, Echigo R, Yoshida H and Tada S (1997), Experimental study on combustion in porous media with a reciprocating flow system, *Combust. Flame*, 11, 32-64.

Howell JR, Hall MJ and Ellzey JL (1996), Combustion of hydrocarbon fuels within porous inert media, *Prog. Eng and Combust. Sci.*, 22, 121-45.

Hsu PF, Howell JR and Matthews RD (1991a), A numerical investigation of premixed combustion within porous inert media, *Proc. ASME /JSME Thermal Engg. Joint Conf.*, 4, Reno, U.S.A., March 17-22, 225-31.

Hsu PF (1991b), Analytical and Experimental study of combustion in porous inert media, *Ph.D. dissertation*, University of Texas.

Hsu PF, Evans WD and Howell JR (1993a), Experimental and numerical study of premixed combustion within non homogeneous porous ceramics, *Combust. Sci. Technol.*, 90, 149-72.

Hsu PF, Howell JR and Matthews RD (1993b), A numerical investigation of pre-mixed combustion within porous inert media, *J. Heat Transfer,* 115, 744-50.

Hsu PF and Matthews RD (1993c), The necessity of using detailed kinetics in models for premixed combustion within porous media, *Combust. Flame*, 93, 457-66.

Hsu PF and Howell JR (1993d), Measurements of thermal conductivity and optical properties of porous partially stabilized zirconia, *Exp. Heat Transfer*, 5, 293-313.

Huang Y, Chao CYH and Cheng P (2002), Effects of preheating and operation conditions on combustion in a porous medium, *Int. J. Heat Mass Transfer*, 4, 4315-24.

Hunt TK, Ivanenok JF and Sievers RK (1994), AMTEC auxiliary power unit for hybrid electric vehicles, *Proc. 29th Intersociety Eng. Conversion Engg. Conf.*, Monterey, U.S.A, August 7-11.

Hunt TK, Sievers RK and Ivanenok JF (1995), Low emission AMTEC automotive power system, *Proc. 30th Intersociety Eng. Conversion Engg. Conf.*, Orlando, U.S.A, July 30 July-August 4, 145-50.

Hwang SJ (2014), Combustion device, Patent No. EP2738459 A1

Ismail KA, Abdullah MZ, Zubair M, Ahmad ZA, Jamaludin AR , Mustafa KF , Abdullah MN (2013), Application of porous medium burner with micro cogeneration System, Energy, 50, 131-142.

Itaya Y, Miyoshi K, Maeda S and Hasatani M (1992), Surface combustion of a premixed methane-air gas on a porous ceramic, *Int. Chem. Eng.*, 32, 123-31.

Itaya Y, Jinno K and Hasatani M (1994), Methane premixed combustion behavior of a porous ceramic surface burner in a furnace, *J. Chem. Eng. Japan*, 20, 301-5.

Jugjai S and Rungsimuntuchart N (2002), High Efficiency heat-recirculating domestic gas burners, *Exp. Therm. Fluid Sci.*, 26, 581-92.

Jugjai S and Anantachai Sawananon (2004), The surface combustor-heater with cyclic flow reversal combustion embedded with water tube bank, *Fuel*, 83, 2369-79.

Kaeding S and Lawrence J (2008), Burner device with a porous body, Patent No. US20080020336 A1.

Kamal MM and Mohamad AA (2005), Enhanced radiation output from foam burners operating with a non premixed flame, *Combust. Flame*, 140, 233-48.

Kamijo T, Suzuki Y, Kasagi N and Okamasa T (2009), High-temperature micro catalytic combustor with Pd/nano-porous alumina, *Proc. Combust. Inst.*, 32, 3019-26.

Kandpal B, Maheswari RC and Kandpal TC (1995), Indoor air pollution from domestic cooking stoves using coal kerosene and LPG, *Energy Convers. Manage*, 36, 1067-1072.

Kendall RM, DesJardin ST and Sullivan JD (1992), Basic research on radiant burners, Final report, *Gas Research Inst.*, Chicago, GRI Report No. 92-7027-171.

Keramiotis C, Stelzner B, Trimis D and Founti M, (2012), Porous burners for low emission combustion: An experimental investigation, Energy, 45, 213-219.

Keramiotis C and Founti MA (2013), An experimental investigation of stability and operation of a biogas fueled porous burner, Fuel, 103, 278-284.

Keshtkar MM and Nassab SAG (2009a), Theoretical analysis of porous radiant burners under 2-D radiation field using discrete ordinates method, Journal of Quantitative Spectroscopy and Radiative Transfer, 110, 1894–1907.

Keshtkar MM, Nassab SAG and Nasr MRJ (2009b), Heat transfer characteristics of a cylindrical porous radiant air heater under the influence of a two-dimensional axisymmetric radiative field. Journal of Power and Energy, 223, 867-872.

Kesting A, Pickenäcker O, Trimis D and Durst F (1999), Development of a radiation burner for methane and pure oxygen using the porous burner technology, *Proc. 5th Int. Conf. Technologies and Combust. Clean Environ. (Clean Air V)*, Lisbon, Portugal, July 12-15, 1999.

Khanna V, Goel R and Ellzey JL (1994), Measurements of emissions and radiation for methane combustion within a porous medium burner, *Combust. Sci. Technol.*, 99, 133-142.

Kline SR and Mc Clintock (1953), Describing uncertainties in single sample experiments, *Mech Engg.*, 75, 1-3.

Koester GE, Kennedy LA and Subramaniam VV (1994), Low temperature wave enhanced combustion in porous systems, *Proc. Central States Section meeting. The Combust. Inst.*, Madison, U.S.A, June 5-7, 55-60.

Korzhavin AA, Bunev VA and Babkin VS (1997), Dynamics of gaseous combustion in closed system with an inert porous medium, *Combust. Flame*, 109, 507-20.

Kulkarni MR and Peck RE (1996), Analysis of bilayered porous radiant burners, *Numerical Heat Transfer*, 30, 219-32.

Lammers FA and De Goey LPH (2004), The influence of gas radiation on the temperature decrease above a burner with a flat porous inert surface, *Combust. Flame*, 136, 533-547.

Leonardi SA, Viskanta R and Gore JP (2002), Radiation and thermal performance measurements of a metal fiber burner, *J. Quant. Spectrosc. Radiat. Transfer*, 73, 491-501.

Leonardi SA, Viskanta R and Gore JP (2003), Analytical and experimental study of combustion and heat transfer in submerged flame metal fiber burners/heaters, *Trans. ASME*, 125, 118-25.

Li BX, Lu YP, Liu LH, Kudo K and Tan HP (2005), Analysis of directional radiative behavior and heating efficiency for a gas-fired radiant burner, *J. Quant. Spectrosc. Radiat. Transfer*, 92, 51-9.

Li Y-H, Chao Y-C and Dunn-Rankin D (2008), Combustion in a meso-scale liquid-fuel film combustor with central-porous fuel inlet, *Combust. Sci. Technol.*, 180, 1900-19.

Lim IG (1997), Effect of properties on CO and NO emission in premixed combustion within porous ceramic burner, *Proc. 4th Int. Conf. on Technologies and Combust. Clean Environ.*, Portugal, July 7-10, II, 28.

Liu JF and Hsieh WH (2004), Experimental investigation of combustion in porous heating burners, *Combust. Flame,*138, 295-303.

Lucke CE (1913), Design of surface combustion appliances, *J Indus Eng Chem.*, 1913, 5, 801-24.

Malico I and Pereira JCF (1999), Numerical predictions of porous burners with integrated heat exchanger for house hold applications, *J. Porous Media*, 2, 153-62.

Malico I, Zhou XY and Pereira JCF (2000), Two-dimensional numerical study of combustion and pollutants formation in porous burners, *Combust. Sci. Technol.*, 152, 57-9.

Malico I and Pereira JCF (2001), Numerical study on the influence of radiative properties in porous media combustion, *J. Heat Transfer*, 123, 951-57.

Marbach TL and Agrawal AK (2006), Heat-recirculating combustor using porous inert media for meso-scale applications, *J Propul Power*, 22, 145-150.

Marbach TL, Sadasivuni V and Agrawal AK (2007), Investigation of a miniature combustor using porous media surface stabilized flame, *Combust Sci Technol.*, 179:1901-22.

Mare L. di, Mihalik TA. Continillo G and Lee JHS (2000), Experimental and numerical study of flammability limits of gaseous mixtures in porous media, *Exp. Therm Fluid Sci.* 21, 117-23.

Min DK and Shin HD (1991), Laminar premixed flame stabilized inside a honeycomb ceramic, *Int. J. Heat Mass Transfer*, 34, 341-56.

Mishra SC, Steven M, Nemoda S, Talukdar P, Trimis D and Durst F (2006), Heat transfer analysis of a two-dimensional rectangular porous radiant burner, *Int. Commu. Heat Mass Transfer*, 33, 467-74.

Mital R, Gore JP and Viskanta R (1997), A study of the structure of submerged reaction in porous ceramic radiant burners, *Combust. Flame*, 11, 175-84.

Mital R, Gore JP and Viskanta R (1998), A radiant efficiency measurement procedure for gas fired radiant burners, *Exp Heat Transfer*, 11, 3-21.

Mjaanes HP, Chan L and Mastorakos E (2005), Hydrogen production from rich combustion in porous media, *Int. J. Hydrogen Energy*, 30, 579-92.

Mohamad AA, Ramadhyani S, Viskanta R (1994), Modelling of combustion and heat transfer in a packed bed with embedded coolant tubes, *Int. J. Heat Mass Transfer,* 37, 1181-91.

Mößbauer S, Pickenäcker O, Pickenäcker K, Trimis D (1999), *5th Int. Conf. Technologies and Combust. for a Clean Environ. (Clean Air V)*, Lisbon, Portugal, July 12-15, I, 519-23.

Mößbauer S, Grüber W and Trimis D (2001), Exhaust gas recirculation in porous burners for the target application zero emission steam engines, *Proc. 6th Int. conf. on technologies and combust. for a clean Environ*, Porto, Portugal, July 9-12, 2, 213-218.

Mujeebu MA, Abdullah MZ, and Mohamad A A, (2011), Development of energy efficient porous medium burners on surface and submerged combustion modes, Energy, 36, 5132-5139.

Muthukumar P, Anand P and Sachdeva P (2011), Performance analysis of porous radiant burners used in LPG cooking stove, Int. J Energy and Environment, 2, 367-374.

Muthukumar P and Shyamkumar P (2013), Development of a novel porous radiant burner for LPG cooking applications, Fuel, 112, 562-566.

Nakamura Y, Itaya Y, Miyoshi K and Hasatani M (1993), Mechanism of methane-air combustion on the surface of a porous ceramic plate, *J. Chem. Eng. Japan*, 26, 205-11.

Nemoda S, Trimis D and Zivkovi G (2004), Numerical simulation of porous burners and hole plate surface burners, Thermal Science, 8, 3-17

Orenstein RM and Green DJ (1992), Thermal shock behavior of open cell ceramic foams, *J. Am. Ceram. Soc.*, 75, 1899-1905.

Pantangi VK, Kumar ASSRK, Mishra SC Sahoo N (2007), Performance analysis of domestic LPG cooking stoves with porous media. Int. Energy Journal 8, 139-144.

Pantangi VK (2010), Development and performance analysis of porous radiant burners for LPG cooking applications. Ph.D thesis, Department of Mechanical Engineering, IIT Guwahati.

Pantangi VK, Mishra SC, Muthukumar P and Reddy R (2011), Performance of PRBs-Cooking Application, Energy, 36, 6074-6080.

Pickenacker O, Pickenacker K, Wawrzinek K, Trimis D, Pritzkow WEC, Muller C, Goedtke P, Papenburg U, Adler J, Standke G, Heymer H, Tauscher W and Jansen F (1999), Innovative ceramic materials for porous-medium burners, *Interceram*, Freiburg, Germany, 48, 424-33.

Prichard R, Guy J J and Conner (1977), Industrial Gas Utilization, New Providence NJ.

Qui K and Hayden ACS (2006), Premixed gas combustion stabilized in fiber felt and its application to a novel radiant burner, *Fuel*, 85, 1094-1100.

Qiu K and Hayden ACS (2007), Thermophotovoltaic power generation systems using natural gas-fired radiant burners, *Solar Energy Mater. Solar Cells*, 91, 588-96.

Raviraj SD and Janrt LE (2006), Numerical and experimental study of the conversion of methane to hydrogen in a porous medium reactor, *combust. Flame*, 144, 698-709.

Redwood DS and John P [2007], High efficiency Radiant Burner, *Patent No.* WO2007027379A1

Sadasivuni V and Agrawal AK (2009), A novel meso-scale combustion system for operation with liquid fuels, *Proc. Combust. Inst.*, 32, 3155-62.

Sahraoui M and Kaviany M (1994), Direct simulation vs volume-averaged treatment of adiabatic, premixed flame in a porous medium, *Int. J. Heat Mass Transfer*, 37, 2817-34.

Sanmiguel JE, Mehta SAR and Moore RG (2003), An experimental study of controlled gas-phase combustion in porous media for enhanced recovery of oil and gas, *Trans. ASME*, 125, 64-71.

Sathe SB, Peck RE and Tong TW (1989a), A numerical analysis of combustion and heat transfer in porous radiant burners, *Heat Transfer Phenom. Radiat. Combust. Fires*, ASME HTD, 107, 461-68.

Sathe SB, Kulkarni MR, Peck RE and Tong TW (1989b), An experimental study of combustion and heat transfer in porous radiant burners, *Meeting of Western Sates Section, The Combust. Inst.*, Livermore, U.S.A, Oct 23–24, 1-19.

Sathe SB, Kulkarni MR, Peck RE and Tong TW (1990a), An experimental and theoretical study of porous radiant burner performance, *23rd Symp. Int. on Combust., The Combust. Inst.,* Pittsburgh, U.S.A, May 21-23, 1011-18.

Sathe SB, Peck RE and Tong TW (1990b), Flame stabilization and multi-mode heat transfer in inert porous media-a numerical study, *Combust. Sci. Technol.*, 70, 93-109.

Scribano G, Solero G and Coghe A (2006), Pollutant emissions reduction and performance optimization of an industrial radiant tube burner, *Exp. Therm Fluid Sci.,* 30, 605-12.

Semenov NN (1928), On the theory of the combustion process, *Z. Physics*, 48, 571.

Shinoda M, Maihara R, Kobayashi N, Arai N and Churchill SW (1998), The characteristics of a heat-recirculating ceramic burner, *Chem. Eng. J.*, 71, 207-12.

Shinoda M, Tanaka R and Arai N (2002), Optimization of heat transfer performances of a heat-recirculating ceramic burner during methane/air and low-calorific-fuel/air combustion, *Energy Convers. Manage.*, 43, 1479-491.

Singh S, Ziolkowski M, Sultzbaugh J and Viskanta R (1991), Mathematical model of a ceramic burner radiant heater, *Foss. Fuel Combust.* ASME-PD, 33, 111-16.

Soete G (1966), Stability and propagation of combustion waves in inert porous media, *11th Symp. Int. on Combust., The Combust. Inst.*, Pittsburgh, U.S.A, July 11-15, 959-66.

Suzukawa Y, Sugiyama S, Hino Y, Ishioka M and Mori I (1997), Heat transfer improvement and NOx reduction by highly preheated air combustion, *Energy Convers. Manage.*, 38, 1061-71.

Takeno T, Sato K (1979), An excess enthalpy flame theory, *Combust. Sci. Technol.*, 20, 73-84.

Takeno T, Sato K and Hase K (1980), A theoretical study on an excess enthalpy flame, *Proc. of 18th Symp. Int. on Combust*., *The Combust. Inst.*, Waterloo, Canada, August 17-22, 465-72.

Takeno T and Hase K (1983), Effects of solid length and heat loss on an excess enthalpy flame, *Combust. Sci. Technol.,* 31, 207-15.

Takeno T and Murayama M (1986), One-dimensional flame with extended reaction zone, *Progr. Astro. Sci.*, 105, 246-62.

Talukdar P, Mishra SC, Trimis D and Durst F (2004) Heat transfer characteristics of a porous radiant burner under the influence of a 2-D radiation field, *J. Quant. Spectrosc. Radiat. Transfer*, 84, 527-37.

Tanaka R, Shinoda M and Arai N (2001), Combustion characteristics of a heat recirculating ceramic burner using low-calorific fuel, *Energy Convers. Manage.*, 42, 1897-1907.

Tomimura T, Hamano K, Honda Y, Echigo R (2004), Experimental study on multi-layered type of gas-to-gas heat exchanger using porous media, *Int. J. Heat Mass Transfer*, 47, 4615-23.

Tong TW and Sathe SB (1988), Heat transfer characteristics of porous radiant burners, *ASME HTD*, 104, 147-55.

Tong TW, Lin WQ and Peck RE (1987), Radiative heat transfer in porous media with spatially-dependent heat generation, *Int. Comm. Heat Mass Transfer,* 14, 627-37.

Tong TW, Sathe SB and Peck RE (1990), Improving the performance of porous radiant burners through use of sub-micron size fibres, *Int. J. Heat Mass Transfer*, 33, 6, 1339-46.

Tong TW and Li W (1995), Enhancement of thermal emission from porous radiant burners, *J. Quant. Spectrosc. Radiat. Transfer,* 53, 235-48.

Trimis D and Durst F (1996), Combustion in a porous medium-advances and applications, *Combust. Sci. Technol.*, 121, 153-68.

Turns SR (2000), An Introduction to Combustion: Concepts and Applications, Second edition, McGraw-Hill, New York.

Viskanta R (1996), Interaction of combustion and heat transfer in porous inert media, *Transport Phenonm. Combust.*, 1, 64-87.

Viskanta R and Gore JP (2000), Overview of cellular ceramics based porous radiant burners for supporting combustion, *Int. J. Environ. Combust. Technol.*, 3, 167-203.

Volkert Jochen and Goebel Peter (2006), Burner for a gas and air mixture, *United States Patent* No. 6997701.

Weclas M (2005), Porous media in internal combustion engines, Cellular ceramics-structure, manufacturing, properties and applications, Wiley-VCH-Publication.

Wei M, Wang Y and Reh L (2002), Experimental investigation of the pre vaporized premixed (vpl) combustion process for liquid fuel lean combustion, *Chem. Eng. Process*, 41, 157-64.

Weinberg FJ (1971), Combustion temperatures: the future? , *Nature*, 233, 239-41.

Williams A, Woolley R, and Lawes M (1992), The formation of NOx in surface burners, *Combust. Flame*, 89, 157-166.

World Bank (2003), India: Access of the poor to clean household fuels, ESM 263, Joint United Nations Development Programme (UNDP)/World Bank Energy Sector Management Assistance Programme (ESMAP), July 2003.

Xiong T (1991), Experimental study of ultra-low emission radiant porous burner, *AFRC 1991 Spring Members Meeting*, Hartford, U.S.A, March 18-19.

Xiong Tian-Yu, Mark JK and Ferol F. Fish (1995), Experimental study of a high-efficiency, low emission porous matrix combustor-heater, *Fuel*, 74, 1641-47.

Yamamoto K, Takada N and Misawa M (2005), Combustion simulation with Lattice Boltzmann method in a three-dimensional porous structure, *Proc 4th Joint Meeting of the US Sections of the Combust. Inst.*, Philadelphia, U.S.A., March 20-23, 30, 1509-15

Yoshida H, Yun JH, Echigo R and Tomimura T (1990), Transient characteristics of combined conduction, convection and radiation heat transfer in porous media, *Int. J. Heat Mass Transfer*, 33, 847-57.

Yoshida M (2011), Burner For Manufacturing Porous Glass Preform, Patent No. US20110259056 A1

Yoksenakul W and jugjai S (2011), Design and development of a SPMB with a submerged flame, Energy, 36, 3092-3100.

Yoshizawa Y, Sasaki K and Echigo R (1988), Analytical Study of the structure of radiation controlled flame, *Int. J. Heat Mass Transfer*, 31, 311-319.

Zeldovich Ya B, Barenblatt GI and Librovich VB (1985), Mathematical theory of combustion and explosions, Plenum Press, New York.

Zhang JM, Sutton WH and Lai FC (1997), Enhancement of heat transfer using porous convection-to-radiation converter for laminar flow in a circular duct, *Int. J. Heat Mass Transfer*, 40, 39-48.

Zhdanok SA, Martynenko VV and Shabunya SI (1993), Obtaining superadiabtic temperatures in combustion of gaseous fuel in a system of two porous plates with a periodic change of the direction of pumping, *J. Eng. Phys. Thermphys.*, 64, 463-69.

Zhdanok SA, Dobrego KV and Futko SI (1998), Flame localization inside axis symmetric cylindrical and spherical porous media burners, *Int. J. Heat Mass Transfer*, 41, 3647-65.

APPENDIX – I

1. Properties of LPG (http://www.gasindia.in)

Particulars		Value
Chemical Formula	:	Propane (C_3H_8) – 60% and Butane (C_4H_{10}) – 40%
Ignition temperature (^oC)	:	488-502
Max. flame temperature (^oC)	:	1985
Higher calorific value in kJ/kg.	:	49540
Lower calorific value kJ/kg.	:	44160
Density	:	1.9 kg/m^3

2. Power/ Thermal load of a burner:

To find the power/thermal load of the burner, kW = Mass flow rate of the fuel × calorific value of the fuel

For example:

If the flow meter shows a reading of 1.23×10^{-5} kg/s

Then the power at which the burner is running = 1.23×10^{-5} kg/s × 44160 kJ/kg

= 0.54 kW

APPENDIX – II

Estimation of Equivalence ratio (*Φ*)

$$\text{The equivalence ratio } \Phi = \frac{(A/F)_{stoich}}{(A/F)_{actual}}$$

Φ>1; fuel rich mixture

Φ<1; fuel lean mixture

Φ=1; stoichiometric mixture

The stoichiometric quantity of air is just that amount needed to completely burn a quantity of fuel. The stoichiometric air fuel ratio is determined by writing simple atomic balances, assuming that the fuel reacts to form an ideal set of products.

For a hydrocarbon fuel given by C_xH_y, the stoichiometric relation is expressed as [Turns, 2002]

$$C_xH_y + a(O_2 + 3.76N_2) \Leftrightarrow CO_2 + H_2O + 3.76 \times a \times N_2$$

we assume composition of air is 21% O_2 and is 79% N_2 (by volume). So for each mole of O_2 in air, there are 3.76 moles of N_2.

$$(A/F)_{Stoich} = 4.76 \times a \frac{(MW)_{air}}{(MW)_{fuel}}$$

Where MW_{air} and MW_{fuel} are the molecular weights of the air and fuel, respectively.

The main constituents of LPG are Propane (C_3H_8) – 60% and Butane (C_4H_{10}) – 40%

Stoichiometric relation:

$$\tfrac{3}{5}C_3H_8 + \tfrac{2}{5}C_4H_{10} + a\left(O_2 + 3.76N_2\right) \rightarrow cCO_2 + bH_2O + 3.76a\,N_2$$

After balancing,

$$\frac{3}{5}C_3H_8 + \frac{3}{5}C_4H_{10} + \frac{28}{5}\left(O_2 + 3.76N_2\right) \rightarrow \frac{17}{5}CO_2 + \frac{22}{5}H_2O + \left(3.76\times\frac{28}{5}\right)N_2$$

$$\left(\frac{A}{F}\right)_{Stoich} = 4.76\times\left(28/5\right)\times\frac{29}{\left(248/5\right)} = 15.58 \approx 15.6$$

For a required wattage, the fuel mass flow rate (F_{actual}) is known.

The equivalence ratio can be changed by changing the mass flow rate of air (A_{actual}) as per the requirement.

$$\Phi = \frac{15.6}{\left(A/F\right)_{actual}}$$

APPENDIX - III

Error Analysis

Klein and McClintock [1953] proposed a procedure for estimating the uncertainty of any measured quantity in experimental studies. If an estimated quantity, R depends on the independent variables like x_1, x_2, x_3,…….x_n then,

$$R = R\ (x_1, x_2, x_3, \ldots\ldots x_n)$$

Then the maximum value of uncertainty is given by:

$$W_R = \left[\left(\frac{\partial x_1}{x_1} \right)^2 + \left(\frac{\partial x_2}{x_3} \right)^2 + \left(\frac{\partial x_3}{x_3} \right)^2 \ldots\ldots\ldots\ldots\ldots \left(\frac{\partial x_n}{x_n} \right)^2 \right]^{1/2}$$

In the present case, the formula for efficiency is as given below:

$$\eta = \frac{\left[m_w C_w \Delta T_w \right] + \left[m_p C_p \Delta T_p \right]}{m_f \times CV}$$

Since $\Delta T_w = \Delta T_p = \Delta T$

$$\eta = \frac{\left[(m_w C_v) + (m_p C_p) \right] \left[\Delta T \right]}{m_f \times CV_f}$$

m_f is the fuel consumed to raise the water temperature from T_1 to T_2

The uncertainty in the thermal efficiency mainly comes due to the measured quantities of mass and temperature.

Assumptions:

1. Temperature rise of water and vessel are equal.

2. No error in values of specific heat of pan (C_p) and water (C_w), and Calorific value (CV) of fuel. The values considered are suggested in the standard (IS: 4246: 2002)

Hence the Calculation formula:

$$\frac{\partial \eta}{\eta} = \left[\left(\frac{\partial \eta}{\partial m_v} \Delta m_v \right)^2 + \left(\frac{\partial \eta}{\partial m_w} \Delta m_w \right)^2 + \left(\frac{\partial \eta}{\partial (\Delta T)} \Delta(\Delta T) \right)^2 + \left(\frac{\partial \eta}{\partial m_f} \Delta m_f \right)^2 \right]^{1/2}$$

where $\Delta m_v = \pm 1$ gm, $\Delta m_w = \pm 1$ gm

$\Delta(\Delta T) = \pm 1°C$, $\Delta m_f = \pm 0.001$ gm

At a condition of $m_v = 0.864$ kg, $m_w = 8$ kg

$\Delta T = (90\text{-}20) = 70°C$, $m_f = 0.1062$ kg

$$\text{We get } \frac{\partial \eta}{\eta} = 0.0155$$

Therefore the maximum uncertainty in efficiency is ±1.5%.

APPENDIX – IV

Technical Specifications of the Instruments Used in the Experiments

1. Digital pressure gauges:

P1		P2	
Make	: DWYER (U.S.A.)	Make	: DWYER (U.S.A.)
Fluid	: LPG	Fluid	: Air
Models	: DPG-003	Models	: DPG-006
Range	: 0-2 bar	Range	: 0-13.8 bar
Accuracy	: ±0.05% full scale	Accuracy	: ±0.05% full scale
Pressure Limit	: 2 x FS range	Pressure Limit	: 2 x FS range
Temperature Limits	: -18 to 66°C	Temperature Limits	: -18 to 66°C
Power requirements	: 3 AAA batteries.	Power requirements	: 3 AAA batteries.

2. Pressure regulator (LPG)

Pressure regulator (A)		Pressure regulator (B)	
Make	: SKN Pvt. Ltd.	Make	: United Works Pvt. Ltd.
Maximum pressure	: 2 bar gauge	Maximum pressure	1.2 bar gauge

Pressure regulator (C)		Pressure regulator (D)	
Make	: United Works Pvt. Ltd.	Make	: United Works Pvt. Ltd.
Maximum pressure	: 1 bar gauge	Maximum pressure	: 0.1 bar gauge

3. Compressor

Make	: Ingersoll Rand
Type	: Reciprocating
Maximum Pressure	: 12 kg/cm^2
Free air delivery	: 400-450 lpm
Type	: 2 stage
Tank capacity	: 250 liters
Accessories	: Precise Pressure regulator, air filter

4. Pressure regulator (Compressed air)

Make	: Norgren
Model	: R73G-2GK-RMN
Fluid	: Compressed air
Maximum pressure	: 10 bar

5. Weighing balance (WB)

Make	: SARTORIUS COMBICS LITE
Model	: CLWP1 – 30ED-I
Capacity	: 30kg
Platform size	: 400X300mm
Readability	: 1g
Power Supply	: 90 to 260V AC & DC
Indicator	:18mm LCD 7 segment backlit

6. Thermocouples

	T1 (For CZ)	**T2 (For PZ)**
Make:	Tempsens Instruments (I) Pvt. Ltd.	Tempsens Instruments (I) Pvt. Ltd.
Type:	metal sheathed K-type	metal sheathed K-type
Junction:	Grounded	Exposed
Range:	20ºC to 1400 ºC	20ºC to 1400 ºC

7. Mass flow meter

Type	: Coriolis mass flow meter
Make	: Emerson Process Management Pvt. Ltd.
Model	: CMF010P323NQB2E222
Flow range	: 0 to 50 g/min
Flow accuracy	: ± 0.35% of full scale
Sensitivity	: 0.001g
Temperature range	: -10 to 100 °C
Operating pressure range	: 0 to 150 bar

8. Portable gas analyser

Make	: GreenLine
Model	: 8000
O_2	: 0 – 25 Vol%
Resolution	: 0.1 Vol%
Accuracy	: <0.1 Vol%
CO	: 0 – 20000 ppm
Accuracy	: <10 ppm (0 – 300 ppm)
Resolution	: 1 ppm
NO	: 0 – 4000 ppm
Accuracy	: <5 ppm (0 – 100 ppm)
Resolution	: 0.1 ppm
NO_2	: 0 – 500 ppm
Accuracy	: <5 ppm (0 – 99 ppm)

9. Data acquisition unit (DAQ)

Make	: Agilent Technologies
Model	: 34970A
Scan rate	: 60 to 250 channels/second
Scan intervals	: 0 to 99 hours; 1 ms time step
Accuracy	: 6 digits of resolution with 0.004%

10. IR camera

Make	: InfraTec
Spectral range	: (7.5 – 14) µm
Temperature measuring range	: (-40 – 1,200) °C, optional > 2,000 °C
Temperature resolution @ 30 °C	: better than 0.05 K, up to 0.03 K
Measurement accuracy	: ± 1.5 K (0 - 100) °C; ± 2 % (< 0 and > 100) °C
Emissivity	: Adjustable from 0.1 to 1.0
IR frame rate	: 50/60 Hz
Zoom function	: Up to 8 times digital, infinitely variable
Power supply	: mains adapter, FireWire (IEEE 1394)
Operation temperature	: (-15 - 50) °C
Dimensions (complete system)	: (133 x 106 x 110) mm
Weight (complete system)	: approx. 1.3 kg

Patents and Publications

Patents

1. Subhash C. Mishra, P. Muthukumar, Niraj Kumar Mishra, Self-Aspirated LPG Domestic Cooking Stove with a Two-Layer Porous Radiant Burner, Indian Patent No: 543/KOL/2015.

2. S. C. Mishra, P. Muthukumar, N. K. Mishra and S. Panigrahi, Medium-Scale Self-Aspirated Improved Air Entrainment LPG Cooking Stove with a Two-Layer Porous Radiant Burner. (Submitted to TIFAC, New Delhi, November 2014).

Journal

1. N. K. Mishra, S. C. Mishra, P. Muthukumar, Performance characterization of a medium-scale liquefied petroleum gas cooking stove with a two-layer porous radiant burner. Applied Thermal Engineering, 89, 44-50, 2015.

Conferences

1. N.K. Mishra, S.C. Mishra, P. Muthukumar, Temperature Measurement in Double Layer Porous Burner for Medium-Scale LPG Cooking Applications. Presented at 22th National and 11th International ISHMT-ASME Heat and Mass Transfer Conference, December 28-31, 2013, IIT Kharagpur, India

2. N.K. Mishra, P. Muthukumar, S.C. Mishra. Performance Tests on Medium-Scale Porous Radiant Burners for LPG Cooking Applications. Presented at International Conference on Energy Resources and Technologies for Sustainable Development (ICERTSD 2013), February 7-9, 2013, Howrah, West Bengal, India.